H. Shibuya

Rock Magnetism and Paleogeophysics

Volume 12

1985

DELP Publication No. 4

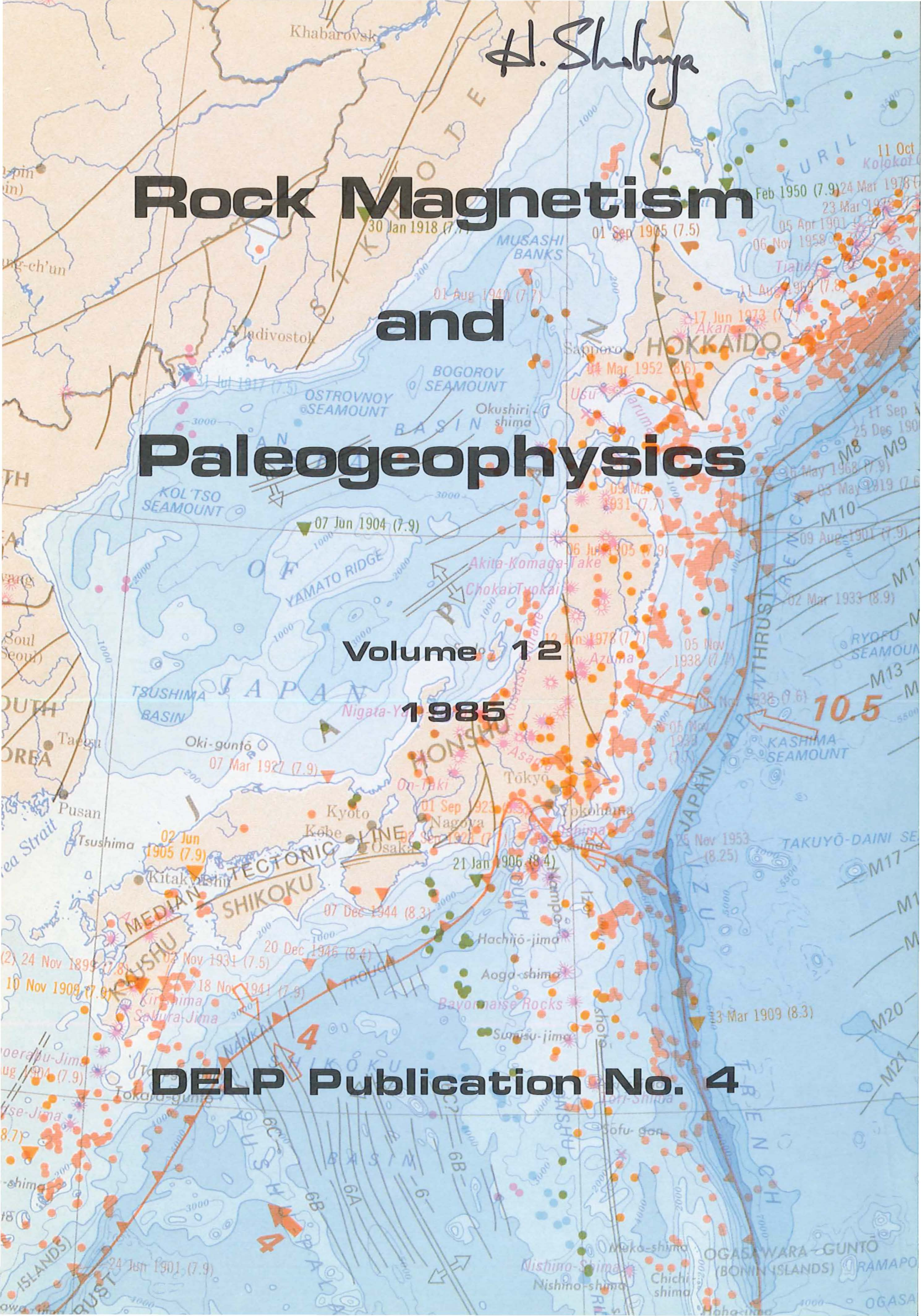

ま　え　が　き

本書は岩石磁気学・古地球物理学研究グループの1985年度の年次研究レポートであり，「国際リソスフェア探査開発計画 (DELP)」の成果報告書第４号として刊行されるものである。

岩石磁気学・古地球物理学研究グループでは，以前から Annual Report の形で英文の報文集を刊行してきた。(Annual Progress Report of the Rock Magnetism (Paleogeophysics) Research Group in Japan, 1963-1968. Rock Magnetism and Paleogeophysics, 1973-) これらの報文集は図書館などからの寄贈要請も多く，諸外国の関連分野の研究者によってかなり広く利用されている。このような経過から，この報告書も全て英文によって編集された。日本国内の研究者の方々にはいく分御迷惑をおかけすることになるが，事情を御理解いただきたい。

岩石磁気学・古地球物理学研究グループは，昭和60年度から実施されたDELP計画において，特に課題５「日本列島の構造発達」の研究で大きな寄与をするべく研究を進めている。本年は４月５日に東京大学地震研究所で「日本海の拡大」に関するシンポジウムを開催した。このシンポジウムでは日本列島の古地磁気データのほか，海洋観測からのデータ（磁気異常，熱流量，年代）や陸上の地質学的証拠(古生物，古気候など)にもとづいて，中新世におこったと思われる日本列島の折れ曲りと日本海拡大との関係が論じられた。このシンポジウムの報文の多くは Journal of Geomagnetisn and Geoelectricity の特集号に収録され現在印刷中である。また，７月24日から25日まで高知大学において第17回岩石磁気古地磁気研究会を開き，日本列島のテクトニクスに関連した多くの問題について活発な討論を行った。この研究会のプログラムは目次の後に集録されている。

本書の刊行および研究会の開催については，国際共同研究等経費「リソスフェア探査開発計画（DELP)」(代表者：秋本俊一，東大物性研）より援助を受けた。ここに記して感謝の意を表する。

1985年12月

PREFACE

This volume is an annual progress report of the Rock Magnetism and Paleogeophysics Research Group in Japan for the year 1985. As the previous reports were so, this volume contains a collection of summaries, extended abstracts or brief notes of the research works carried out in our group this year. Many of the reports contain materials which may undergo a significant change or may be revised as the research activity continues. In this respect, the readers are warned to regard them as tentative, and are also requested to refer from a complete paper if such is published as a final result. (Names of journals appear at the end of individual articles if they are in press, submitted, or in preparation for submission to some scientific journals).

The Japanese national program (for five years) for the International Lithosphere Project (dubbed DELP, for Dynamics and Evolution of the Lithosphere Project) started from this year. As a part of this year's activity, a symposium on the opening of the Japan Sea was held on 5 April, 1985 at Earthquake Research Institute, University of Tokyo. The papers presented in this symposium are now in press in a special issue of Journal of Geomagnetism and Geoelectricity. The readers may find an up-to-date collection of research results related to many aspects of the evolution of the Japanese islands and its environs.

This volume is published with financial aid from Ministry of Education, Science and Culture. It is Publication No. 4 of the DELP Committee. We thank other members of the Lithosphere Project for help and encouragements.

Tokyo
December 1985

Hidefumi Tanaka
Associate Editor

Masaru Kono
Editor

Rock Magnetism and Paleogeophysics
Research Group in Japan

TABLE OF CONTENTS

ARCHEOMAGNETISM

PALEOMAGNETISM: JAPANESE ISLANDS

PALEOMAGNETISM: OTHER AREAS

ROCK MAGNETISM

MISCELLANEOUS STUDIES

Cover

Japan and its surrounding area from "Plate Tectonic Map of the Circum-Pacific Region", Northwest Quadrant. Copyright 1981 by the American Association of Petroleum Geologists (AAPG), Box 979, Tulsa, Oklahoma, U.S.A. Reproduced by the permission of the AAPG. Circum-Pacific Plate Tectonic Maps can be purchased from the AAPG, or in Japan, from Naigai Koeki, Ltd. (Tel. 03-400-2326).

ROCK MAGNETISM AND PALEOGEOPHYSICS SYMPOSIUM 17

The seventeenth Rock Magnetism and Paleogeophysics Symposium was held on 24-25 July, 1985 at Kochi University. Most of presentation was concerned to paleomagnetism in Japan. Two speakers of Kochi University (asterisks below) were invited to summarize current status in researches.

24 July Afternoon

1. H. Morinaga (Kobe Univ.)
   Paleomagnetism of a stalagmite from Ryuga-Do Cave, Kochi

2. M. Homma (The Women's Highschool attached to Tokyo Univ. of Home-economy)
   Paleomagnetism of Myoken Formation, the Lower Part of Ninomiya Group in Oiso Area

3. M. Torii (Kyoto Univ.)
   Note on remanent directions from Neogene igneous rocks of Ishizuchi area

4. N. Ishikawa (Kyoto Univ.)
   Paleomagnetism of Ohsumi Granite

5. Y. Itoh (Kyoto Univ.)
   Paleomagnetism of tne Nohi Rhyolite

25 July Morning

6. K. Tokieda (Shimane Univ.)
   Remanent magnetization of clay material from archeological ruin and its application for dating

7. Y. Fujiwara (Hokkaido Univ.)
   Paleomagnetism of the Kamuikotan tectonic Belt in Hokkaido

8. K. Hirooka (Toyama Univ.)
   Paleomagnetic dating of paleoearthquake

9. K. Hirooka (Toyama Univ.)
   Paleomagnetic study of Koshikijima Island, Kyushu

10. Y. Otofuji (Kobe Univ.)
    Spreading mode of the Japan Sea Basin

25 July Afternoon

11. T. Kawasaki* (Kochi Univ.)
    Paleogeotherms: olivin-orthopyroxene-garnet geothermometry

12. H. Ishizuka* (Kochi Univ.)
    Geology of the Kamuikotan Belt in Hokkaido

13. K. Maenaka (Hanazono College)
    Paleomagnetism of Lower Cretaceous sediments in outer zone of southwest Japan I

14. S. Sasajima (Hanazono College)
    Paleomagnetism of Lower Cretacious sediments in outer zone of southwest Japan II

15. H. Shibuya (Univ. Osaka Pref.)
    Secondary magnetization on Paleozoic-Mesozoic rocks in Japan and Korea

16. H. Tanaka (Tokyo Inst. Technology)
    Paleomagnetism of Southern Peru

17. A. Hayashida (Doshisha Univ.)
    Paleomagnetism of the Early Miocene Series in Kakegawa Area

PRELIMINARY REPORT OF CONSTRUCTION OF A STANDARD GEOMAGNETIC SECULAR VARIATION CURVE FROM GIANT CORE SEDIMENTS IN JAPAN

Masayuki HYODO* and Katsumi YASKAWA**

* Cryogenic Center, Kobe University, Nada, Kobe 657, Japan
** Department of Earth Sciences, Faculty of Science, Kobe University, Nada, Kobe 657, Japan

In this paper preliminary result of stacking of the paleomagnetic data of Holocene marine and lake sediments from middle to south-west Japan is described.

Paleomagnetic data of five core sediments are used for stacking ; one from lake Yogo at 34.6°N 135.3°E (core YG1), two from lake Kizaki at 36.6° N 137.8°E (cores KZ1 and KZ3), one from Osaka Bay at 34.6°N 135.3°E (core OS2) and one from Mizushima Nada, the Inland Sea at 34.4°N 133.6°E (core MZ1). All the cores have been taken by a giant core (20 cm in diameter) sampling thechnique. Remanent magnetization of these sediments are very stable against AF-demagnetization. Detailed description of cores KZ3, OS2 and MZ1 are given in Horie et al.(1980), Hyodo and Yaskawa (1980), and Hyodo and Yaskawa (1986). Directions of natural remanent magnetization (NRM) are illustrated in Fig. 1. Magnetization vectors of four to five subsamples in each depth level are analyzed using Fisher statistics. Closed circles and error bars in Fig. 1 show mean directions and α_{95} confidence limits in each depth level. Declination is relative because the geographical north could not be assigned to the cores.

Declination and inclination of individual cores exhibits very similar pattern of variation. Using the similarity we attempt to transfer depth scale of individual cores to a common depth scale and further to a time scale.

The core YG1 is adopted as a master core because it covers the widest range of secular variation (~10500 yrBP). Equivalent depths between the master core and others are determined correlating maxima and minima of declination and inclination change. Correlative features are tied over 29 levels in YG1 ; seventeen tie points are defined in both declination and inclination, in which five are overlapped. Within-lake correlation using lithology and remanent intensity is possible for cores KZ1 and KZ3. The correlation provide many sharp tie points which quite closely coincide with those by correlation of declination and inclination.

On the basis of the transformation of depth to depth, ^{14}C-ages obtained in individual cores are transfered to the depth scale of the master core YG1. All the ages are plotted to the depth of YG1 in Fig.2. The core YG1 has its own ages ; three ^{14}C-ages and two tephrochronological ages. The two tephras were identified by Arai (1981) as Akahoya (6300 yrBP) for that of depth 565 cm and Oki (9300 yrBP) for that of depth 822 cm (Arai, 1981). All the ages except two erratic ages of YG1 are well consistent with each other.

The ages of YG1 at depths of 267 and 567 cm are too old. This is considered due to incorporation of old carbon as often observed in lake sediments (Mothersill, 1979 ; Creer and Tucholka, 1982). Dating method for YG1 is different from that for other cores in sample used. Fine fraction of organic carbon separated from some volume of sediments was used for dating of YG1. On the other hand, some pieces of shell or wood as large as possible were collected for dating of other cores. The ^{14}C-age at the basement of YG1 seems to be unaffected by old carbon according to the extrapolation with the trend by the two tephrochronological ages.

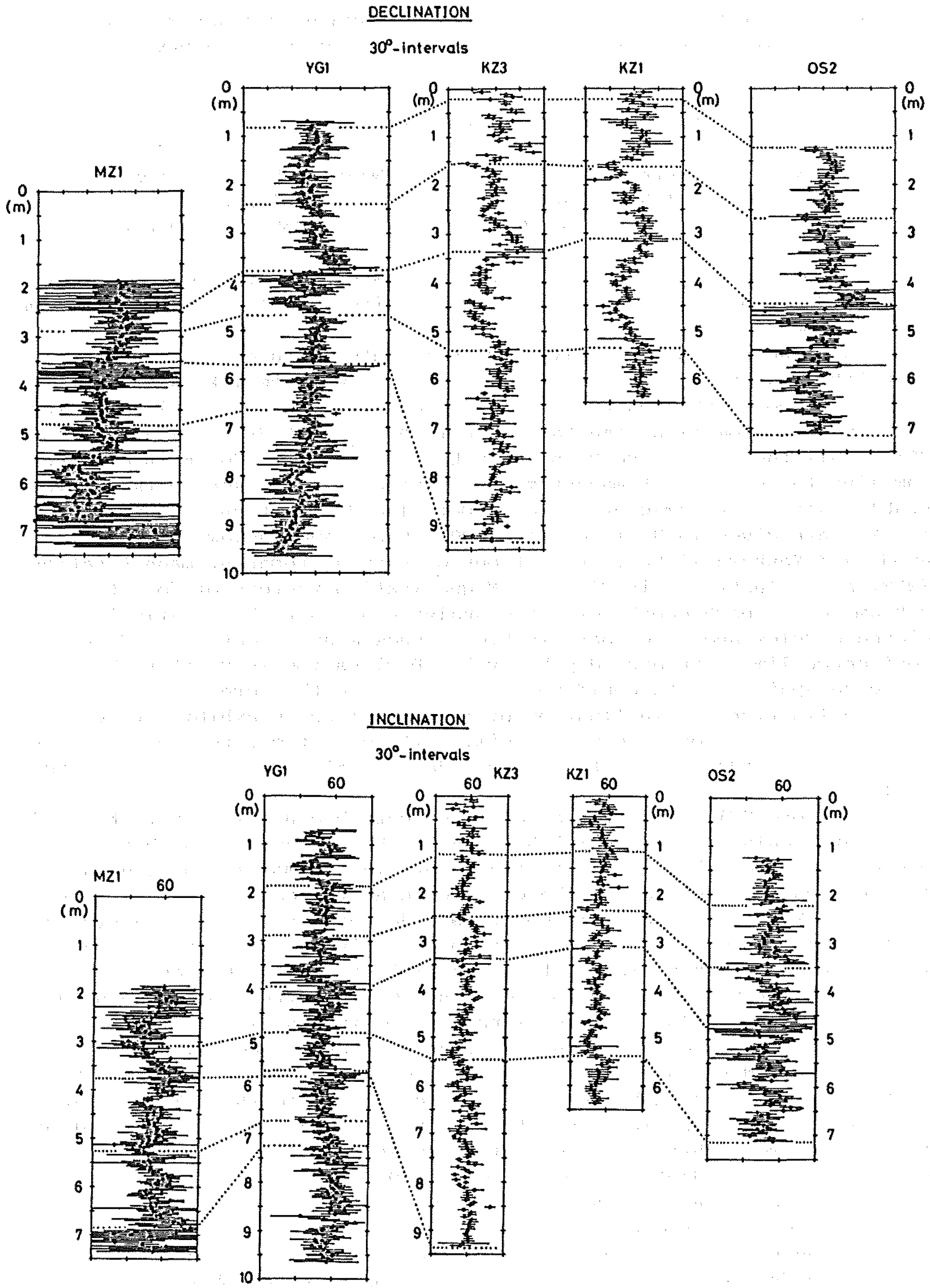

Fig.1 Declination and inclination logs plotted on depth scale ; MZ1 from Mizushima Nada, the Inland Sea ; YG1 from lake Yogo ; KZ3 and KZ1 from lake Kizaki ; OS2 from Osaka Bay. Closed circle represents horizon mean. Error bar shows α_{95} confidence limit. Some major common features of variation are tied by dotted line.

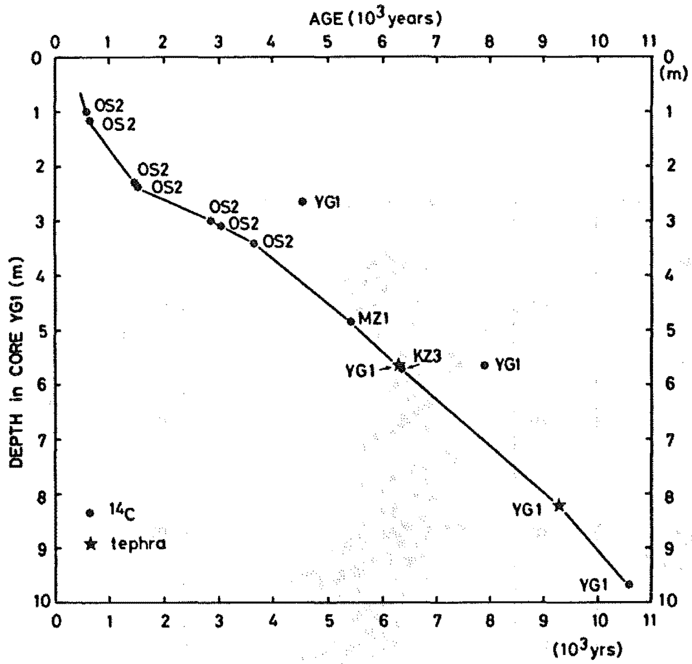

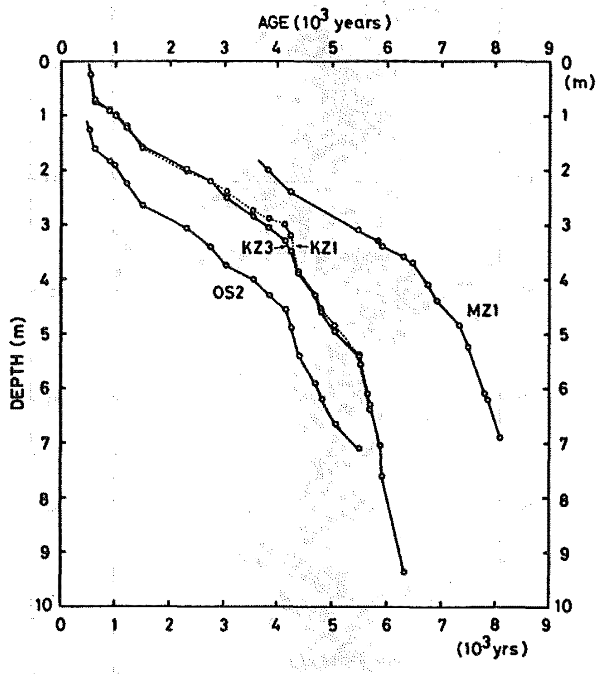

Fig.2 Depth-age relation of core YG1. Ages in other cores are transformed to the depth scale of YG1 on the basis of fine correlation of declination and inclination. Two aberrant ages of YG1 are possibly due to old carbon effect.

Fig.3 Depth-age relation of individual cores. Open circles show tie points of common features dated by the depth-age relation in Fig.2.

Depth-age relation of YG1 was determined with twelve ages as drawn by solid line in Fig.2, eliminating the aberrant ages in YG1. The twenty nine tie points were dated by a linear interpolation between the age data points. The top section above the top ^{14}C-age was dated with the trend of the adjacent section. The ages of the tie points were reduced to the depth scale of individual cores (Fig.3).

Reference frame of each core is adjusted before stacking for better fitting of magnetization direction. First, tilt correction is made. Average of inclinations from 500 to 5100 yrBP is calculated for cores YG1,

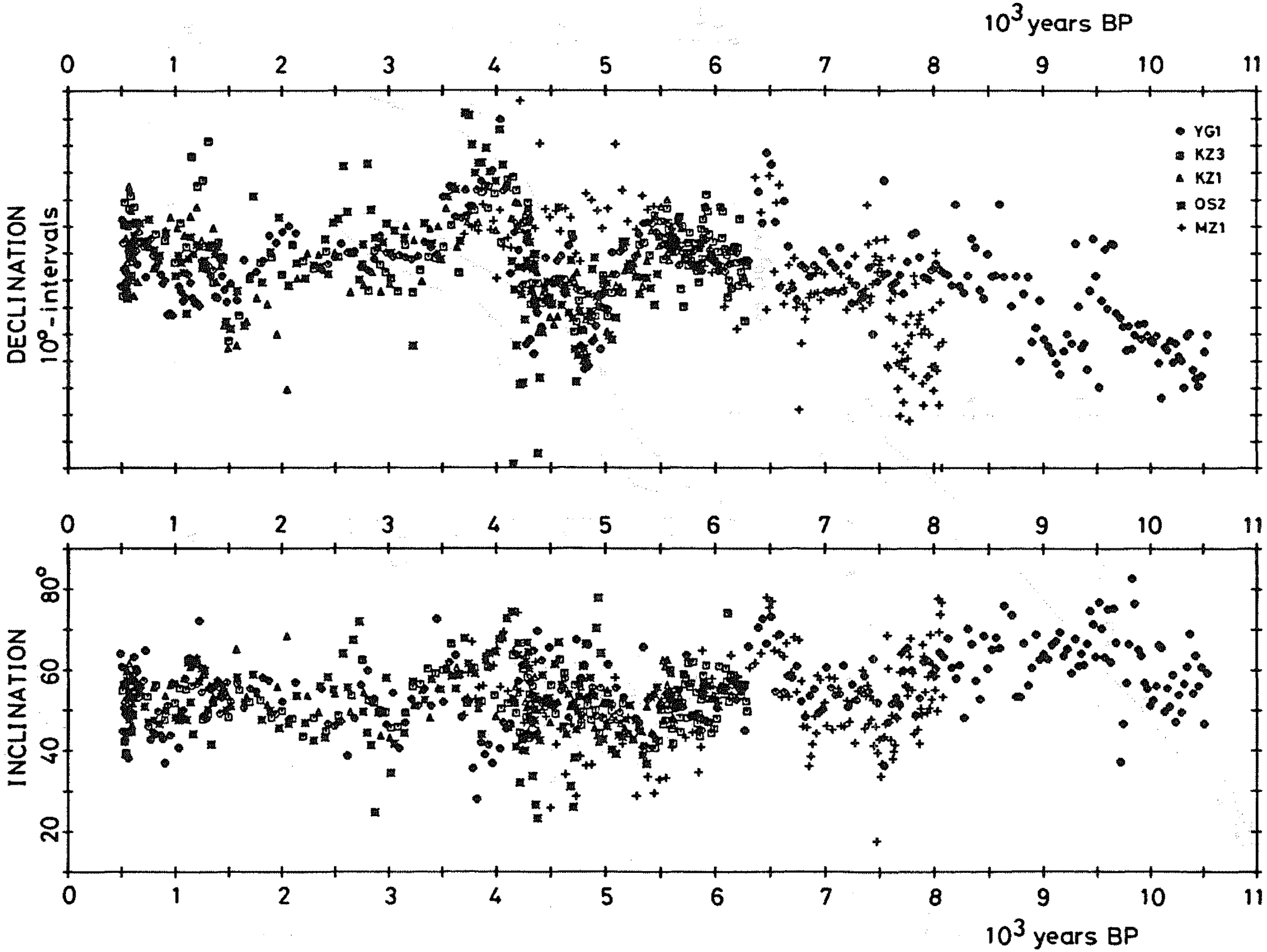

Fig.4 Horizon mean magnetization direction of overall cores plotted on a time scale.

KZ3, KZ1 and OS2. The time span is determined by that of OS2, the shortest one. The average of the core average inclinations is 53.8°. Frame of a core was rotated in a plane including its vertical axis and mean declination so as to adjust the core average to 53.8°. The frame of MZ1 was adjusted fitting the inclination to that of YG1. As a result, angles of tilt correction are +3.9°, -5.1°, +0.2°, +0.9° and -12.9° for YG1, KZ3, KZ1, OS2 and MZ1, respectively. The frame of core MZ1 in Fig.1 is already rotated by -12.7° to correlated with an other standard curve (Hyodo and Yaskawa, 1986). Next, the frame of KZ3, KZ1, OS2 and MZ1 were rotated in the new horizontal plane to minimize the sum of the squres of declination difference between YG1 and other cores.

Horizon mean magnetization directions of overall cores are plotted on a time scale obtained above (Fig.4). The data of the basal interval of 50 cm in core MZ1 were removed. The portion is considered to be an old sediment before the Holocene transgression (Hyodo and Yaskawa, 1986). The stacked declination and inclination magnetograms still exhibit oscillation of fairly high amplitude.

Results of stacking paleomagnetic data from small cores of lacustrine deposits has been obtained from North America (Creer and Tucholka, 1982), Australia (Barton and McElhinny, 1981) and Argentine (Creer et al., 1983). Superiority of our result is as follows. (a) Our core samples spread over four sedimentary basins of quite different depositional environment. (b) We consistently treated our data as a vectorial change of the geomagnetic field not as a scalar change of declination and inclination.

Geomagnetic secular variation for 500 - 10500 yrBP is mainly characterized by (i) high amplitude fluctuations from 3500 to 6500 yrBP, (ii) a long term linear trend before 6500 yrBP.

References

Arai, F., T. Oba, H. Kitazawa, Y. Horibe and H. Machida (1981) The Quaternary Research, 20, 209.

Arai, F. (1981) Personal communication.

Barton, C.E. and M.W. McElhinny (1981) Geophys. J. R. astr. Soc., 67, 465.

Creer, K.M. and P. Tucholka (1982) Canadian Journal of Earth Sciences, 19, 1106.

Creer, K.M., D.A. Valencio, A.M. Sinito, P. Tucholka and J.F.A. Vilas (1983) Geophys. J. R. astr. Soc., 74, 199.

Mothersill, J.S. (1979) Canadian Journal of Earth Sciences, 16, 1016.

Horie, M., K. Yaskawa, A. Yamamoto, T. Yakoyama and M. Hyodo (1980) Arch. Hydrobiol., 89, 407.

Hyodo, M. and K. Yaskawa (1980) J. Geomag. Geoelecr., 32, 581.

Hyodo, M. and K. Yaskawa (1986) Geophys. J. R. astr. Soc. (in press).

(To be submitted to Nature)

PALEOMAGNETISM OF A SEDIMENT CORE COLLECTED FROM HARDING LAKE IN INTERIOR ALASKA, USA

Hayao MORINAGA[1], Kazuko S. MORINAGA[2*], Katsumi YASKAWA[2]

1. The Graduate School of Science and Technology, Kobe University, Rokkodai-cho, Kobe 657, Japan
2. Faculty of Science, Kobe University, Rokkodai-cho, Kobe 657, Japan
* Present Adress: Motoyama Junior High School, Okamoto, Kobe 658, Japan

1. Introduction

Many paleomagnetic studies of various sediments have been carried out with the aim of investigating the fine scale behavior of the geomagnetic field and the possible relation between paleomagnetic parameters and paleoclimatic indicators (Verosub, 1977). Some studies have found out certain magnetic "excursions" mainly in sedimentary cores and in igneous rocks (Verosub and Banerjee, 1977). If these excursions are a true behavior of the geomagnetic field, they would have application as high-resolution chronostratigraphic marker horizons and would provide an opportunity to test models of the geomagnetic field behavior (Verosub and Banerjee, 1977; Hoffman, 1981; Negrini et al., 1984).

Referring to facies, granulometric features, pollen zones and ^{14}C ages reported, and climatic changes inferred by Nakao and Ager (1985), we report here on paleomagnetic investigation of a core of lacustrine sediments collected from Harding Lake in Interior Alaska. We discuss particularly on implications of intensity change of natural remanent magnetization (NRM) concerning climatic change and anomalous NRM directions in the sediment core, which seem to be possible excursions.

2. Geological setting and core sample

Lake Harding is situated on the Interior Alaska, which lies between the Brooks Range to the north and the Alaska Range to the south, at latitude 64° 25'N and longitude 146° 50'W. Most of areas around this lake were unglaciated even during the most severe climatic changes in the Quaternary Period. Of course, the high mountain areas of both Ranges were extensively glaciated several times during the Quaternary. Even now, some small ice sheets are seen in the winter time (Yokoyama and Tanoue, 1980). This lake is closed lake with none of outlet and inlet rivers. Its morphometric features are; 9.88 Km^2 in area, 43 m in maximum depth and 16 m in mean depth, the lake surface being 217 m above sea level.

Core sample was collected at a site HD-1 of the Harding Lake covered with ice 80 cm in thickness in March 1979 (Nakao et al., 1980). The site HD-1 was at the deepest point of this lake, 42.3 m in water depth from the ice surface. The Core sample was 65.9 mm in diameter and 6.59 m in length.

Facies, results of granulometric analysis and pollen records through this core have been offered by Nakao et al. (1980). Climatic changes and vegetational history inferred from pollen records and ^{14}C ages of six horizons in this core also have been presented by Nakao and Ager (1985). The granulometric features, the ^{14}C ages, the climatic changes and the pollen zones (the vegetational features) are shown in Fig.1. Also, variation of the NRM intensity is shown in this figure for later discussions. The curve is drawn with five-point moving averages.

Nakao et al. (1980) have recognized from vertical changes in the

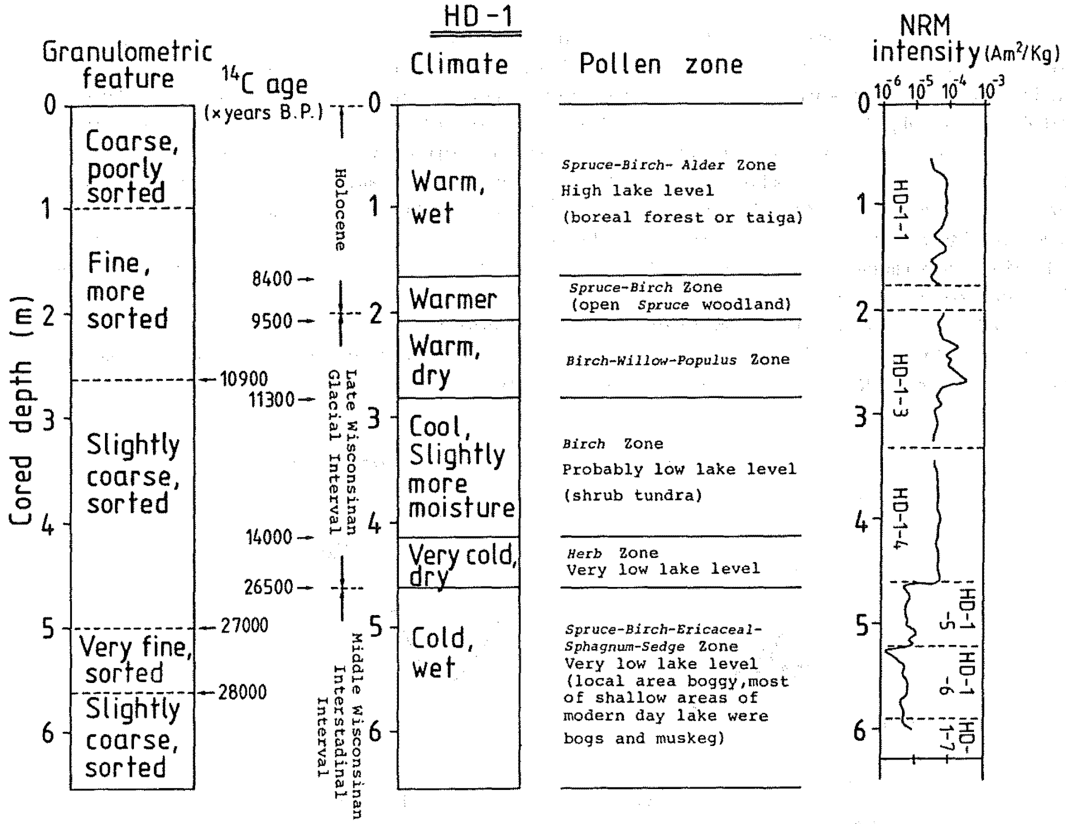

Fig.1 Granulometric features, climatic changes, pollen zones (vegetational features) after Nakao and Ager (1985), and NRM intensity change throughout HD-1 core since about 30,000 years B. P..

facies that lacustrine sediments had been present through this core. They have detected from the granulometric analysis that the mean diameter slightly decreases above the depth of about 2.7 m (age; 10,900 years B. P.), and suddenly changes into coarser and more variable above the depth of 1.0 m. They have described that the slight decrease in the mean diameter showed the beginning of rapid rise in the lake level and have analogized from this decrease that a catastrophic epoch had taken place about 11,000 years B. P. at the beginning of the regression of Last Glaciation. It has been expected from the sudden change of the mean diameter at the depth of 1.0 m that the wet climate had lasted from 5,000 to 2,500 years B. P. in contrast with the preceding age when the climate was slightly dry, making sediments fine and sorted (Nakao and Ager, 1985).

The ^{14}C age at the depth near 5.4 m is 15,900±1,300 years B. P.. This ^{14}C age is anomalously younger than those at the shallower depth level. This younger age came about from contamination of the deepest horizon due to the inflow of groundwater (Nakao and Ager, 1985).

Taking into consideration of the ^{14}C ages, sedimentation rate during Late Wisconsinan Glacial maximum from 26,500 years B. P. to 14,000 years B. P. is lower of 3.9 cm/kyrs than that during other periods (20 to 55 cm/kyrs).

3. Magnetic measurements and results

Core HD-1 consists of seven slugs 0.6 to 1.3 m long which were separately collected. Individual slugs were not oriented with respect to azimuth. Paleomagnetic specimens were continuously cut from six slugs (HD1-1, 3, 4, 5, 6 and 7), excluding a slug HD1-2, to 366 cube specimens in a 1×1×1 cm^3 cube with a knife; only twelve specimens were extracted from the upper part of a slug HD1-7, 66 cm long. A nominal time resolution of each specimen, on the basis of the ^{14}C ages (Nakao and Ager, 1985), is averagely about 30 years during other periods excluding Late Wisconsinan Glacial maximum period, when the nominal time resolution of each specimen is averagely about 250 years.

All specimens were measured on a cryogenic magnetometer whose sensitivity is 10^{-11} Am^2 (10^{-8} emu). The NRM intensities range from 10^{-6} to 5×10^{-4} Am^2/Kg. As a test of the stability and reliability of the

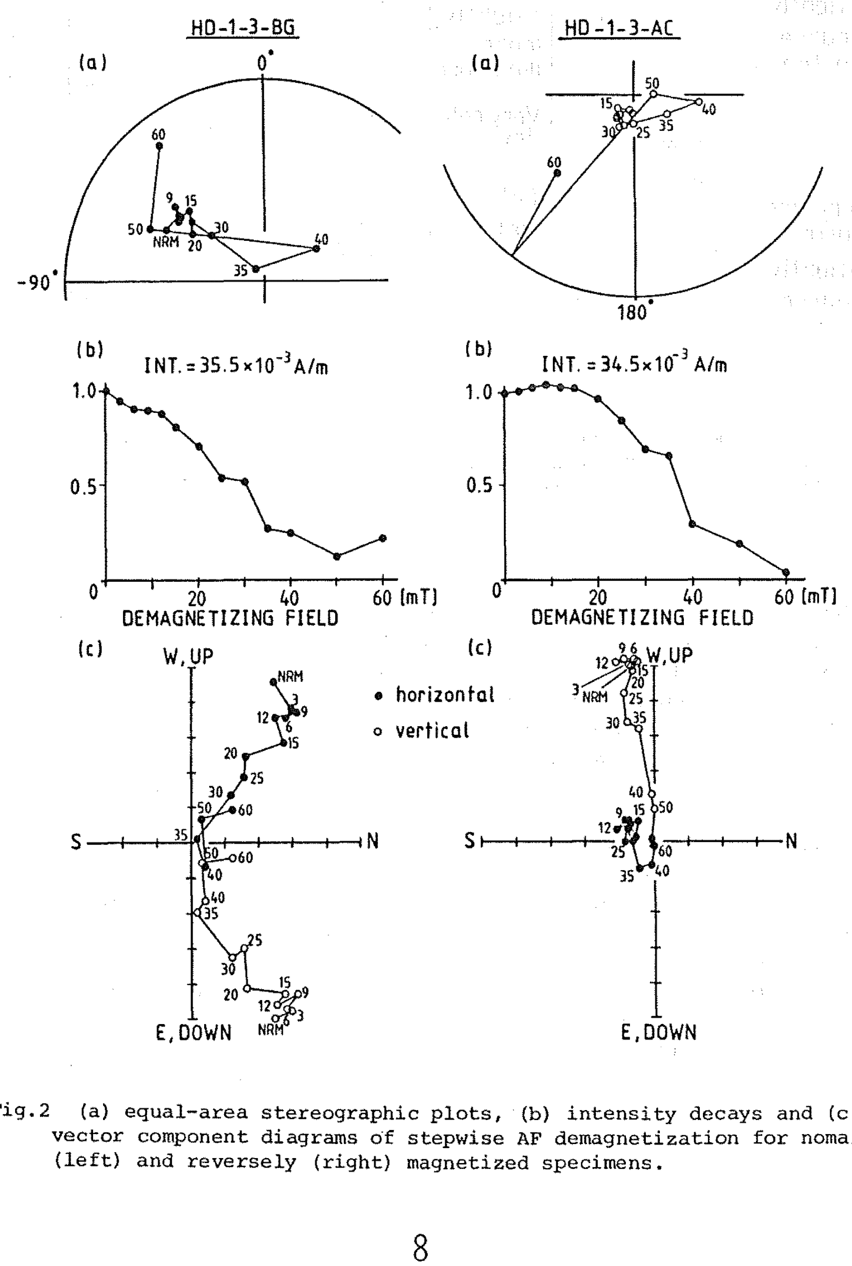

Fig.2 (a) equal-area stereographic plots, (b) intensity decays and (c) vector component diagrams of stepwise AF demagnetization for nomally (left) and reversely (right) magnetized specimens.

remanence, eleven pilot specimens were subjected to routine stepwise alternating-field (AF) demagnetization, in peak fields of 3, 6, 9, 12, 15, 20, 25, 30, 35, 40, 50 and 60 mT. Nine of eleven pilot specimens were normally magnetized and the rest was reversely magnetized. These stepwise AF demagnetizations indicated that these specimens possessed strong and stable remanences with median destructive field ranging from 20 to 40 mT and their direction scarcely changed against the AF level up to 30 mT (Fig.2). Thus, the NRMs before the AF demagnetization were sufficient to discuss large-scale fluctuations in their intensity and direction, although the declination was fairly variable because of the steep inclination (Fig.2-right). The declination, inclination and intensity of the NRM are shown in Fig.3. These curves are drawn with their five-point moving averages.

As stated above, the individual slugs were not azimuthally oriented, so that it is only possible to determine the relative declination of specimens within a given slug. In Fig.3, the declinations were reset so as to agree the average value of all specimens excluding those of relatively low and reversed inclinations, with 0°; no correlation in declination is implied from slug to slug.

4. Discussions and conclusions

(1) NRM intensity change

Variation in the NRM intensity throughout the core sample may imply the past climatic change in the area around the Harding Lake. The NRM intensity variation of sediments is mainly affected with change in two parameters; (a) intensity of the geomagnetic field in which the NRM was fixed, and (b) natures of sediments and magnetic particles which carried the NRM (e.g. quantity ratio of the magnetic particles to the nonmagnetic particles, and their size and sort). Three sudden changes in the NRM intensity, which occur near the depth levels of 2.7 m, 4.6 m and 5.2 m (Figs.1 and 3), are caused by that in the latter parameter (b) rather than the former one (a). Because (i) intensity of saturation isothermal remanent magnetization, which was measured for some discontinuous specimens, shows a similar variation to that of the NRM, supporting that

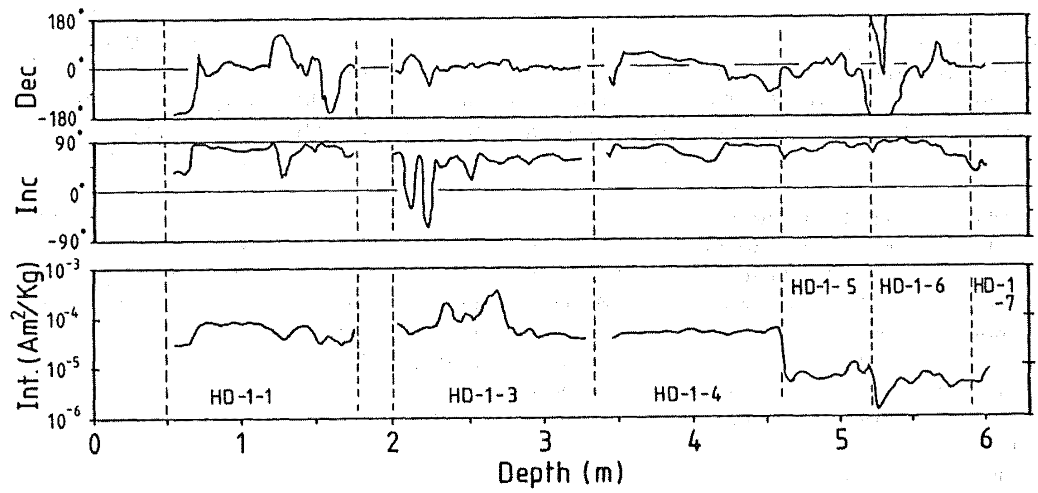

Fig.3 Declination, inclination and intensity of NRM throughout HD-1 core.

the variation of the NRM intensity mainly depends on quantity change of the magnetic constituents in the lake sediments, (ii) the mean diameter also changes near the same levels as the NRM intensity (Fig.1) and (iii) the facies also alter variously near the depth levels of 4.6 m and 5.2 m. At the high latitude such as interior Alaska, the nature of sediments can alter with change in quantity of melt water of glacier which carries constituents of sediments and with change in passage of its supply. These changes are accompanied with volume change of ice sheet, which is induced by climatic change. Thus, the sudden changes in the NRM intensity have a good possibility of finding out catastrophic timings of the past climate.

Pollen record (Fig.1) is an indicator of the past climatic change. There are four boundaries at the depth levels of 1.65 m, 2.05 m, 2.80 m, 4.15 m and 4.60 m in a record of this core. A boundary between "*Spruce-Birch* Zone" and "*Birch-Willow-Populus* Zone" (2.05 m; 9,500 years B. P.) corresponds to that between Holocene and Late Wisconsinan Glacial Interval. It is known from granulometric analyses that the lake level have started to rise around the depth level of a boundary between "*Birch-Willow-Populus* Zone" and "*Birch* Zone" (2.80 m; 11,300 years B. P.) (Nakao et al., 1980). The NRM intensity suddenly changes at almost the same depth level of this boundary and relatively fluctuates in shallower range above this depth level, suggesting a subsequent gradual rise in the lake level. A boundary between "*Herb* Zone" and "*Spruce-Birch-Ericaceal-Sphagnum-Sedge* Zone" (4.60 m; 26,500 years B. P.) corresponds to that between Late Wisconsinan Glacial Interval and Middle Wisconsinan Interstadial Interval. Also around the depth level of this boundary, the NRM intensity suddenly changes. Thus, a sudden change in the NRM intensity apparently offers information of a transition point in the past climate. It seems to be probable that a sudden falling of the NRM intensity around the depth level of 5.20 m would suggest a transition period in the past climate.

(2) Anomalous NRM directions

In the case of sediments from Harding Lake, it is capable to find out short-period (<100 yrs) excursions such as possible excursions, "Starno event" (Nøel and Tarling, 1975) and "Gothenburg flip" (Morner, 1977; Morner and Lanser, 1974 and 1975), because the nominal time resolution of one specimen is averagely about 30 years during other periods excluding Late Wisconsinan Glacial maximum period.

Three declination swings with lower or reversed inclinations occur around the depth levels of 0.6, 1.3 and 2.2 m (Fig.3), which correspond to ages of about 3,000, 6,600 and 10,000 years B. P., respectively. These ages are determined by interpolation of the ^{14}C ages at six horizons, so that they may rather differ from the true ages. In addition, these ages must be slightly old to be considered as the ages of the declination swings, because the NRM is acquired after deposition of sediments (Verosub, 1977).

The declination swing with low inclination at 0.6 m (age; about 3,000 years B. P.) may correspond to a proposed "Starno" event (Nøel and Tarling, 1975). Nøel and Tarling (1975) have inferred the event from a 30° shallowing in the inclination of demagnetized post-glacial sediments from Blekinge in southern Sweden. Age of the event, 2,800 years B. P., corresponds to that of a possible excursion which has been suggested by Ransom (1973) on the basis of archeomagnetic data from Italy and Greece. This swing, however, might be only apparent, because it occurs in coarse, poorly sorted and loose clay zone from 0.50 to 0.56 m.

The declination swing with low inclination and partly with reversed inclination at 1.3 m (age; about 6,600 years B. P.) can not be found out by any other paleomagnetic investigations (Jacobs, 1984). This swing occurs in fine, more sorted and laminated clay zone from 1.26 to 1.80 m. This swing seems to indicate a true geomagnetic behavior and to be considered as a new possible excursion dated about 6,600 years B. P., because no post-depositional slumping was found out in this clay zone (Nakao and Ager, 1985). Two declination swings accompanying with reversed inclination swings occurs in the depth range from 2.1 m to 2.3 m (age range; about 9,800 to 10,600 years B. P.). These swings occurs in fine, more sorted and laminated silt zone from 2.00 to 2.92 m. They seems to indicate the true geomagnetic behavior, because no post-depositional slumping was found out in this silt zone. Either or both of them can correspond to a proposed excursion "Gothenburg flip" dated at 12,350 years B. P. (Morner and Lanser, 1974) and a possible excursion dated around 12,000 years B. P. (Nøel and Tarling, 1975), although the ages of the swings are younger than those of the reported excursions and the period for a set of the swings (800 yrs) is about eight times as long as that of the reported excursions (<100 yrs). Because, no swing but these swings occurs in the depth range from 2.0 to 4.1 m (age range; about 9,500 to 14,000 years B. P.). The swings, however, might be considered as a new possible excursion or as a set of new possible excursions.

Many excursions have been reported from studies of sediments and igneous rocks in the period ranging from 14,000 to 26,500 years B. P. (Jacobs, 1984); e.g., Laschamp (e.g., Bonhommet and Zahringer, 1969), Mono lake (e.g., Denham and Cox, 1971), Gulf of Mexico (e.g., Clarke and Kennett, 1973) and Lake Biwa (Nakajima et al., 1973). All of them were not able to be recognized in this core in the identical period. This is due to poor time resolution of one specimen (250 years).

References

Bonhommet, N. and J. Zahringer (1969) Earth Planet. Sci. Lett., 6, 43.

Clarke, H. C. and J. P. Kennett (1973) Earth Planet. Sci. Lett., 19, 267.

Denham, C. R. and A. Cox (1971) Earth Planet. Sci. Lett., 13, 181.

Hoffman, K. A. (1981) Nature, 294, 67.

Jacobs, J. A. (1984) Reversals of the Earth's magnetic field, 1st ed. (Adam Hilger Ltd., Bristol), 86.

Morner, N.-A. (1977) Quat. Res., 7, 413.

Morner, N.-A. and J. P. Lanser (1974) Nature, 251, 408.

Morner, N.-A. and J. Lanser (1975) Earth Planet. Sci. Lett., 26, 121.

Nakajima, T., K. Yaskawa, N. Natsuhara, N. Kawai, and S. Horie (1973) Nature Phys. Sci., 244, 8.

Nakao, K. and T. A. Ager (1985) Hydrological Regime and Climatic Changes in the Arctic Circle, edited by K. Nakao, (Hokkaido University, Sapporo), 43

Nakao, K., J. Laperriere, and T. A. Ager (1980) Climatic Changes in the Interior Alaska, edited by K. Nakao, (Hokkaido University, Sapporo), 16.

Negrini, R. M., J. O. Davis, and K. L. Verosub (1984) Geology, 12, 643.

Nøel, M. and D. H. Tarling (1975) Nature, 253, 705.

Ransom, C. J. (1973) Nature, 242, 518.

Verosub, K. L. (1977) Rev. Geophys. Space Phys., 15, 129.

Verosub, K. L. and S. K. Banerjee (1977) Rev. Geophys. Space Phys., 15, 145.

Yokoyama, T. and R. Tanoue (1980) Climatic Changes in the Interior Alaska, edited by K. Nakao, (Hokkaido University, Sapporo), 45.

(To be submitted to J. Geomag. Geoelectr.)

VARIATION OF THE GEOMAGNETIC INTENSITY DEDUCED FROM ARCHEOLOGICAL OBJECTS IN JAPAN

Hideo SAKAI and Kimio HIROOKA

Department of Earth Sciences, Faculty of Science, Toyama University, Toyama 930, Japan

Introduction

Paleointensity for archeological periods in Japan was first studied by Nagata et al. in 1963. About 200 pieces of data were so far obtained by several researchers such as Sasajima and Maenaka (1966), Kono (1969), Kitazawa (1970), Domen(1977) and Tanaka (1982). Several features of the paleointensity such as the sinusoidal variation with time were discussed in their study. However, their findings do not agree with one another in some time periods. As a whole, the paleointensity data in Japan for archeological ages seems to be inadequate. In this study, over 300 archeological samples were submitted to the paleointensity studies. Conventional Thellier's double heating method(Thellier and Thellier; 1959, Coe; 1967) is mainly used for analysis. Natural remanent magnetization (nrm) of some altered or weathered samples contain the remanent magnetization called chemical remanent magnetization (crm). Estimation of the geomagnetic intensity from crm is difficult and crm causes the error in intensity studies. For the crm bearing samples, modification of the method is deviced and applied in order to enhance the efficiency of measurements.

From the analysis, 172 paleointensity data were newly obtained. The time periods involved are from 5,000 years B.C. to 1,800 A.D.

Samples and ages

The samples used in this study are archeological objects such as potsherds, ceramics, roof tiles, kiln walls and so on. Localities of sample excavated are shown in Fig. 1.

As for the ages of these samples, we accepted the dates determined by several researchers. These dates were obtained by the radiocarbon method, the thermoluminescence method (Ichikawa, 1980) and the archeological evidences (Hirooka, 1967;Shibuya, 1980).

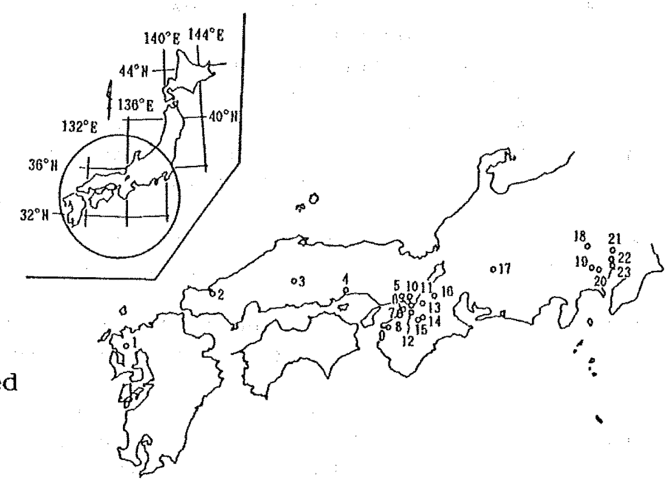

Fig. 1.
A map showing distribution of the localities from which samples were collected; corresponding sites to each number are as follows.
1.Ureshino C., 2.Hagi C., 3.Tojo T., 4.Bizen T., 5.Suita C., 6.Osaka C., 7.Sakai C., 8.Izumi C., 9.Wakayama C., 10.Takatsuki C., 11.Yao C., 12.Domyoji T., 13.Nara C., 14.Sakurai C., 15.Asuka V., 16.Shigaraki T., 17.Toki C., 18.Fukaya C., 19.Hachioji C., 20.Inagi C., 21.Showa T., 22.Kawaguchi C., 23.Bunkyo W.
C:City, T:Town, W:Ward, V:Village.

As the ages of Jomon type potteris, radiocarbon ages and TL ages are referred. Radiocarbon ages of the Jomon potteries are the mean values of many reported dates of the same type potteries(Keally and Muto, 1982). Some ages are those communicated by the archeologists. Dates for the potteries of Yayoi period are referred from Tanabe and Sahara(1961) and Uno(1985) Ages , collected sites and materials of the sample are summarized in Table 1.

Thellier's method

The conventional double heating Thellier's method is used for analyses. The method consists of two stages of heating process. The sample was first heated and cooled in zero field, and the remanence measured. Then the process was held in the laboratory field. The sequence was repeated for various temperatures up to the Curie temperature. Heating of the sample was mainly in a nitrogen atmosphere. Some samples were heated in air. Shielding of the magnetic field was provided by the Helmholz coils and mu-metal box, so that the magnetic field at the heating position could be shielded near to 50 nT(equivalent to approximately 1/900 of the geomagnetic field in the laboratory). Measurements of the residual magnetization were mostly carried out with an astatic magnetometer of Osaka University. Some were undertaken by the Shonstedt spinner magnetometer of Toyama University.

Analysis of the data is made by the familiar diagrams such as in Fig 2., where natural remanent magnetization, nrm, and its thermally demagnetized component is seen on the ordinate and the thermoremanent magnetization, trm, acquired in the laboratory is shown on the abscissa. The intensity of each remanence was normalized by that of the nrm before demagnetization. The examples of the successful results are shown in Fig. 2. From here on, we refer to this diagram as the nrm-trm diagram.

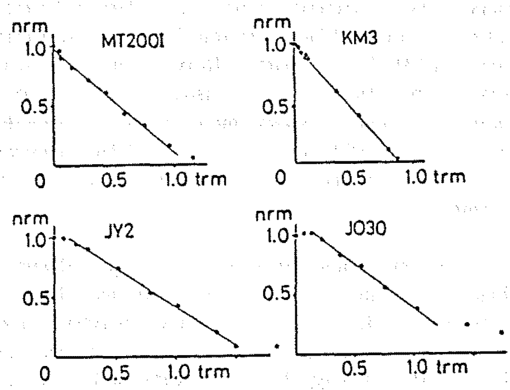

Fig. 2.
Some typical examples of Thellier's experiments; successful results.

Deviation of the plots from the linear line in nrm-trm diagram

It has been sometimes observed that the some plots of the lower and/or higher temperature region deviate from the linear line of the data of intermediate temperature range. Deviation occurred in the plots of higher temperature range might be the effects of thermo-chemical remanent magnetization caused by the oxidation process(Nagata and Kobayashi, 1963). Deviation of the plots in the lower temperature region is considered to be originated by several causes. The reheating effect of the sample is one of the cause. This effect was discussed in Kitazawa and Kobayashi(1968), Barbetti(1976) and Sakai(1978).

In some samples, the plots of the lower temperature region are on the line of very steepned slope in nrm-trm diagram as shown in Fig. 3. The figure shows the result of potsherd of 14th century. Its trm component is very weak compared with the demagnetized nrm component in the low temperature region. It is also clear, as shown on the Schmidt's equal area projection in the figure, that the remanent vector changed its direction by thermal demagnetization. Directional change of the vector is almost along the large circle of the projection. These features may occur when the sample has the secondary remanence in addition to the original one.

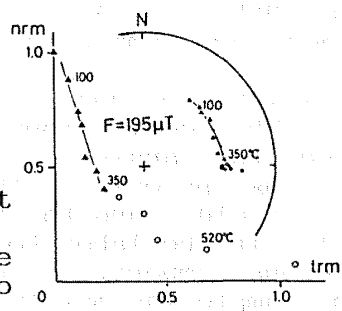

Fig. 3.
Nrm-trm diagram for the sample SG23; Directional change of the nrm vector during thermal demagnetization is also shown on the equal-area projection net.

In the case of this sample, the estimated paleointensity from the steepened slope is over 200 μT which is unconceivable value as the geomagnetic field intensity of 14th century. We conceive therefore that the remagnetized component is overprinted and it is no longer of trm origin. As such a strong secondary component, chemical remanence is conceivable. The chemical remanence, so-called crm may be acquired in the alteration process of magnetic minerals in the sample. Several researchers such as Collinson(1967) and Roy and Park(1974) showed that chemical cleaning method is useful for removing the secondary crm component in sedimentary rocks. This method seems particularly effective for the porous sample. The potsherd of Fig 3. is porous and chemical cleaning method is submitted to this sample.

Thellier's method modified by chemical cleaning

The chemical cleaning method is the method to dissolve and remove the secondary magnetized minerals by acid. For chemical cleaning, samples were cut into cubic in shape and 15mm in edge length. Hydrochloric acid of 20% concentration was used as the cleaning solvent. The procedure of the method is as follows. Soaking the sample in acid for several hours. Then take it out and wash it with water. Then the remanence is measured. The whole process was repeated. And when the change in magnetization becomes negligible small, the experiments stopped. Fig. 4 shows the example of chemical cleaning. Here, the abscissa axis shows the cleaning time. The intensity of the remanence gradually decreases. After cleaning of about 18 hours, it reaches about 1/4 of the pre-cleaned sample's intensity. The directional change of the magnetization resulting from the chemical cleaning is almost identical with the result of thermal cleaning. The sample applied the adequate cleaning is submitted to the Thellier's experiment.

The result of Thellier's experiments both on the chemically cleaned sample and that prior to cleaning are compared in Fig. 5. By chemical cleaning, remanence of low blocking temperature region is preferably removed and the steepened feature of the slope disappeaed. The directional change observed in the sample before cleaning also disappeared with the cleaned specimen. In the case of the chemically cleaned specimen, the linear relation was obtained by the temperature region up to the 520°C. The paleointensity obtained corresponds with the value of other samples from the same period(Table 1, Fig. 7). This shows the residual component after etching is the reliable and suitable trm for Thellier's method. The easily etched remanent component might be secondary component acquired by the chemically synthesis of magnetic minerals of sample. This method was submitted to the several samples. Many samples from the Jomon potteries Jomon were submitted to the chemical cleaning. In the practical magnetical cleaning by etching, however, the sample itself was often broken by the acid on the way of experimental process and intensity experiment cannot be continued any further. Two pieces of potsherd(SG23 and TM) were successfully applied this method so far. Thellier's method modified by chemical cleaning becomes more effective, when the porous but hard sample contains secondary component of crm origin.

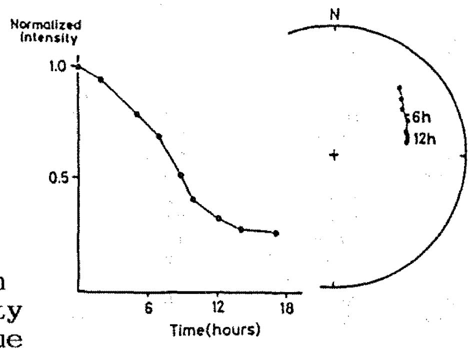

Fig. 4.
Change of nrm vector during chemical cleaning; Decrease of the intensity with time is shown in the left diagram and the directional change is shown in the net.

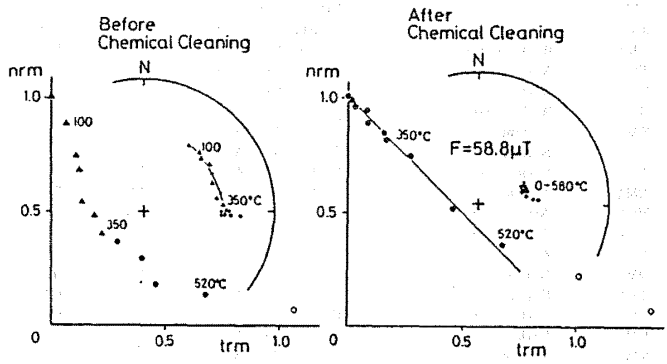

Fig. 5
Results of the Thellier's experiment of the sample SG23; the result of the pre-eched sample is shown in the left and the result of after chemical cleaning is in the right.

Reliability of the data

The reliability of the data obtained in this study was examined from the view of the following points.

1. The number of the data points satisfying the linear relation in a nrm-trm diagram; in the case that the number of the data in linear relation increases, the intensity data will be more reliable.

2. Degree of the deviation in the intensity obtained from the samples of the same or similar age; when the diviation is smaller, the results will be more reliable.

As seen in Fig. 2, fairly straight lines are displayed in nrm-trm diagram by the ceramic and potsherd samples of a few centuries A. D. However, the older samples such as Jomon potteries and Yayoi potteries sometimes show the deviation of the plots from the linear line in the nrm-trm diagram. When

Table 1. Resuts of present study

Sample	Locality	Age	Method	Sample type	N	F (μ Tesula)	Ref
JO4	Kawaguchi C.	5100 ± 300 B.C.	AR, C14	PSJ	2	37.3 ± 2.0	1
JK1	Inagi C.	3900 ± 300 B.C.	AR, C14	PSJ	2	39.8 ± 3.0	1
JY1	Tojo T.	3850 ± 115 B.C	TL	PSJ	3	33.6 ± 2.2	2
JK2	Bunkyo W.	3200 ± 500 B.C.	AR, C14	PSJ	3	31.7 ± 2.6	1
JO14	Hachioji C.	3000 ± 200 B.C.	AR, C14	PSJ	2	43.2 ± 4.5	1
JO17	Bunkyo W.	2840 ± 400 B.C	AR, C14	PSJ	3	40.0 ± 4.5	1
JY2	Tojo T.	2710 ± 210 B.C.	TL	PSJ	2	38.3 ± 1.7	2
JY3	Tojo T.	2350 ± 130 B.C.	TL	PSJ	3	44.1 ± 3.2	2
JS1	Fukaya C.	2200 ± 200 B.C.	AR, C14	PSJ	4	58.0 ± 3.8	1
JO23	Hachioji C.	2140 ± 110 B.C.	AR, C14	PSJ	2	41.6 ± 2.3	1
JS2	Showa T .	1600 ± 200 B.C.	AR, C14	PSJ	2	37.3 ± 2.6	1
JO28	Kawaguchi C.	1200 ± 200 B.C.	AR, C14	PSJ	2	44.4 ± 3.0	1
JO30	Kawaguchi C.	1040 ± 130 B.C.	AR, C14	PSJ	5	55.7 ± 5.8	1
JN1	Asuka V.	650 ± 350 B.C.	AR	PSJ	3	53.8 ± 2.9	3
JY4	Tojo T.	230 ± 110 B.C.	TL	PSJ	3	56.7 ± 1.9	2
JM	Yao C.	2C-3C B.C.	AR	PSY	3	60.7 ± 1.9	4,5,6
KM1	Yao C.	0-1C B.C.	AR	PSY	3	62.3 ± 2.1	4,5,6
KM2	Yao C.	1C B.C.-1C A.D.	AR	PSY	2	57.7 ± 2.3	4,5,6
KF	Domyoji T.	2C A.D.	AR	PSY	3	61.6 ± 0.4	7
KM4	Yao C.	2C A.D.	AR	PSY	2	60.8 ± 3.4	4,5,6
YS1	Tojo T.	210 ± 45 A.D.	TL	PSY	3	59.8 ± 2.1	2
AM	Takatsuki C.	330 ± 35 A.D.	AR	PS	4	64.3 ± 3.7	8
MT84	Sakai C.	490 ± 10 A.D.	AR	CM	2	62.6 ± 2.8	8
WT	Wakayama C.	5C-6C A.D.	AR	TE	3	64.0 ± 3.5	7
SR4-II	Wakayama C.	525 ± 25 A.D.	AR	BE	2	61.4 ± 4.0	9
TM	Nara C.	6C A.D.	AR	CM	3	65.2 ± 3.1	7
NT1	Nara C.	6C A.D.	AR	CM	3	67.3 ± 5.2	7
SR3	Wakayama	585 ± 15 A.D.	AR	KW	3	63.2 ± 3.5	9
KM3	Izumi C.	610 ± 10 A.D.	AR	CM	3	67.8 ± 3.0	8
TG41I	Sakai C.	630 ± 10 A.D.	AR	KW	3	56.3 ± 3.8	9
TH	Sakurai C.	Late 7C A.D.	AR	TE	4	56.8 ± 3.5	7
NM1	Asuka V.	Late 7C A.D.	AR	TE	2	60.7 ± 2.0	7
NK2	Asuka V.	Late 7C A.D.	AR	TE	3	59.9 ± 1.9	7
NK4	Asuka V.	Late 7C A.D.	AR	TE	3	58.2 ± 4.2	7
NY	Asuka V.	Late 7C A.D.	AR	TE	4	62.5 ± 2.5	7
NM2	Suita C.	8C A.D.	AR	TE	3	57.2 ± 1.7	7
TK230	Sakai C.	8C A.D.	AR	CM	4	65.4 ± 1.9	8
TK57	Sakai C.	760 ± 10 A.D.	AR	CM	2	57.8 ± 2.1	8
KM38-II	Sakai C.	770 ± 10 A.D.	AR	CM	4	68.6 ± 2.3	8
KM22	Izumi C.	780 ± 10 A.D.	AR	CM	3	54.6 ± 2.3	8
Kishibe	Suita C.	790 ± 10 A.D.	AR	CM	3	60.7 ± 2.8	8
SR1	Wakayama C.	825 ± 25 A.D.	AR	CM	3	55.5 ± 1.7	9
MT200-I	Sakai C.	875 ± 25 A.D.	AR	CM	4	52.6 ± 2.0	8
TK314	Sakai C.	925 ± 25 A.D.	AR	CM	3	55.1 ± 3.7	8
NH3	Osaka C.	10-11C A.D.	AR	PS	3	51.7 ± 1.8	10
NH5	Osaka C.	Late 11C A.D.	AR	PS	3	49.4 ± 2.9	10
NH4	Osaka C.	12C A.D.	AR	PS	5	49.9 ± 2.0	10
NH1	Osaka C.	13C A.D.	AR	PS	4	50.1 ± 2.7	10
TK3	Sakai C.	13C A.D.	AR	TE	2	54.2 ± 1.6	11
IW	Asuka V.	13-14C A.D.	AR	PS	3	50.6 ± 2.9	7
BI3	Bizen T.	1330 ± 30 A.D.	AR	BE	4	52.1 ± 2.7	8
NH2	Osaka C.	14C A.D.	AR	PS	3	52.2 ± 2.2	10
MOZU	Sakai C.	1350 ± 50 A.D.	AR	PS	3	54.8 ± 2.4	8
SG23	Shigaraki T.	1350 ± 50 A.D.	AR	PS	2	56.4 ± 3.2	8
JR3	Toki C.	1550 ± 15 A.D.	AR	BE	3	46.2 ± 1.7	9
HA	Hagi C.	1670 ± 20 A.D.	AR	KD	3	48.7 ± 1.4	11
SU	Ureshino T.	1680 ± 30 A.D.	AR	KD	3	47.8 ± 1.9	12
KN	Toki C.	1760 ± 50 A.D.	AR	BE	3	47.0 ± 1.7	8

Definitions.

F: mean paleointensity and standard deviation.
N: number of samples.
Method: AR shows that the age is estimated by archeological evidence,
ARC14 denotes archeological evidence with C14 dating,
TL denotes thermoluminescence method.
Material: PS is the potsherd, PSJ represents the Jomon type pottery,
PSY is the Yayoi type pottery, TE is the rooftile, CM denotes the ceramics, BE is the baked earth, KT is the kiln wall,
KD is the kamadogu**.
** Kamadogu is the tool for setting the potteries in the kiln.
Ref. : References for age estimation.
1. Keally and Muto(1982) 2. Ichikawa(1980) 3. Ishino(1980)
4. Center of Osaka Cultual Properties(1982)
5. Tanabe and Sahara(1961) 6. Uno(1985) 7. Aboshi(1980)
8. Hirooka(1967) 9. Shibuya(1980)
10. Association of Osaka Cultural Properties(1982)
11. Nakamura(1980) 12. Kakimoto(1980) 13. Higashinakagawa(1980)
3,6,7,11,12 and 13 are the dates of personal communication.

Thellier's method was applied to the Jomon type potteries, over a half of the data were rejected in view of the point 1.

Variation of the geomagnetic field intensity in Japan

In this study, more than 300 samples were submitted to nrm-trm analysis. Several check points reffered above were taken to select reliable paleointensity data and we accepted 172 data in number as the paleointensity data. From the samples of the age after 0 A.D., paleointensities were efficiently obtained.

Table 1 gives the obtained paleointensities in this study.

In Fig. 6, all data in this study are summarized. The abscissa and the ordinate show the geomagnetic paleointnsity and the age respectively. Each plot of the data is the mean value of the each site. The present intensity of this studied area is ranging from 460-475 μT. The intensity from 5,000 B.C. to 1,000 B.C. was lower than the present value except for that around 2,000 B.C. The intensity seems to increase gradually in this period. Strong intensity around 2,000 B.C. is also denoted in the data of Sasajima(1966) and Tanaka(1982). The rate of increase in intensity rises after 1,000 B.C. Around 0 A.D., the intensity reaches about 1.3 times as strong as that of the present.

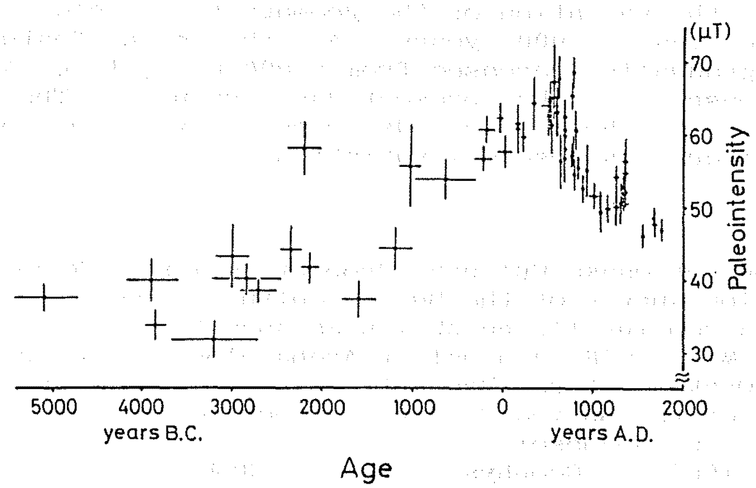

Fig.6
Variation of the geomagnetic field intensity obtained from this study.

The paleointensities for the last two thousand years are also shown in Fig. 7. Variation of the paleointensity of this period was formerly studied by Nagata et al. and Sasajima et al. in 1960's. Their data are shown in the same diagram. We can see a minimum at around 1,000 years A.D. A similar trend is also reported by Nagata et al(1963). The intensity peakes are shown around 600 A.D. and around 1,300 A.D. That of 600 A.D. is about 1.4 times as large as the present and that of 1,300 A.D. is about 1.2 times as large as the present. We can distinguish two trends in the variation of the paleointensity of this period. One is the monotonous decreasing trend from 0 A.D. to the present, and the other is the intensity fluctuation of a period of several hundred years interval.

Although the data before 0 A.D. is still inadequate, we can summarize that the paleo-intensity variation of the last 7,000 years shows the fluctuations of periods of several hundred years overlapping on the main longer variation of quasi-sinusoidal.

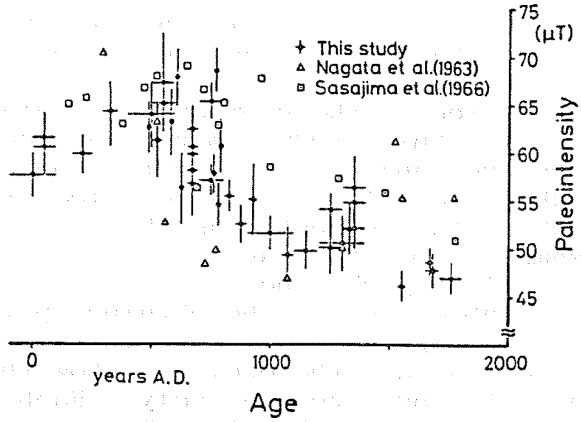

Fig.7
Variation of the geomagnetic field intensity after 0 A.D.; results of Nagata et al. and Sasajima and Maenaka are also shown.

Conclusion

The geomagnetic field intensities were determined by Thellier's method. The improved method by chemical cleaning was successfully applied to the samples whose remanent magnetization consists of trm and crm.

The study of the archeological objects of Japan elucidated the variation of the geomagnetic field intensity during the last 7,000 years. As the main feature, the intensity gradually increased from 5,000 B.C. to 0 A.D. and then decreased to the present-day value. The secular variation with shorter periods seems to exist superposed on the gradual quasi-sinusoidal variation.

References

Association of Osaka Cultural Properties (1982) Report on the excavation survey of the Buried Cultural Properties in Nagahara remains II, pp322 (in Japanese).

Barbetti, M. (1976) Journal of Archaeological Science 3, 137.

Center of Osaka Cultural Properties (1982) Report on the excavation survey of the Buried Cultural Properties in Kamei remains, pp 251 (in Japanese).

Coe, R.S. (1967) J. Geophys. Res., 72, 3247.

Collinson, D.W. (1967) Methods in Paleomagnetism, edited by D.W. Collinson, K.W. Creer and S.K. Runcorn ,Elsevier, Amsterdam, 306.

Domen, H. (1977) Phys. Earth Planet. Interiors, 13, 315.

Hirooka, K. (1967) Mem. Fac. Sci. Kyoto Univ., Ser.Geol. Mineral., 38, 167.

Ichikawa, Y. (1980) the Editorial Committee of Kobunkazai, edited by Natural Scientific Approaches in Archaeology and Art History. The Japan Society for the Promotion of Science, Tokyo, 3 (in Japanese).

Keally, C.T. and Y. Muto (1982) Research of Culture of Jomon Era 1, edited by S. Kato, T. Kobayashi and T. Fujimoto. Yuzankaku, Tokyo, 246.

Kitazawa, K. and K. Kobayashi (1968) J. Geomag. Geoelectr., 20,7.

Kitazawa, K. (1970) J. Geophys. Res., 75, 7403.

Kono, M. (1969) D.Sc. Thesis, Univ. Tokyo, Japan, pp.58.

Nagata, T., Y. Arai, and K. Momose (1963) J. Geophys. Res.,68,5277.
Nagata, T., K. Kobayashi (1963) Nature, 197, 476.
Roy, J.L. and J.K. Park (1974) Can. J. Earth Sci., 11, 437.
Sakai, H. (1978) SUEMURA III, Osaka Prefectural Board of Education, 156 (in Japanese).
Sasajima, S. and K. Maenaka (1966) Mem. Coll. Sci., Univ. Kyoto, Ser. B, 33, 53.
Shibuya, H. (1980) M.Sc Thesis, Univ. Osaka, Osaka, Japan, pp58.
Tanabe, S and M. Sahara. (1961) Archeology of Japan III - Yayoi Era, edited by S. Wajima et al., Kawade, Tokyo.
Tanaka, H. (1982) J. Geomag. Geoelectr., 34, 601.
Thellier, E. and O. Thellier (1959) Ann. Geophys., 15, 285.
Uno, T., personal communication (1985).

PALEOINTENSITIES OF THE GEOMAGNETIC FIELD OBTAINED FROM PRE-INCA POTSHERDS NEAR, CAJAMARCA, NORTHERN PERU

Masaru Kono[1], Naoko Ueno[2], and Yoshio Onuki[3]

1 Department of Applied Physics, Tokyo Institute of Technology, Ookayama 2-12-1, Meguro-ku, Tokyo 152
2 Department of Natural Sciences, Toyo University, Hakusan 5-28-20, Bunkyo-ku, Tokyo 112
3 Department of Cultural Anthoropology, University of Tokyo, Komaba 3-8-1, Meguro-ku, Tokyo 153

1. Introduction

Variation of the the geomagnetic paleointensities in the last few thousand years in Peru has already been studied by Nagata et al. (1965), Kitazawa and Kobayashi (1968), Games (1977), and Gunn and Murray (1980), but there appears a large scatter among the reported data. This discrepancy seems to be largely caused by inappropriate age assignments for the materials used in experiments. In archeologically well studied areas, the ages of the materials are cross-checked in many ways, but such is not the case in Peru and other places in South America.

C-14 ages of archeomagnetic samples (potsherds, bricks, etc.) from Peru were usually obtained from carbonized wood, etc., from the same horizon. However, it is not very uncommon that one excavation locality contains several different cultural levels, and mixtures of materials belonging to different stages are often found even in a same horizon. Even if C-14 ages were obtained for the materials in the same horizon, they may be not sufficient by themselves to give the ages of potsherds. Moreover, C-14 ages contain errors much larger than the statistical errors quoted as the uncertainties, because of the non-ideal effects such as leaching of elements, weathering, and so on. Therefore, some of the assigned C-14 ages may be erroneous and are not good time measures for the samples.

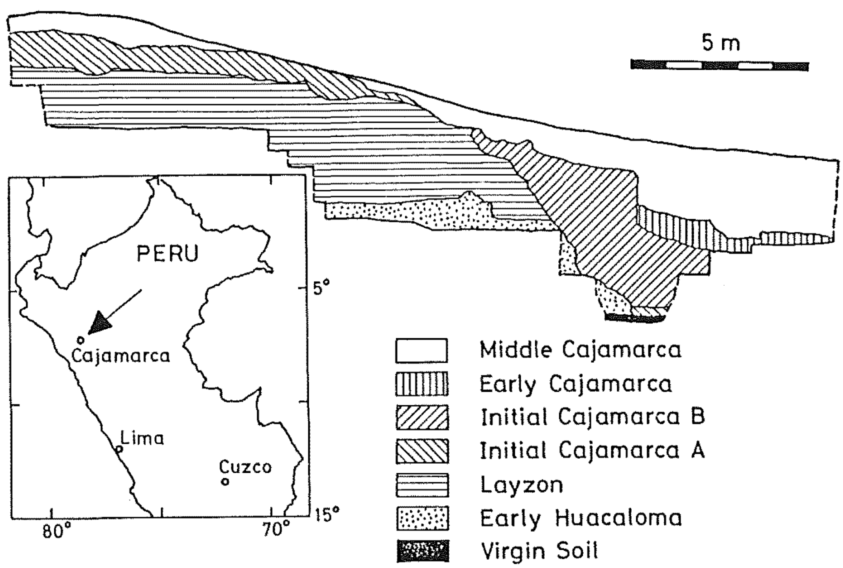

Fig. 1 Simplified chlonological section of Huacaloma excavation site, near Cajamarca. Inset shows the location of the site. (after Terada and Onuki, 1982).

To circumvent these difficulties, we used potsherds which have reasonably well determined ages. They are from Pre-Inca ruins of Cajamarca, northern Peru, where the Tokyo University Team has been continuing excavations for many years (Terada and Onuki, 1982, 1985). The location of the site and the vertical section of the layers in the excavated trench are shown in Fig. 1. This site contains several layers of different cultures in succession, for which ages were assigned by the Tokyo University Team in the following manner.

The stratigraphic section clearly tells us the order of cultural evolution at this site. The total period was therefore divided into several cultural stages based on stratigraphy. More than twenty C-14 data were obtained for these cultural stages. In most cases, C-14 age data from the same layer are consistent, but quite scattered ages were obtained in others. For some, the scatter of ages for the same layer is real and defines the length of time covered by the period, but in others they represent errors as the ages of adjacent periods overlap. The third method was stylistic changes in the ceramics and other materials, based on the comparison of cultural development in Northern Peru. Best estimate ages were determined by combining these three methods: stratigraphy, C-14 dates, and evolution in the style of ceramics. The last of these methods is quite useful and also important, since ceramics of a certain age are often found in layers belonging to later stages.

The time covered in Huacaloma excavation site is 1500 B.C. to 1300 A.D. and is divided into six cultural stages or periods; Early Huacaloma (assigned period of 1500 B.C. to 1000 B.C.), Late Huacaloma (1000 B.C. to 500 B.C.), Layzon (500 B.C. to 200 B.C.), Initial Cajamarca (200 B.C. to 200 A.D.), Early Cajamarca (200 A.D. to 600 A.D.), and Middle Cajamarca (600 A.D. to 1300 A.D.). Initial Cajamarca period is subdivided into Phase A (older) and B (younger) based on stratigraphy (Terada and Onuki, 1982, p. 255), though C-14 ages were not discriminated.

2. Paleointensity Experiments and Results

The magnetic minerals in all the samples were Ti-poor titanomagnetite with Curie points in excess of 550°C. Most of the samples showed a nearly reversible heating and cooling curves (Fig. 2a) in thermomagnetic analysis, and even when irreversibility was observed, the change due to

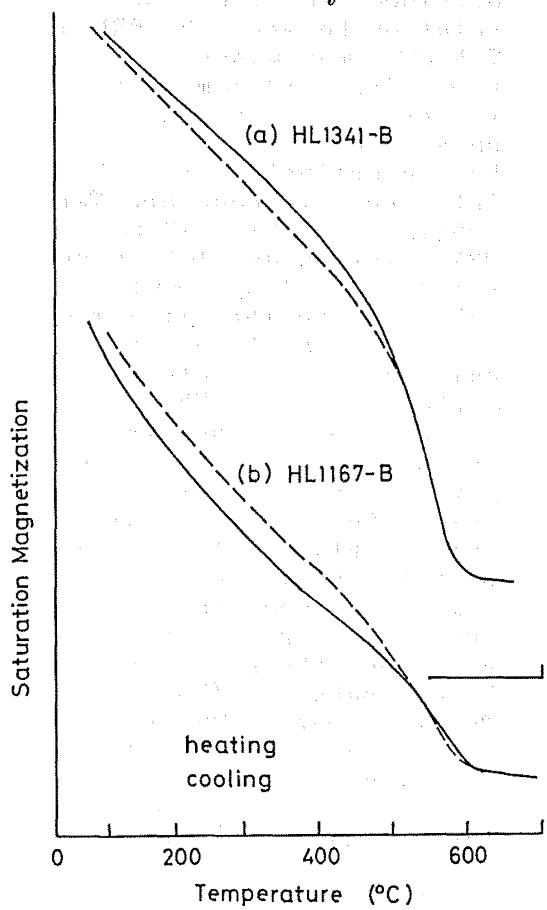

Fig. 2 Thermomagnetic curves of typical samples.

heating was not severe (Fig. 2b).

Paleointensity experiments were carried out by the Thellier's method (Thellier and Thellier, 1959) modified by Coe (1967). After the measurement of the natural remanent magnetization (NRM), samples were heated and cooled in nitrogen atmosphere at 50°C steps until the Curie temperature was reached. Heatings were made twice to the same temperature, first in a nonmagnetic space (residual field less than 200 nT) and then in a field of 50 μT. The results are plotted on Arai diagrams (NRM-TRM diagrams). In the course of heat treatments, the directions of remanence did not change much up to about 500°C, indicating the good stabiliby of the NRM. From these results, these samples seem to be well suited for paleointensity experiments.

Examples of successful paleointensity experiments are given in Fig. 3. In these figures, filled and open circles indicate data points included or excluded from the regression analysis. The latter points are affected by viscous remanene (VRM) at low temperatures or alteration due to high temperature oxidation near Curie point. In calculating the slope (and therefore the paleointensity), it was made sure that six or more points belonged to the linear portion, and that this portion covered at least a third of the first quadrant in the NRM-TRM diagram. Paleointensity estimates were obtained from the linear relation between the NRM and TRM (thermoremanent magnetization) components on the Arai diagrams, using least squares method where errors in both coordinates are taken into account (Kono and Tanaka, 1984). The slope of the NRM-TRM relation was determined for 21 out of 24 samples subjected to the experiment.

The quality of the calculated paleointensities differ greatly. The standard error (s_F) was calculated for each datum to give the reliability of paleointensity estimate. This value combines the effects of both the variance in linear regression and that in quadratic regression to represent the non-ideal, non-linear behavior (Kono and Tanaka, 1984). The mean paleointensities for the individual cultural period were calculated using the inverse square of the standard error ($1/s_F^2$) as the weight of individual data (Table 1). In doing so, all the data were included regardless of their standard errors.

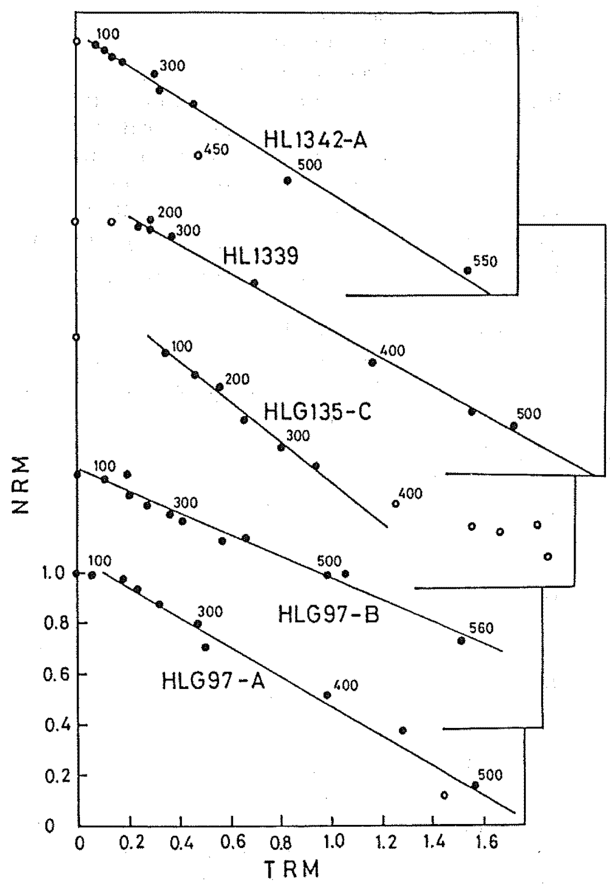

Fig. 3 Examples of Arai diagrams for Thellier's method. Intensities normalized by the NRM magnitudes of samples.

Because small weights were attached to these data, there is no significant changes if they were neglected or not; when data with $s_F > 9$ uT were excluded, change in the mean intensity was always smaller than 0.2 μT and that in the standard error was less than 0.3 μT except for Middle Cajamarca for which s_F became 15.6 μT.

Table 1. Summary of the Paleointensity Results

Cultural Period	Age Range	n_0	n	$\bar{F}$ μT	s.e. μT
Middle Cajamarca	600 AD - 1300 AD	4	3	34.2	13.3
Early Cajamarca	200 AD - 600 AD	5	5	43.0	2.1
Initial Cajamarca, B	0 AD(?) - 200 AD	3	3	37.2	3.0
Initial Cajamarca, A	200 BC - 0 AD (?)	2	2	25.4	1.7
Layzon	500 BC - 200 BC	4	3	28.4	2.6
Late Huacaloma	1000 BC - 500 BC	2	2	42.4	11.6
Early Huacaloma	1500 BC - 1000 AD	4	3	27.9	1.3

n_0: Number of samples subjected to Thellier's method; n: Number of paleointensity data; $\bar{F}$: Mean paleointensity for the period; s.e.: Standard error of the mean paleointensity.

3. Discussion and Conclusions

The Thellier's method was applied to 24 potsherd samples from pre-Inca ruins of northern Peru, and 13 good ($s_F < 9$ uT) and 8 acceptable ($s_F > 9$ μT) paleointensity data were obtained. The high rate of success is perhaps related to good stabilities in both magnetic and chemical sense. As the ferromagnetic minerals in these samples are Ti-poor titanomagnetites (see Fig. 2), the original firing of these ceramics should have been carried out at temperatures in excess of 600°C and in oxidizing conditions.

Samples used in the present study came from different fragments of broken potteries bearing different patterns even when sample names are quite similar, such as HL521-A to E. Nevertheless, most of the data in one period agrees with each other quite well. This is probably because the age assignments were appropriate.

Only the samples of Middle Cajamarca period show a large scatter among obtained values. Although the number of data are not very large, at least two of them are quite well defined. It seems, therefore, that the difference among them is real. One possibility is errors in age assignments for some of these samples and the other is that large amplitude fluctuation of geomagnetic intensity really occurred in this period. In this respect, it is interesting that Gunn and Murray (1980) reported a fluctuation between 40-60 μT for the period of 600-1300 A.D., though our data suggest that the range of fluctuation was somewhat smaller, 23-45 μT.

Fig. 4 compares the present results with previous data reported as "good" by the original authors. Our data are broadly consistent with data already reported for the time interval of 1500 B.C. to 500 A.D. From 1500 B.C., the intensity increased to a maximum of about 40 uT at about 700 B.C. and then decreased again. An intensity minimum at about 0 A.D. seems well defined by the present data. As the standard error for each period is

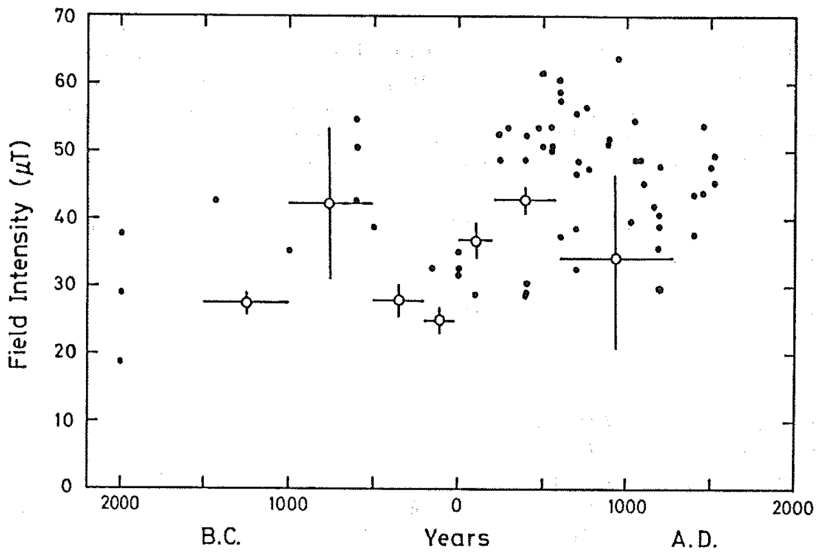

Fig. 4 "Good" paleointensity data reported by previous authors (dots) and the present data (open circles with error bars). Our data are shown as the mean and standard errors for each period.

small, small amplitude fluctuation can also be distinguished. We may therefore conclude that the use of well dated materials for paleointensity determination will clarify the real changes in the geomagnetic field.

In concluding, we must emphasize the importance of proper age assignments in archeomagnetic studies. The large scatter in the previous "good" data between 0 and 1600 A.D. (Fig. 5) may, in part, be attributed to large errors in the ages. The succes we had in the present study owes much to the good age control for our samples. It should always be kept in mind that the standard deviations attached to C-14 ages are only statistical errors, and not a true measure of the actual errors in the age data.

References

Coe, R.S. (1967) J. Geophys. Res., 72, 3247.
Games, K.P. (1977) Geophys. J. Roy. Astron. Soc., 48, 315.
Gunn, N.M. and A.S. Murray (1980) Geophys. J. Roy. Astron. Soc., 62, 345.
Kitazawa, K. and K. Kobayashi (1968) J. Geomag. Geoelectr., 20, 7.
Kono, M. and H. Tanaka (1984) J. Geomag. Geoelectr., 36, 267.
Nagata, T., K. Kobayashi, and E.J. Schwarz (1966) J. Geomag. Geoelectr., 17, 399.
Terada, K. and Y. Onuki (1982) Excavations at Huacaloma in the the Cajamarca Valley, Peru, 1979, Univ. of Tokyo Press, Tokyo.
Terada, K. and Y. Onuki (1985) The Formative Period in the Cajamarca Basin, Peru: Excavations at Huacaloma and Layzon, 1982, Univ. of Tokyo Press, 1985.
Thellier, E. and O. Thellier (1959) Ann. Geophys., 15, 285.

(Submitted to Journal of Geomagnetism and Geoelectricity)

A PRELIMINARY PALEOMAGNETIC RESULTS FROM THE CENTRAL AXIAL ZONE OF HOKKAIDO

Yoshiki FUJIWARA

Department of Geology & Mineralogy, Hokkaido University
Sapporo, 060

The major tectonic units in Hokkaido are generally accepted to be divide into following five tectonic belts; the West Hokkaido belt, the Kamuikotan belt, the Hidaka belt, the Tokoro belt and the East Hokkaido (Nemuro) belt from west to east. The west Hokkaido belt which is characterized by a large amount of andesitic volcanic volcanic terrain of Lower Cretaceous age in that eastern margin is extension of the northern Honshu arc. In the Kamuikotan belt and eastern margin of the Hidaka belt, a thick submarine basalts associated with chert, shale and acidic tuff are frequently recognized. This strata has been called the Sorachi Group since its recognition in the middle 1930's. The sequence is uncomformably overlain by a thick detrital sequence (Yezo Group) ranging from Lower to Uppermost Cretaceous. These two geologic units are the main object for the present paleomagnetic investigation.

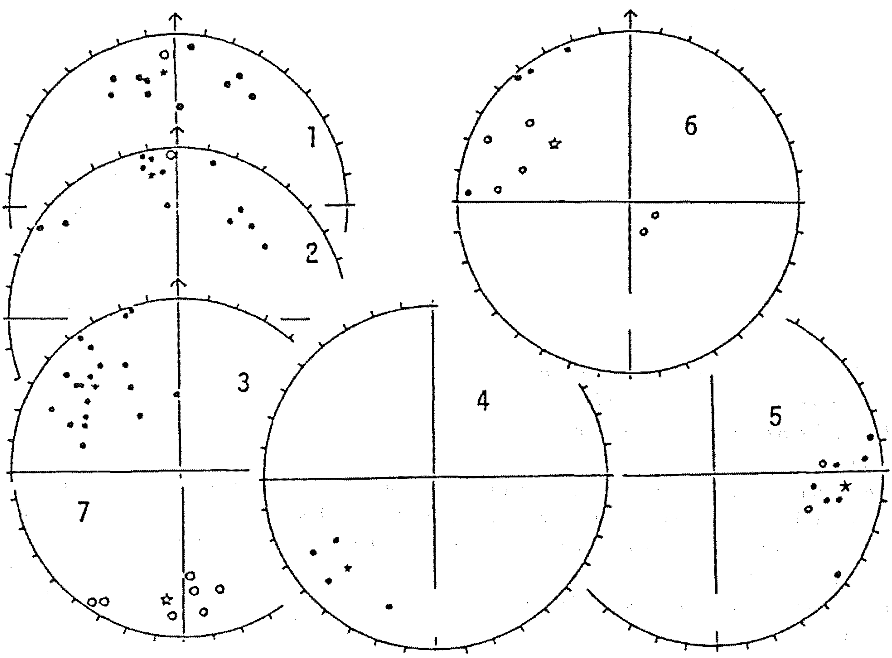

Fig. 1 Paleomagnetic directions from the Sorachi Group on equal area projections. Solid (open) circles are on the lower (upper) hemisphere; solid (open) stars represent mean directions projected on the lower (upper) hemisphere.
1,2,3,4,5,7 : pillow basalt, 6: dolerite sheet

Fig. 1 represents the directions of magnetization after AF cleaning collected from 7 localities belonging to the Sorachi Group. The site mean directions from each site clearly show very low inclinations and scatted declinations. The mean normal directions are almost antipodal to no. 7 reversed site mean direction. This may suggest some stabilty of remanence. Low inclinations are also defined by chert samples which were collected from the melange complex where distributed at co-parallel along eastern margin of the Sorachi Group bounded by steep strike-slip fault (Fig. 2).

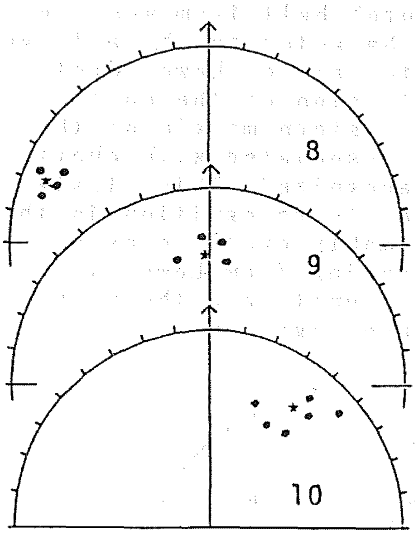

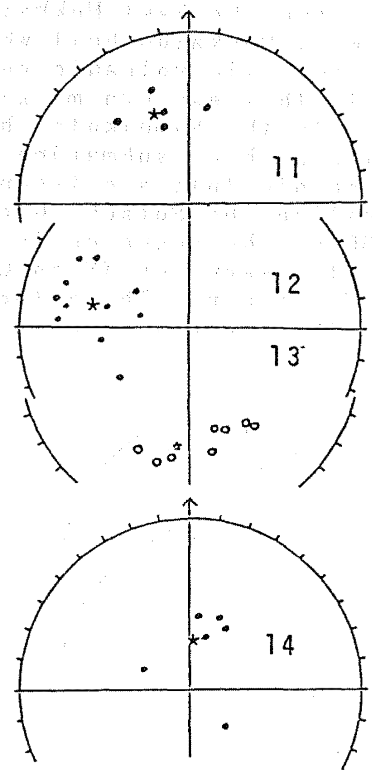

Fig. 2 Directions of remanent magnetiztion of individual site after AF cleaning : conventions as in Figure 1. Site Nos. 8, 9, 10 are from chert blocks collected from the melange complex tectonically divided from the Sorachi Group by steep strike-slip fault. Tectonic correction was made by using bedding orientation of individual block. 11, 12, 13, 14 represent directions of after AF cleaned remanence of sedimentary rocks collected from the Lower Yezo Group.

The results obtained from 4 sites belonging to the Lower Yezo Group, flysch type sedimentary sequence overlying on the Sorachi Group, also represented in Fig. 2. The mean direction of magnetiztion of the Lower Yezo Group has northward declination and relatively high inclination in comparison with the mean direction inferred from the Sorachi Group.

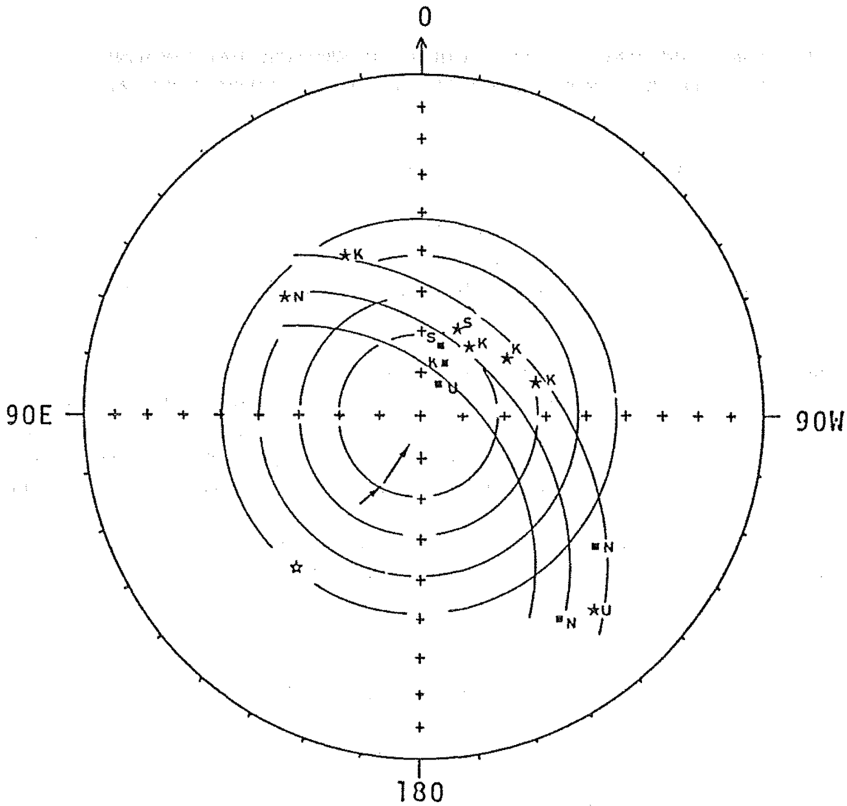

Fig. 3 Paleomagnetic pole positions inferred from the Messozoic rocks in the Central Axial Zone of Hokkaido. open star: sampling locality, solid strars : pole positions from the Sorachi Group, soid square :Lower Yezo Group, arrow indicates APWP from Eurasia.

Calculation of paleolatitudes from the mean inclination resulted from paleomagnetic treatments will be most effective to estimate the position of the Central Axial Zone of Hokkaido in the late Jurassic to early Cretaceous time.

Preliminary paleomagnetic results from the Sorachi Group suggest the location of formation of submarine basalts was approximately 11 N, while the results from the Lower Yezo Group represent approximately 23 N. The evidence representing such low paleolatitudes may introduce some interpretation concerning to a large scale displacement of the Northern Japan.

The formation of the Sorachi Group was equatorial at late Jurassic time, probably situated at around somewhere of the triple junction of the Izanagi, Farallon and Pacific plate. Low paleolatitude obtained from the Lower Yezo Group also suggests that deposition of this sedimentary sequence took place at far southern sub-tropical place.

Detailed discussions will be apeared in forthcoming paper.

(To be submitted to Journal Geophysical Research)

TECTONIC SETTING OF THE CHUBU DISTRICT: PALEOMAGNETIC STUDY ON THE NOHI RHYOLITE OF LATE CRETACEOUS AGE

Yasuto ITOH*, Masayuki TORII* and Takaaki MATSUDA**

* Department of Geology and Mineralogy, Kyoto University, Kyoto 606, Japan
** Department of Geology, Himeji Institute of Technology, Himeji 671-22, Japan

The Chubu district is the conjunction area of southwestern and northeastern arcs of the Japanese island arc system. These two arcs have undergone differential rotation which was closely related to the opening of the Japan Sea in Middle Miocene (Otofuji et al., 1985). To investigate complex tectonic history of the Chubu district, paleomagnetic studies on various ages and locations of the district are indispensable. The paleomagnetic data of Neogene rocks have been obtained from the following areas as shown in Fig. 1: Niu (Nakajima and Hirooka, 1986), Shidara (Torii, 1983), Morozaki (Hayashida, 1986), Mizunami (Hayashida, 1986) and Yatsuo (Itoh, 1986). The characteristic paleomagnetic direction about Early Miocene rocks of the Yatsuo area, northern part of the Chubu district, showed a easterly deflection of about 13°, while much more deflected data (more than 40°) were obtained from the synchronous rock units in the rest areas. The significant difference of deflection indicates that a differential rotation has occurred within the Chubu district in Miocene.

Older tectonic events should be reconstructed with the aid of paleomagnetic data on the pre-Neogene rocks. Geological framework of the Chubu district is characterized by accreted blocks, Mino belt and the Outer Zone, and the host Hida terrane (Fig. 1). The data on the pre-Neogene rocks have been obtained mainly from greenstones and siliceous rocks in the Mino belt (Hattori, 1982), until now. These rocks are

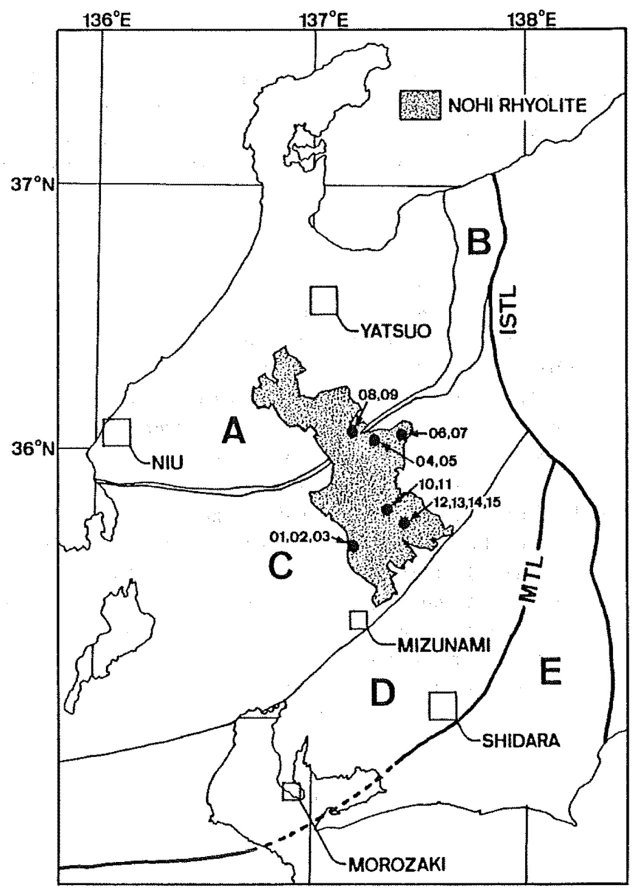

Fig. 1 Summary of geological provinces and areas of Neogene paleomagnetic data in the Chubu district. Solid symbols denote sampling sites of this study. A: Hida belt, B: Hida marginal belt, C: Mino belt, D: Ryoke belt, E: Outer zone, MTL: Median tectonic line, ISTL: Itoigawa-Shizuoka tectonic line.

considered to be allochthonous blocks in a subduction complex (Mizutani and Hattori, 1983). To investigate the tectonic events after the accretion of the Mino belt at Jurassic age, it is necessary to collect paleomagnetic data on the rocks which were autochthonously formed on the accreted blocks. In this paper, results of the paleomagnetic study are described on the Nohi rhyolite, a body of extrusive rocks which overlies the Hida and the Mino belts (Fig. 1).

The Nohi rhyolite consists exclusively of rhyolitic to rhyodacitic welded tuffs and small amount of intrusive rocks (Yamada et al., 1971). Harayama and Koido (1983) compiled the radiometric ages of the Nohi rhyolite and concluded that most part of the Nohi rhyolite had been formed from 85 to 70 Ma (Late Cretaceous).

Paleomagnetic sampling was carried out at 15 sites (Fig. 1). Samples were collected only from the following rocks; (1) tilting of rocks were clearly observed through the eutaxitic structure of welded tuff and (2) they have not been thermally and/or chemically altered by associated intrusive rocks. Each site comprised 8 to 11 hand samples which were independently oriented using a magnetic compass. Cylindrical specimens of 25 mm in diameter and 22 mm in length were prepared from each sample. A cryogenic magnetometer (ScT C-112) was used to measure remanent magnetizations.

Stability of remanence was tested through progressive thermal demagnetization. One specimen was chosen from each site as a pilot sample and thermally demagnetized in more than 8 steps using a noninductively wound electric furnace. The furnace is enclosed by three-layered cylindrical mu-metal shield in which the

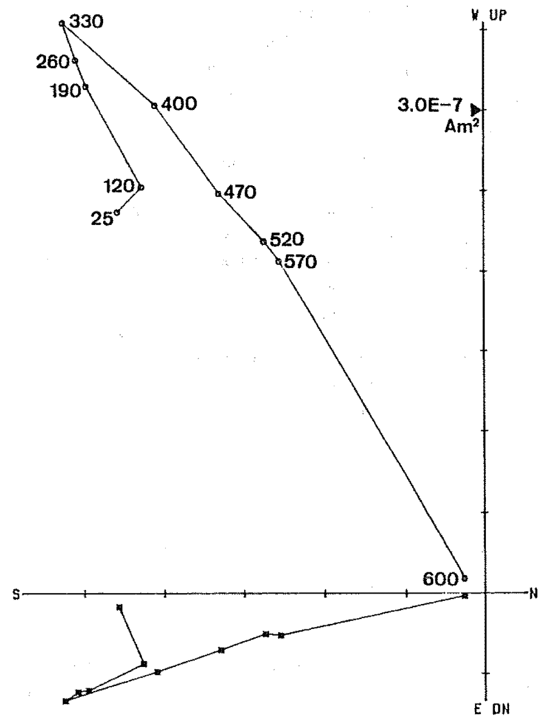

Fig. 2 Typical vector-demagnetization diagram of progressive thermal demagnetization of a pilot specimen from Site 13. Solid and open circles are projections of vector end-points on horizontal and N-S vertical planes, respectively. Numbers attached to symbols are temperature in °C.

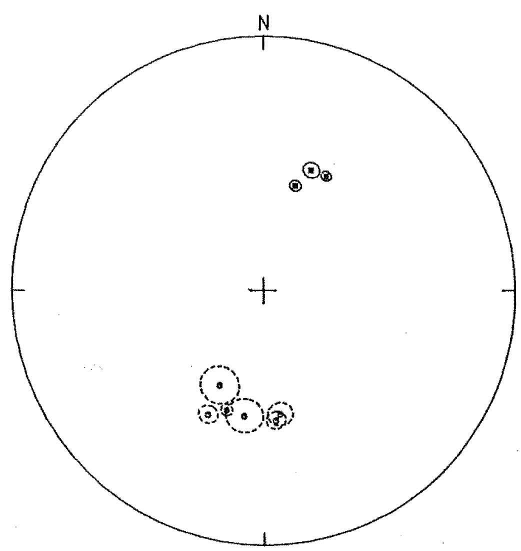

Fig. 3 Equal area projection of site-mean directions of the Nohi rhyolite with 95% confidence circles. Open and solid symbols denote negative and positive inclinations.

Table 1 Paleomagnetic site-mean directions from the Nohi rhyolite. DEMAG.: demagnetization level in °C or mT, Dec.,Inc.: mean declination and inclination in degree, N: number of specimens, α_{95}: radius of 95% confidence circle in degree, k: Fisher's precision parameter, PHI,LMD: latitude and longitude of virtual geomagnetic pole position (north-seeking pole) in degree.

Site	DEMAG.	Dec.	Inc.	N	α_{95}	k	Polarity	PHI	LMD
01	20 mT	-162.6	-49.3	12	1.9	544.4	R	74.4	-117.2
02	550 °C	-155.5	-45.6	12	3.0	212.6	R	67.5	-117.2
03	15 mT	-154.9	-56.2	12	6.2	49.3	R	69.8	-143.4
04	10 mT	29.0	47.4	12	1.6	762.2	N	64.5	-123.9
05	20 mT	21.9	47.8	11	2.6	310.6	N	70.2	-117.7
06	500 °C	17.1	54.5	12	1.8	586.4	N	76.1	-133.3
10	560 °C	172.5	-49.5	12	3.9	124.8	R	81.7	8.6
11	20 mT	174.7	-47.6	12	3.0	203.6	R	81.6	-8.8
13	500 °C	-171.1	-48.8	12	5.7	58.3	R	80.4	-96.4

residual magnetic field is less than 10 nT in cooling cycle. Six sites among the 15 were rejected because thermal demagnetization failed to find a stable component. The other 9 sites survived the stability test and showed straight trends which converge to the origin on the vector-demagnetization diagrams (Fig. 2). For the surviving 9 sites, alternating field (AF) demagnetization experiment was carried out progressively. Identical stable components found by the thermal demagnetization were also detected by the progressive AF demagnetization in 5 sites.

Routine demagnetizations were made for 11 to 12 specimens of each site at 3 to 4 steps of the demagnetization level. AF method was employed for the 5 sites in which the stable components were detected by progressive AF demagnetization. For the other 4 sites, thermal demagnetization was carried out. An optimum demagnetization level was decided as to give the minimum within-site scatter of direction (minimum α_{95}).

Site-mean directions after tilt correction are listed in Table 1 and plotted on the equal area projection with 95% confidence circles (Fig. 3). Three normal and six reversed polarity sites are revealed. As clearly shown in the figure, the site-mean directions are distributed in antipodal

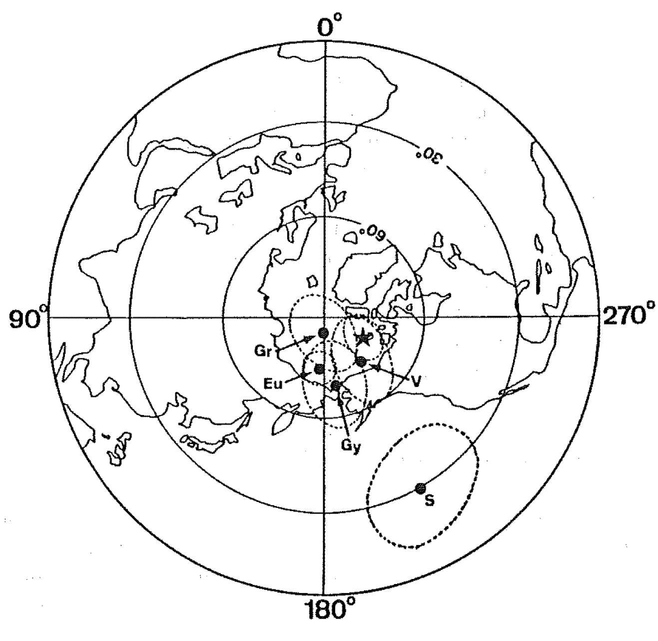

Fig. 4 Cretaceous pole positions and cones of 95% confidence. VGP of the Nohi rhyolite is shown by star. Eu: Eurasia (Irving and Irving, 1982), Gy: Gyeongsang basin in Korea (Otofuji et al., 1983), Gr: granitic rocks in Korea (Ito and Tokieda, 1980), V: volcanic rocks in Korea (Kienzle and Scharon, 1966), S: San'in district in Southwest Japan (Otofuji and Matsuda, 1983a).

Table 2 Average paleomagnetic directions obtained from the Nohi-Yatsuo district (Itoh, 1986 and this study) and the San'in district (Otofuji and Matsuda, 1983a,b). N: number of sites, D,I: mean declination and inclination for each period, α_{95}: circle of 95% confidence.

	Nohi-Yatsuo				San'in			
	N	D	I	α_{95}	N	D	I	α_{95}
Late Cretaceous	9	14.5	50.3	5.9	6	71.3	44.2	20.3
Early Miocene	4	12.6	47.1	7.0	6	69.9	49.5	14.5
Middle-Late Miocene	4	-2.5	55.6	6.6	4	1.3	56.3	16.9

relation. This fact strongly suggests that composite mean of 9 sites yields a characteristic direction of the Nohi rhyolite of Late Cretaceous age. When reversed polarity directions are inverted to the normal ones, site-mean directions from 9 sites yield the formation-mean: D=14.5°, I=50.3° and α_{95}=5.9°.

The virtual geomagnetic pole (VGP) position of the Nohi rhyolite is 77.0°N and 114.9°W. The VGP position is illustrated in Fig. 4 with the VGPs of Cretaceous rock units from Eurasia, Southwest Japan and the Korean Peninsula. Southwest Japan could be represented by the well-dated rock units in the San'in district, of which paleomagnetic directions (Otofuji and Matsuda, 1983a) are only usable data with tilt correction for pre-Neogene rocks in Southwest Japan. The VGP position of the Nohi rhyolite is not significantly different from those of Korea and Eurasia, but is quite discordant with the VGP of Southwest Japan (San'in district). This result implies that the Korean Peninsula and the block which contains the Nohi rhyolite have not relatively rotated to Eurasia, whereas the San'in district has rotated clockwise around a vertical axis. Because the geologic provinces of Paleozoic and Mesozoic rocks (e.g. Ryoke belt) extend continuously from the Chubu to the San'in district, the difference in rotational movement between the two districts after Cretaceous is attributed to a bending inside Southwest Japan.

The timing of the bending could be estimated from the paleomagnetic data of Neogene rocks which cover the Nohi rhyolite. From the study of Sudo (1979), northernmost margin of the Nohi rhyolite is unconformably overlain by Early Miocene volcanic rocks at the southwestern part of the Yatsuo area, in which paleomagnetic directions were determined about Early to Late Miocene rocks (Itoh, 1986). Assuming that the Nohi rhyolite and the Yatsuo area have formed a rigid tectonic block since Early Miocene, interesting information is obtained about the bending of Southwest Japan. In Table 2, paleomagnetic data of the Nohi-Yatsuo district and the San'in district are listed for the following three periods: Late Cretaceous, Early Miocene and Middle-Late Miocene. Changes in declinations indicate that major bending of Southwest Japan occurred in Miocene.

References:

Harayama, S. and Y. Koido (1983) MAGMA, 67, 51.
Hattori, I. (1982) Tectonophysics, 85, 313.
Hayashida, A. (1986) J. Geomag. Geoelectr., in press.
Irving, E. and G. A. Irving (1982) Geophys. Surveys, 5, 141.
Ito, H. and K. Tokieda (1980) J. Geomag. Geoelectr., 32, 275.
Itoh, Y. (1986) J. Geomag. Geoelectr., in press.
Kienzle, J. and L. Scharon (1966) J. Geomag. Geoelectr., 18, 413.
Mizutani, S. and I. Hattori (1983) Accretion Tectonics in the Circum-

Pacific Regions, edited by M. Hashimoto and S. Uyeda, TERRAPUB, Tokyo, 169.
Nakajima, T. and K. Hirooka (1986) J. Geomag. Geoelectr., in press.
Otofuji, Y. and T. Matsuda (1983a) Earth Planet. Sci. Lett., 62, 349.
Otofuji, Y. and T. Matsuda (1983b) Rock Mag. Paleogeophys., 10, 69.
Otofuji,Y.,T. Matsuda and S. Nohda (1985) Earth Planet. Sci. Lett., 75, 265.
Otofuji,Y., J. Y. Oh, T. Hirajima, K. D. Min and S. Sasajima (1983) The Tectonic and Geologic Evolution of Southeast Asian Seas and Islands: Part 2, Geophys. Monogr. 23, edited by D. E. Hayes, 388.
Sudo, S. (1979) Geol. Soc. Japan Mem., 17, 187.
Torii, M. (1983) PhD Thesis of Kyoto University.
Yamada, N., K. Kawada and T. Morohashi (1971) Chikyukagaku (Earth Science), 25, 52.

Timing of Rotational Motion of Southwest Japan Inferred from Paleomagnetism of the Setouchi Miocene Series

Akira HAYASHIDA

Laboratory of Earth Science, Doshisha University, Kyoto

Abstract

Paleomagnetic measurements have been made on tuff and mud samples from 25 sites of the Morozaki Group and the Mizunami Group, typical sequences of the Setouchi Miocene Series distributed in the eastern part of Southwest Japan (Fig. 1). Stability tests by alternating field and thermal demagnetization reveal the existence of characteristic remanent magnetization, of which directions show significant clockwise deflection; the mean declination shift exceeds 50° in the late Early Miocene members (N6-N8), and is less than 30° in the early Middle Miocene members (N9). This result, compared with the other paleomagnetic data from the Setouchi Miocene Series and the volcanic rocks in the San'in district (Fig. 2), suggests that coherent rotation of Southwest Japan began between the late Early Miocene and the early Middle Miocene. Nearly a half of the rotation might have attained in the stage of Zone N9, which possibly corresponds to the period of the opening and increasing subsidence in the Japan Sea.

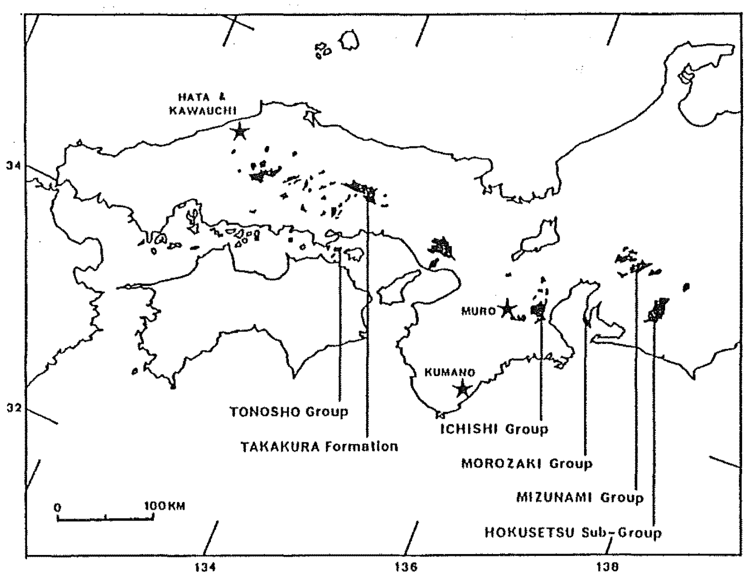

Fig. 1 Map showing the distribution of the Setouchi Miocene Series. The Morozaki Group and the Mizunami Group are located in the eastern part of Southwhest Japan. Location of some volcanic rocks refered are shown with stars.

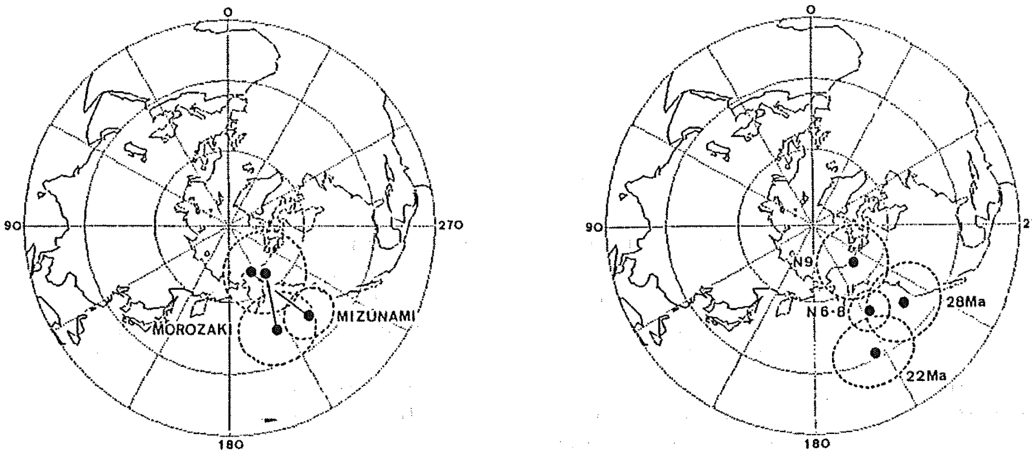

Fig. 2 Virtual geomagnetic pole (VGP) positions plotted on the Northern Hemisphere of equal-area projection. (Left) VGP's of the Morozaki and the Mizunami Group. Transition of the poles from the late Early Miocene to the early Middle Miocene are shown by arrows. (Right) VGP positions determined from the volcanic rocks in the San'in district (Kawauchi: 28 Ma, Hata: 22 Ma), and the Setouchi Miocene Series (late Early Miocene: N6-8, early Middle Miocene: N9). Confidence circles of the 95% level are shown except for the younger pole of the Mizunami Group (left).

(To be published in J. Geomag. Geoelectr.)

REVERSE MAGNETIZATIONS FOUND FROM THE IZUMI GROUP IN NORTHWESTERN SHIKOKU, SOUTHWEST JAPAN

kazuto KODAMA

Department of Geology, Faculty of Science, Kochi University
Kochi 780, Japan

Paleomagnetic measurements were conducted on sedimentary rocks of the Izumi group distributing in the northwest of Shikoku (Fig. 1). The Izumi group in this area as well as other regions consists generally of alternations of sandstone, shale and shaly mudstone showing almost synclinal and partly anticlinal folding with bedding strike directing N50^{o} to 90^{o}E. Geologic age of the sediments can be assigned to Upper Campanian (Uppermost Cretaceous) by the occurrence of radiolarians (Okamura et al., 1984) and megafossils (e.g., Matsumoto, 1954), and seems to be somewhat older than that of eastern Shikoku because of their structural relationships and fossil age difference so far reported.

A total of 17 sites were visited in this study and their initial and magnetically demagnetized magnetizations were measured with a cryogenic magnetometer in the Kyoto University. We report in this brief note the preliminary paleomagnetic data whilst rockmagnetic behaviors and interpretations from tectonic and statistic viewpoints will be discussed elsewhere in more detail. Fig. 2 illustrates the in-situ and tilt-corrected site-mean remanence directions whose statistics are summarized in Table 1. Although five sites (sites 2,10,11,16 and 17) had to be rejected due to their too divergent directions (k<10), the others except one (site 14) seem to show reverse magnetizations with declinations deflected significantly westward. Referring the previous paleomagnetic data from the eastern extension of the Izumi belt (Kodama, 1986), the present data set can be thought as a counterpart of a pair of normal and reverse polarities during the Upper Cretaceous.

Table 1. Paleomagnetic data from the Izumi group in northwestern Shikoku, southwest Japan.

Site	N	I	D	I_c	D_c	k	α_{95}
1	5	-10.4	215.8	-39.3	251.2	15.8	19.8
3	6	-18.0	227.7	-30.1	263.8	22.5	14.4
4	7	-42.3	217.3	-54.9	242.6	49.0	8.7
5	8	-29.6	159.2	-45.2	238.4	83.7	6.1
6	5	-17.3	193.9	-36.7	227.5	42.9	11.8
7	7	-59.4	242.9	-45.8	300.6	46.2	9.0
8	9	-51.6	228.2	-48.3	304.7	138.8	4.4
9	9	-10.0	332.0	-17.4	331.3	23.9	10.8
12	8	-62.4	306.3	-63.0	243.6	22.3	12.0
13	5	-31.4	205.4	-48.1	194.6	21.4	16.9
14	5	36.6	76.4	50.2	44.2	13.8	21.4
15	7	-47.4	232.3	-1.9	218.9	29.5	11.3

N; number of specimens. I,D; in-situ inclination and declination, I_c,D_c; inclination and declination after correction for bedding tilt. k, α_{95}; Fisher's precision parameter and semi-angle of 95% confidence cone.

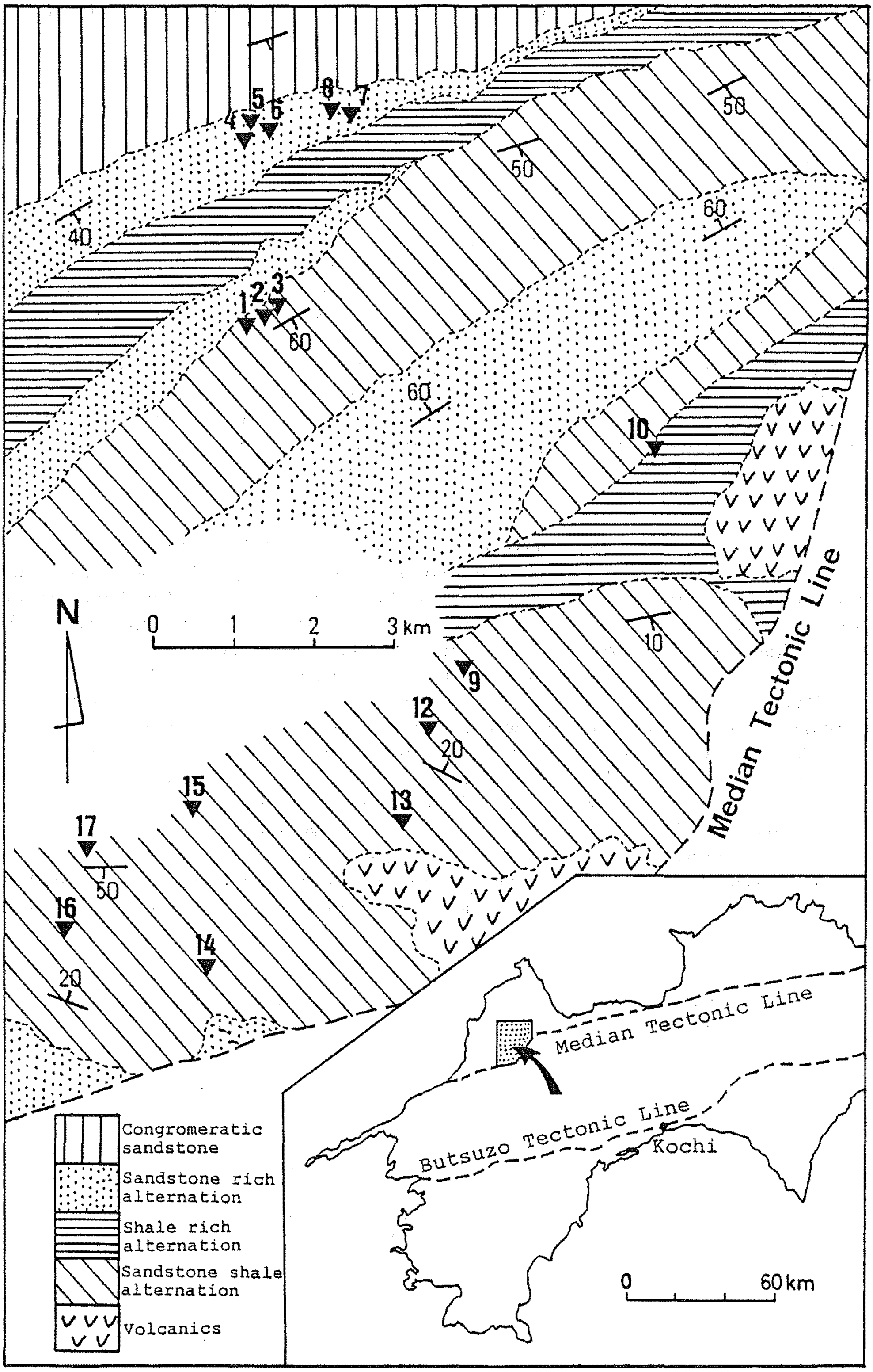

Fig. 1 Generalized geologic map of the Izumi belt in northwestern Shikoku, Southwest Japan, showing sampling localities for paleomagnetic study (reproduced partly from Okamura et al., 1984).

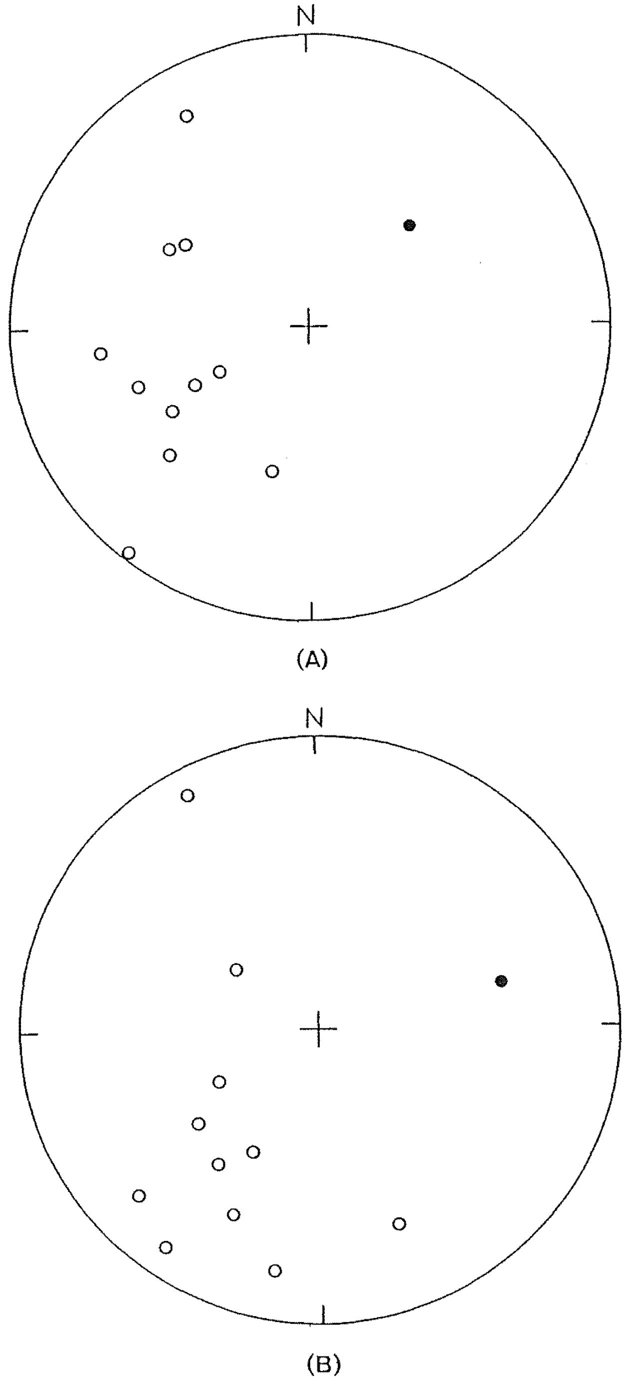

Fig. 2 Site mean directions after (A) and before (B) the corrections for bedding tilt. Equal-area projection on the lower (solid) and upper (open) hemisphere.

References

Kodama, K. (1986) J. Geomag. Geoelectr., 38 (in press).
Matsumoto, T. (1954) The Cretaceous system in the Japanese Islands (J.S.P.S., Tokyo), 324.
Okamura, M., Y. Kagawa, and M. Tashiro (1984) Research Reports of the Kochi University, 32, 339.

PRELIMINARY PALEOMAGNETIC STUDY ON THE LOWER CRETACEOUS SERIES IN THE OUTER ZONE OF SOUTHWEST JAPAN

Kazuaki MAENAKA and Sadao SASAJIMA

Hanazono College , Nishinokyo-Tsubonouchi, Nakagyo
Kyoto, 604

INTRODUCTION

In Southwest Japan, the geotectonic unit is divided with the Median Tectonic Line into two zones: that is the inner zone and the outer zone. Both of them are also characterized by the zonal structure. From the recent paleomagnetic researches, it is concluded that most of terranes excepting the Hida terrane in Southwest Japan have been formed at some regions of the equatorial zone and have accreted as subduction complex to the proto-Japanese island during Mesozoic Era. Cretaceous paleo-position of the inner zone of the Southwest Japan with respect to the Korean Peninsula was proposed by Sasajima (1984). On the other hand, the paleolatitude of the outer zone is not still established, though Silurian Kurosegawa microcontinent has been inferred to have situated in the paleoequatorial zone (Shibuya et al., 1983).

In order to clarify whose Cretaceous situation, the writers have tried to measure paleomagnetic directions of the terrigenous clastic samples from the Lower Cretaceous Series of the outer zone in Southwest Japan.

GEOLOGICAL SETTINGS AND SAMPLING

Samples were collected from two regions (Wakayama Prefecture and Kochi Prefecture) in Southwest Japan.

In the western Kii Peninsula, more than 2000m thick succession of the Cretaceous clastic deposits occuping the east-northeast-trending narrow basin on the Chichibu Belt. The Yuasa Formation forms the lowest member of the Cretaceous succession. The formation is distributed only in the vicinity of Yuasa and ranges in thickness from 25 to more than 200m, thickning to the south. The conformably overlying Arida Formation yields abundant molluscan fossils of Baremian age (Maejima, 1984). Consequently, the Yuasa Formation is considered to be Hauterivian (125-131 Ma) in age (Harland et al., 1982). Samples were collected from various kinds of lithology accross stratigraphic thickness of about 100m. Seventy oriented samples (silt, sand and shale) were collected from 7 sites.

The Ryoseki Formation, corresponding to the Yuasa Formation, is distibuted in north of Kochi City, central Shikoku (Tsuchiya, 1982). Twenty samples were collected from the outcrop of serpentinite-derived sandstone in Lower Cretaceous formation in the Kurosegawa Tectonic zone as shown in Fig. 1.

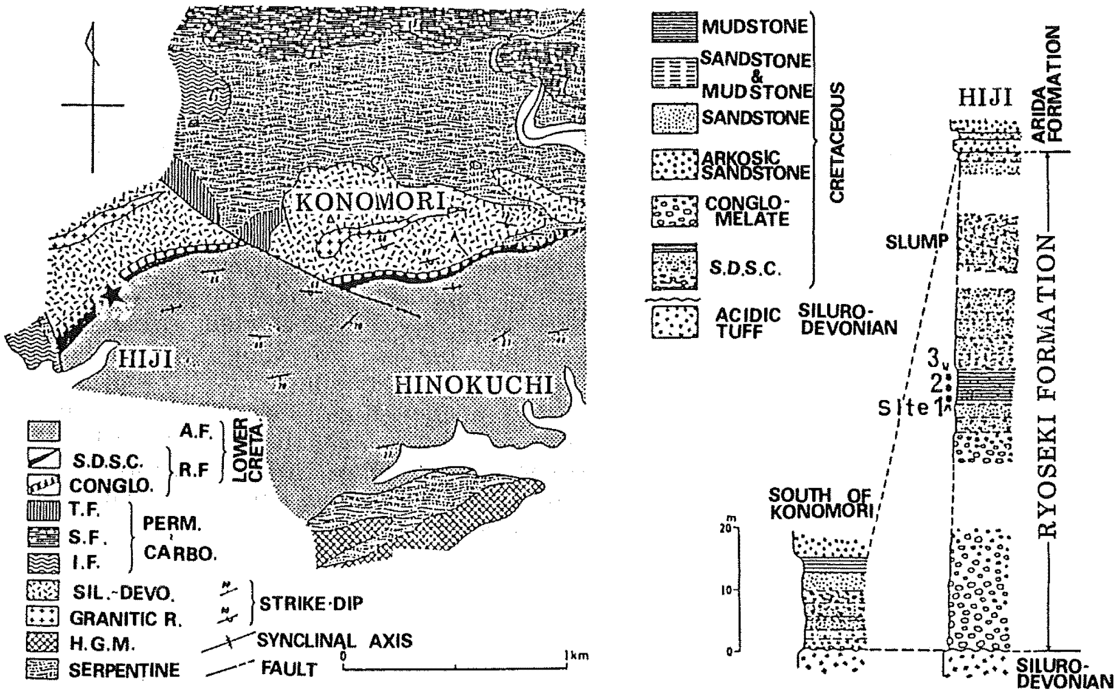

Fig. 1. Location map of sampling site (star mark) and stratigraphic position of the collected samples. A.F.; Arida Formation. I.F.; Ino Formation. R.F.; Ryoseki Formation. S.F.; Sirakidani Formation. T.F.; Takaoka Formation. H.G.M.; High grade Metamorphic rock. S.D.S.C.; Serpentinite derived sandstone and conglomerate (after Tsuchiya, 1982).

MAGNETIC MEASUREMENT

From the collected samples, some pilot specimens from many core specimens were demagnetized using an alternating field (AF) demagnetizer and a laboratory-made furnace (Ito and Torii, 1984). Measurement of the remanent magnetization were performed with a spinner magnetometer. An example of thermal demagnetization on the specimen from Yuasa is shown in Fig. 2. It shows that two components were isolated by thermal progressive demagnetization. The first component (component B) is destroyed below 300°C, whereas the second component (component A) has a final unblocking temperature of 500-550°C. Component B coincides with the present field dierction strongly suggest a secondary component. From only one site samples among seven collected sites of Yuasa region, the reliable primary magnetization can be successfully obtained.

On the contrary, the serpentinite-derived sandstone specimens collected from Ryoseki series show a high intensity in an order of magnitude 10^{-4}emu/cc. The result of AF and thermal demagnetization display a highly reliable remanent magnetization as shown in Fig. 3. Fig. 4 shows the direction in situ and after tilting correction. The result after tilting correction shows that a reversed magnetization of site 2 is antipodal to those of normal magnetization from site 1.

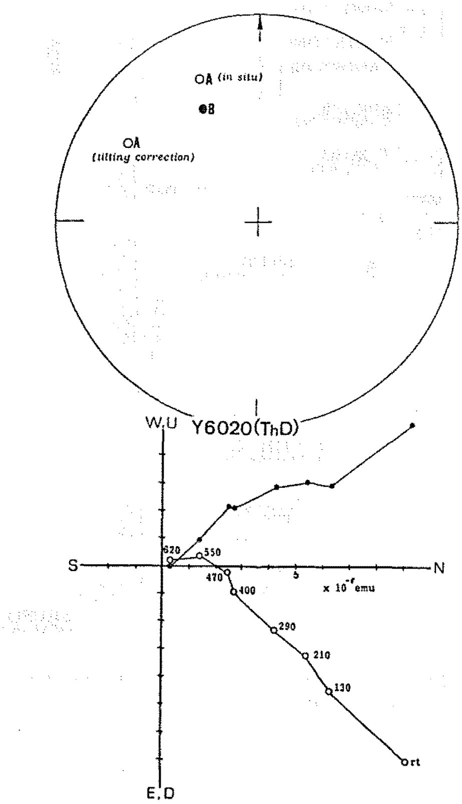

Fig. 2. Example of Zijderveld (1967) projection of the successive end point of the magnetization vector during progressive thermal demagnetization. Demagnetization temperatures are indicated in degrees Celesius. Solid circles represented projections on the horizontal plane, and open circles on vertical plane. A shows a higher temperature component and B shows a lower temperature component. A(in situ) and A(tilting correction) respectively show the direction of magnetization before and after tilting correction.

Fig. 3. Example of Zijderveld projection of samples from the Ryoseki Formation. Symbols are the same as those in Fig. 2. Numerals nearby open circles give A.F. field in Oe(left figure) and temperature (right figure).

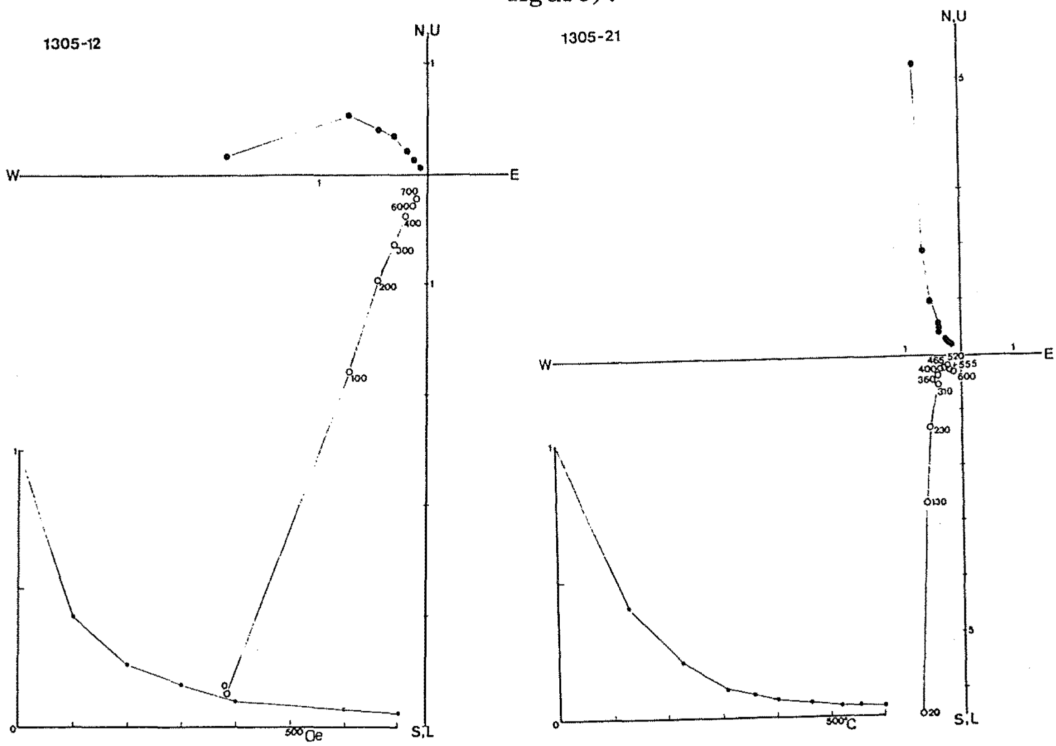

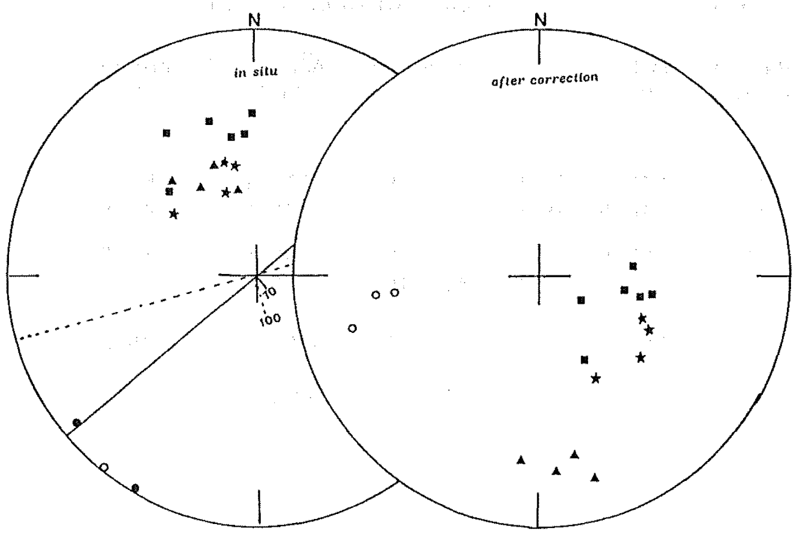

Fig. 4. Equal-area projection of the direction obtained from the samples of Ryoseki Formation. Open (solid) symbols represents projections on the upper (lower) hemisphere. Left and right figures respectively show the direction before and after the tilting correction.

DISCUSSION

Site mean directions of remanent magnetizations are given in Table 1 and Fig. 5. The value of paleolatitude calculated from the obtained inclination is listed in the last column of Table 1. The averaged value (23°) of paleolatitude (PAL in Table 1) gives considerably lower value compared with that (34°) of the present position. The results agrees well with the data from South China block obtained recently by Lin et al. (1985). This is also concordant with the results from the paleobotanical view-point that Ryoseki floral province was in close proximity to Yangtze landmass.

Basing on these paleomagnetic and paleobotanical informations (Kimura, 1984), the writers tentatively estimate the paleoposition of the Kurosegawa-Chichibu terrane and assambled terranes of the inner zone of Southwest Japan as shown in Fig. 6. Taking into consideration the accompanied error of the average paleolatitude, the paleogeographic position of the Kurosegawa-Chichibu terrane might not be conclusive as shown in Fig. 6. It may be possible to suppose that the terrane has almost contacted with the inner Ryoke micro-continent on the basis of the error range of the present paleomagnetic precision. The reconstruction in general agreement with other geological observations.

Table 1. Site mean direction, statics and paleolatitude.

Locality	Number of Specimens	Before tilt correction D(°)	I(°)	*k*	*α*	After tilt correction D(°)	I(°)	PAL
RYOSEKI								
Site 1A	10	340.5	47.9	29.4	9.1	114.1	57.5	38.1
B	10	346.5	58.9	73.1	5.7	120.3	46.8	28.0
2A	3	229.0	2.5	63.1	15.7	262.8	-31.0	16.7
B	4	331.3	54.9	74.1	10.7	173.6	24.1	12.6
YUASA	4	350.5	-25.5	6.0	41.1	303.5	-39.3	22.3
						Mean	39.7 ± 12.5	$22.5\left\{\begin{matrix}+10.3\\-8.1\end{matrix}\right.$

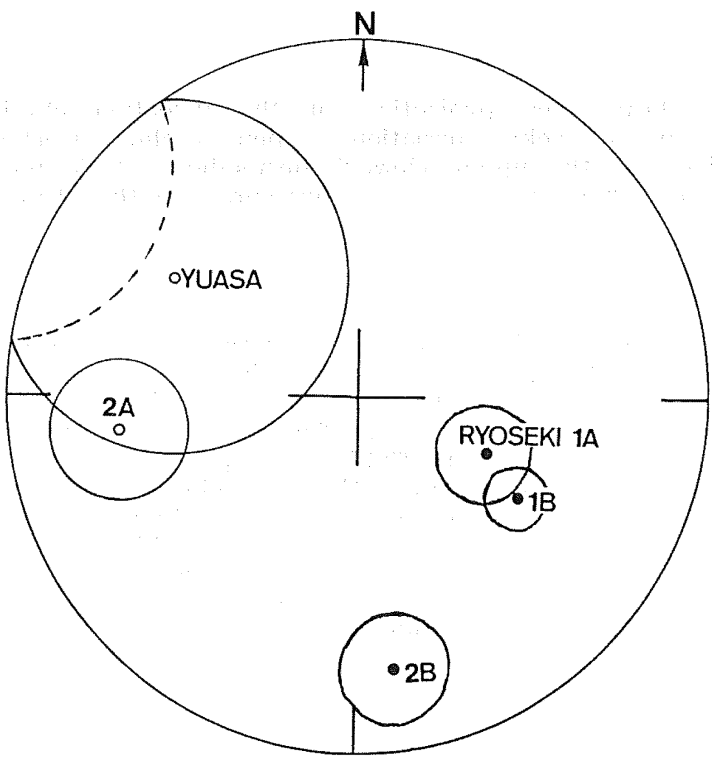

Fig. 5. Equal-area projection of the site mean directions with their circles of 95% confidence for this investigation.

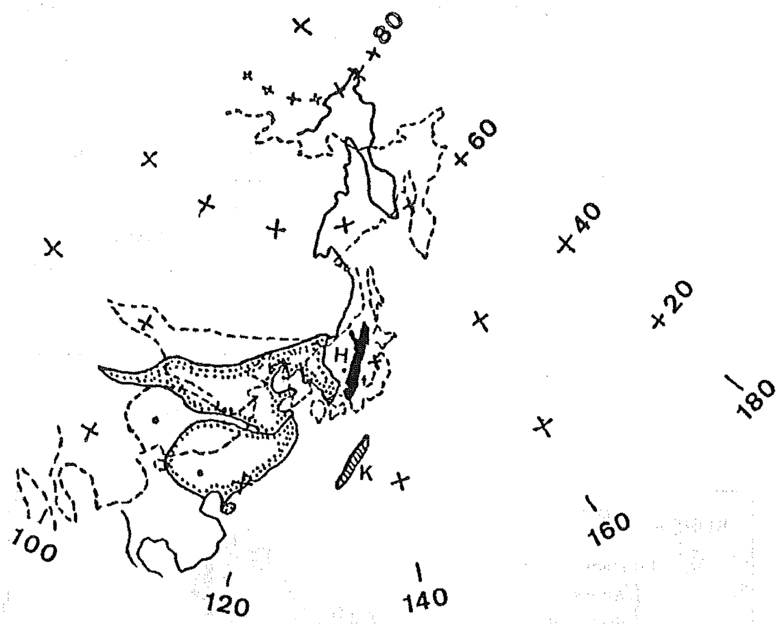

Fig. 6. Reconstruction map of East Asia for Early Cretaceous Age. Dotted line represents the present geographic map. The reconstruction for China block are due to the data of Lin et al. (1985). H; Hida terrane. K; Kurosega terrane.

REFERENCES

Harland, W. B., A. V. Cox, P. G. Llewellyan, C. G. A. Pickton, A. G. Smith and R. Walters (1982), A geological time scale, Cambridge Univ., Press.

Ito, Y. and M. Torii (1984), Rock Mag. Paleogeophys., 11, 51-54.

Kimura, T. (1984), Geology and paleontology of Southeast Asia, 25, 325-350.

Lin, J. L., M. Fuller and W. Zhang (1985), Nature, 313, 444-449.

Maejima, W. (1984), Jour. Geosci., Osaka City Univ., 27, 105-118.

Sasajima, S. (1984), Mobile zone in Asia, ed. by K. Fujita, 239-256.

Shibuya, H., S. Sasajima and S. Yoshikura (1983), Jour. Geol. Soc. Japan, 89, 307-309.

Tsuchiya, N. (1982), Bull. Geol. Surv. Japan, 33, 381-387.

Zijderveld, J. D. A. (1967), Method in Paleomagnetism, ed. by Collinson et al., 254-286.

COUNTER-CLOCKWISE ROTATION OF TSUSHIMA ISLANDS, WESTERNMOST AREA OF SOUTHWEST JAPAN, INFERRED FROM PALEOMAGNETIC STUDY OF OLIGOCENE TO MIOCENE ROCKS

Naoto ISHIKAWA*, Masayuki TORII*, and Kazuhide KOGA**
*Department of Geology and Mineralogy, Kyoto University, Kyoto 606
**Department of Applied Geosciences, Nihon University, Tokyo 159

1. Introduction

Considerable paleomagnetic studies now outline the opening process of the Japan Sea (e.g., Otofuji et al., 1985); Southwest Japan is supposed to have undergone a clockwise rotation through about 50° at 15 Ma, possibly as a result of the formation of the Japan Sea (Otofuji et al., 1985). Regional extent of the rotated Southwest Japan has been roughly assumed from somewhere of the Kyushu Island to the central part of the Honshu Island (Otofuji et al., 1985). The pivot of the clockwise rotation has been tentatively assumed to be situated in the western margin of Southwest Japan (Otofuji and Matsuda, 1983). To investigate tectonic deformation of the westernmost area of Southwest Japan is indispensable to define the rotated area and further to give a clue to the opening mode of the Japan Sea.

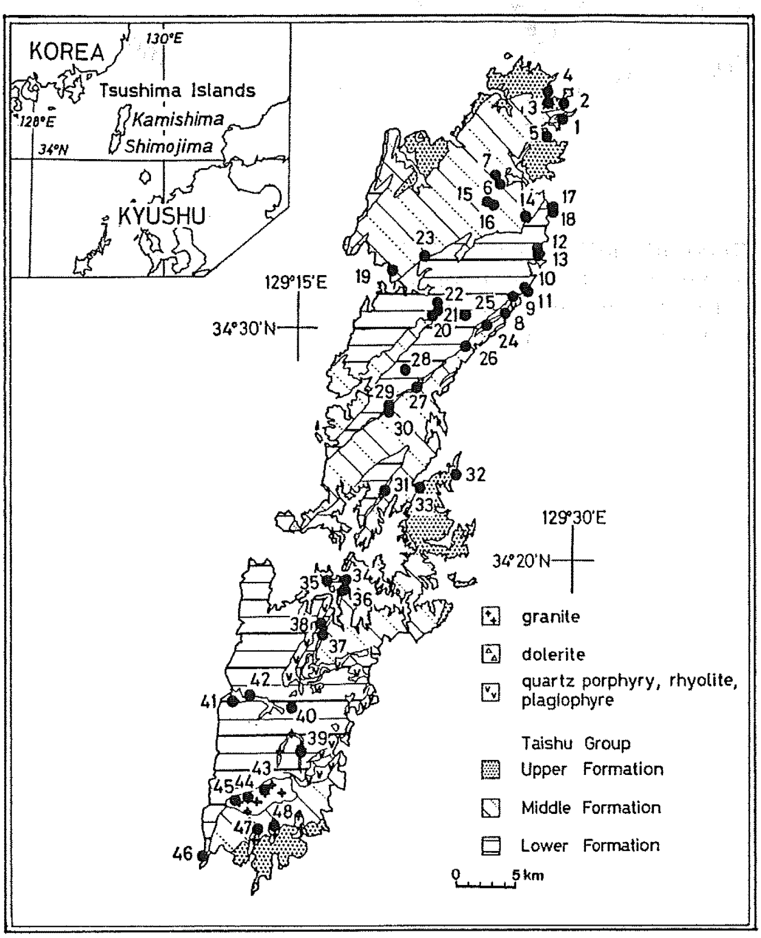

Fig. 1. Simplified geologic map and sampling site. (Compiled from MITI, 1972, 1973, 1974; Shimada, 1977; Chiba, 1984). Numerals indicate site number.

Tsushima Islands are located 150 km off northern Kyushu, and comprise mainly two big islands, Kamishima in north and Shimojima in south (Fig. 1). Thick marine sediments of the Late Oligocene to the Early Miocene in age (Taishu Group) are ubiquitously exposed and various types of intrusive rocks of the Early to Middle Miocene are sporadically distributed in the islands (Fig. 1, Table 1, 2). From viewpoints of their geologic ages, the paleomagnetic directions of the rocks may imply some tectonic events occurred in the Middle Miocene, possibly related to the opening of the Japan Sea. The previous paleomagnetic study was limited to granitic rocks from the southern part of Shimojima (Ito et al., 1980). Our study was, thus, designed to obtain paleomagnetic directions from various geologic units all over the the islands.

Table 1. The major stratigraphic units and their ages in Tsushima Islands (Compiled from MITI 1972, 1973, 1974,1975 and Shimada 1977).

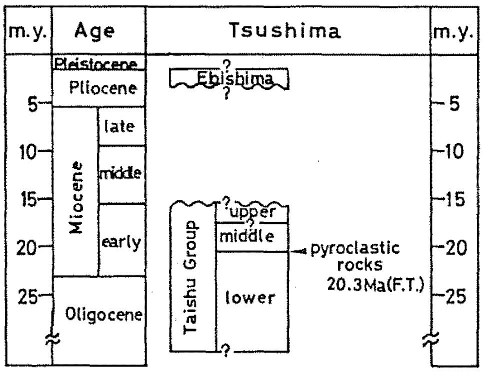

Table 2. The sequence of igneous activities in Tsuhsima Islands (Compiled from MITI 1972, 1973, 1974, Shimada 1977) and radiometric ages (*Takahashi and Hayashi, 1985; **Kawano and Ueda, 1966).

1st	Volcanic eruption to form pyroclastic seams	: tuff	20.3 Ma(F.T.) *
2nd	The intrusion of plagiophyre	: Pp	18.7 Ma(F.T.) *
3rd	The intrusion of quartz porphyry (and rhyolite)	: Qp	14.2 Ma(F.T.) *
4th	The intrusion of dolerite		
5th	The intrusion of granite	: Gr	14.9 Ma(F.T.) * 12 Ma(K-Ar) **

2. Geologic setting and sampling

The Taishu Group is a thick marine sequence of mudstone, shale and sandstone. The group is subdivided into three formations: Lower, Middle, and Upper Formation (Matsumoto, 1969; Shimada, 1977; Matsuhashi et al., 1974; MITI*, 1972, 1973, 1974; Chiba, 1984; Table 1). Intercalations of thin layers of pyroclastic rocks are found mainly in the lowermost part of the Middle Formation. The Taishu Group is intruded by many types of igneous rocks: plagiophyre, quartz porphyry, dolerite, rhyolite, and granite. Plagiophyre and quartz porphyry are found as a sill intruding into the Lower Middle Formaton near the horizons of the pyroclastic rocks. Some of the sills are folded concordantly with the Taishu Group. The dolerite, rhyolite and granite are intruding and intersecting the fold structure of the Taishu Group. The granite is considered to have intruded

* MITI; Ministry of International Trade and Industry

at the latest stage of the igneous activities (MITI, 1972, 1973, 1974; Shimada, 1977; Table 2).

The geologic age of the Taishu Group has been considered to range from Late Oligocene to Early Miocene on the basis of plant and molluscan fossils (Ishijima, 1954; Kanno, 1955; Takahashi, 1962; Kitamura, 1962; Masuda, 1970; Matsuo, 1970; Takahashi and Nishida, 1974). Several radiometric ages (Kawano and Ueda, 1966; Takahashi and Hayashi, 1985) indicate that the igneous activities occurred in the Early to Middle Miocene. The radiometric age estimation supports the geologic age deduced from fossil data.

Samples for the paleomagnetic study were collected at 48 sites: 35 sites from the Taishu Group and 13 sites from the intrusive rocks (Fig. 1). At each site, about ten hand samples were collected and oriented with a magnetic compass. Strike and dip angles of stratified rocks were measured.

3. Paleomagnetic analysis

More than two cylindrical specimens about 25 mm in hight were prepared from each hand sample. Remanent magnetizations were measured with a cryogenic magnetometer (ScT C-112) and partly with a spinner magnetometer (Schonstedt SSM-1A). Stability of natural remanent magnetization (NRM) was assessed by progressive demagnetizations of alternating field (AF) and thermal (TH) methods. Two or more pilot specimens, which showed representative initial NRM directions and intensities for each site, were submitted to the progressive demagnetizations. When a stable component of pilot specimens was recognized decaying toward the origin on vector-demagnetization diagram (Zijderveld, 1967), other specimens were also demagnetized at the appropriate level to determine the direction of the stable component.

Magnetic directions of sedimentary rocks and of some igneous rocks such as a sill were corrected for the tilt of the strata. When the fold axis was found to be plunged, magnetic vectors and bedding planes were firstly corrected so that the slant axis of the fold is made horizontal. Tilt correction of the plunge-corrected remanent direction were then carried out for the plunge-corrected bedding planes. Our field observations and detailed geological maps of MITI (1972, 1973, 1974) showed that the axial planes were almost vertical.

It was difficult to make an effective demagnetization for most of sedimentary rocks from the Taishu Group because of their weak magnetic intensity and irregular behaviors during the high temperature and/or high AF treatments. Fig. 2a is an example of the progressive demagnetization from the fine grained pyroclastic rock (site 34), which shows an exceptionally smooth change of vector end-points. Pilot specimens from site 42 (shale) were also found to have stable remanence. For these sites, AF cleaning was also effective to remove unstable components. The pilot specimens from site 14, 15, 16, and 35 were found to have stable components which were recognized as a trend toward the origin in the temperature range below 500° (Fig. 2b). The linear trends, however, were obscured in the higher tenperature range. Consequently, 6 of 35 sites of the Taishu Group were found to have stable remanent directions after the demagnetization experiments of pilot specimens.

All the pilot specimens from intrusive rocks (13 sites) yielded stable magnetic components by the demagnetizations. Two different types of demagnetization behaviors were observed during the progressive thermal demagnetizations. Magnetization of the pilot specimens from site 24 (plagiophyre), 32 (plagiophyre), 38 (quartz porphyry), 43 (granite), 44 (granite), and 47 (granite) comprises an essentially single stable component, while a small soft component was easily removed by the low

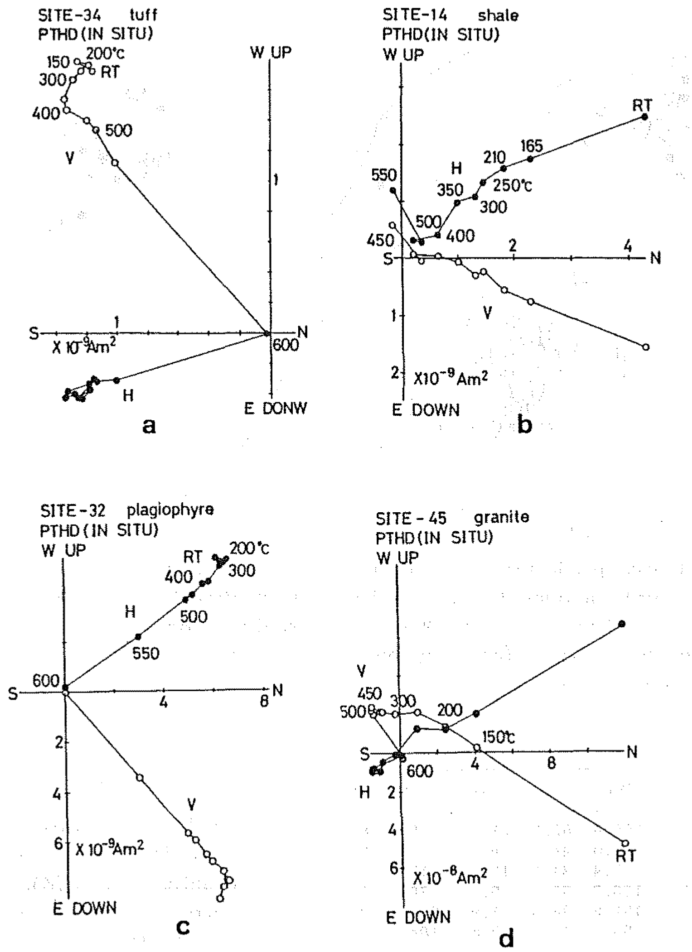

Fig. 2. Typical examples of progressive thermal demagnetization (PTHD) shown by vector-demagnetization diagram. Solid (open) circles are projection on horizontal (N-S vertical) plane. Unit of coordinate is bulk remanent intensity. a: tuff (fine grained pyroclastic rock) in the lower most part of the Middle Formation, b: shale of the Middle Formation, c: plagiophyre d: granite at Uchiyama.

temperature treatment (150 or 200°, Fig. 2c). For pilot specimens from the rest sites, site 1 (dolerite), 10 (plagiophyre), 25 (dolerite), 28 (dolerite), 39 (granite), 45 (granite), and 48 (granite), a stable component was recognized as a linear trend toward the origin only at a higher temperature range (400 to 550°, Fig. 2d). The same stable components were also recognized in progressive AF demagnetizations.

Site-mean directions from 19 sites were obtained after the partial demagnetizations and the tectonic corrections as mentioned above (Table 3, Fig. 3). The radius of 95% confidence limit (α_{95}) are all smaller than 30°. As shown in Fig. 3, site-mean directions make two tight clusters in the antipodal relation on the NW quadrant of lower hemisphere and SE quadrant of upper hemisphere. The antiparallel clusters can be assumed a record of the geomagnetic field in normal and reversed polarity. Several times of the geomagnetic field reversal are observed in order of stratigraphic sequence. The samples cover the age from the Late Oligocene to the Middle Miocene, that is, long enough to average out the paleo-secular variation. Two exceptional remanent directions are those of the dolerite (site 28) and the tuffaceous sandstone (site 35). We regard them

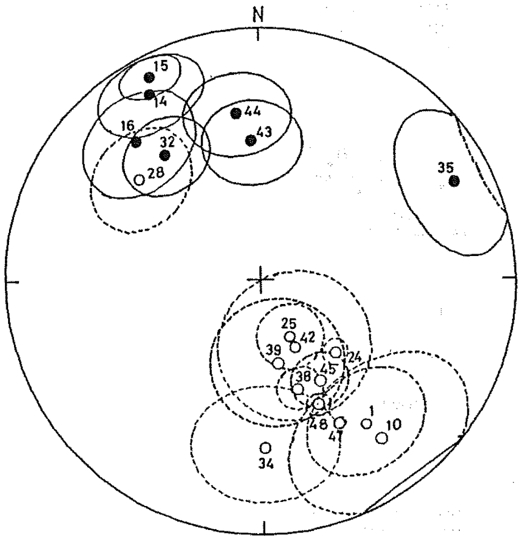

Fig. 3. Equal-area projection of site mean directions. Ovals around the directions indicate 95% confidence limit. Numerals denote site number. Solid (open) symbol is on the lower (upper) hemisphere.

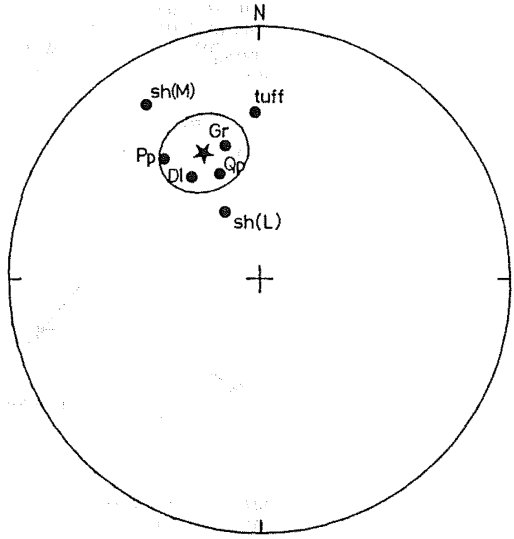

Fig. 4. Equal-area projection of formation-mean directions. Star symbol indicates the regional mean direction. Oval indicates 95% confidence limit.

Table3. Paleomagneticsite-mean directions.

LITH.	Site	Demag.	Dec.	Inc.	α_{95}	k	N	Corr.
Gr	39	500 °C	169.4	-62.5	21.0	8	8	-
	43	15 mT	-3.0	44.6	14.9	13	9	-
	44	15 mT	-7.4	34.1	15.4	10	11	-
	45	500 °C	150.2	-52.4	9.1	38	8	-
	47	30 mT	151.8	-36.3	1.9	854	8	-
	48	20 mT	156.0	-45.2	3.8	184	9	-
Dl	1	500 °C	144.2	-30.8	18.0	12	7	-
	25	550 °C	153.4	-69.7	10.5	22	10	-
	28	550 °C	-49.5	-38.3	16.3	9	11	-
Qp	38	400 °C	160.0	-53.4	7.1	48	10	-
Pp	10	550 °C	143.0	-23.1	26.7	9	5	B
	24	30 mT	134.3	-57.1	4.2	155	9	B
	32	400 °C	-36.5	38.2	13.3	22	7	-
sh(M)	14	300 °C	-29.9	15.9	14.6	10	12	P.B
	15	300 °C	-27.7	9.7	8.2	40	9	P.B
	16	400 °C	-41.4	28.3	17.4	13	7	P.B
t-ss	35	400 °C	63.7	15.3	19.9	6	12	P.B
tuff	34	500 °C	178.8	-34.3	21.2	9	7	P.B
sh(L)	42	500 °C	153.2	-65.7	24.2	7	7	B

LITH=lithology (Gr: granite, Dl: dolerite, Qp: quartz porphyry, Pp: plagiophyre, sh(M): shale of the Middle Formation, t-ss: tuffaceous sandstone of the Middle Formation, tuff: graind pyroclastic rock at the lowermost part of the Middle Formation, sh(L): shale of the Lower Formation).
Demag.=demagnetization level (in °C or mT). Dec., Inc.=mean declination and inclination in degrees. $_{95}$=radius of 95% confidence circle in degrees. k=precision parameter. N=number of specimens. Corr.=tilt correction (B: tilt correction relative to bedding plane, P.B.: tilt correction relative to the plunge-corrected bedding plane)

LITH.	Dec.	Inc.	α_{95}	k	N''
Gr	-14.0	44.7	37.2	47.3	6
Dl	-33.2	50.3	-	-	2
Qp	160.0	-53.4	-	-	1
Pp	-38.2	39.2	7.6	1074.9	3
sh(M)	-32.7	17.9	18.3	46.4	3
tuff	178.8	-34.3	-	-	1
sh(L)	153.2	-65.7	-	-	1
mean	**-23.6**	**44.5**	**13.5**	**20.8**	**7**

Table 4. Paleomagnetic formation-mean directions and regional-mean direction.

N''=number of site

as a record of transient feature of the geomagnetic field or as the results of improper tectonic corrections, and discard them from the further consideration.

Formation means were calculated from site means of a correlative rock unit by inverting reversed polarity directions to the normal (Table 4, Fig. 4). The regional mean direction was calculated from seven formation means, and depicted in Fig. 4; the mean declination is -23.6°, and the mean inclination is 44.5°, the radius of 95% confidence circle is 13.5° and precision parameter (k) is 21. This direction can be regarded as the characteristic paleomagnetic direction of the Late Oligocene to the Middle Miocene in Tsushima Islands.

4. Interpretation

Ito et al. (1980) previously obtained the westerly deflection of remanent directions of the granitic rocks collected at the southern part of Shimojima. They stressed a possibility that the deflected direction was caused by recording a transitional field during a polarity change of the geomagnetic field. The present study, however, revealed that the westerly deflection is, however, observed throughout all the stratigraphic units of the islands. An instantaneous record of the transitional field, thus, cannot be approved to explain the deflected paleomagnetic directions.

The westerly deflection of the paleomagnetic direction implies a tectonic displacement of Tsushima Islands. Because the pole position at 20 Ma (with 30 Ma window) determined from North Eurasia is not significantly apart from the geographic pole (Irving and Irving, 1982), we herein refer to the geographic pole as the expected geomagnetic pole in interpretation of the characteristic direction of Late Oligocene to Middle Miocene from Tsushima Islands. The mean inclination of the characteristic direction from Tsushima Islands is 9.5° shallower than that of the axial geocentric dipole field (54°). This difference is not significant because the 95% confidence limit of the mean inclination (ΔI)is calculated as 10.1° (Demarest, 1983). On the other hand, the mean declination is significantly deflected to the west: 23.6°±14.9°.

The westerly deflected declination suggests a counter-clockwise rotation of the islands through about 24°. The rotation postdates the intrusion of granites, which was dated as 12 Ma by K-Ar method (Kawano and Ueda, 1966) and as 14.9 Ma by fission track method (Takahashi and Hayashi, 1985). The present results suggest that Tsushima Islands was a tectonic block seperated from Southwest Japan; Tsushima Islands might be rotated counter-clockwise when the Japan Sea was opened.

Geologic structure of Tsushima Islands is characterized by an intensive folding of Taishu Group. The fold axes are trending in NE-SW direction and disposing left-hand en echelon (e.g., Matsumoto, 1969; Inoue, 1982). The fold system is assumed to have been formed by a horizontal compressive force in NW-SE direction at sometime between Middle and Late Miocene (Minami, 1979; Inoue, 1982; Hosino, 1984). Inoue (1982) and Koga (1982) proposed the models for the process of tectonic displacements in Tsushima Islands. Those models imply that the deformation of the Taishu Group occurred with a sense of a counter-clockwise rotation and a left-lateral translation along two large tectonic lines off the eastern and western coast of the islands (Murauchi, 1972; Tomita et al., 1975; Minami, 1979; Katsura and Nagano, 1976; Inoue, 1982; Hoshino, 1985). The present paleomagnetic result gives independently evidence for the above-mentioned tectonic models.

References

Chiba, T. (1984) Journal of the Nikkan Tunnel Study Group, **1**, 35-47.
Demarest, H. H. Jr. (1983) J. Geophys. Res., **88**, 4321-4328.
Hoshino, K., Kong, P. C. et al. (1984) ITIT Report (Project No.8014).
Irving, E. and G. A. Irving (1982) Geophys. Surv., **5**, 141-188.
Inoue, E. (1982) U.N. ESCAP CCOP Tech. Bull., **15**, 85-121.
Ishijima, W. (1951) J. Geol. Soc. Japan, **57**, 457-458.
Ito, H., K. Tokieda, and Y. Notsu (1980) Mem. Fac. Sci. Shimane Univ., **14**, 85-93.
Kanno, S. (1955) Trans. Proc. Palaent. Soc. Japan, N. S. **18**, 31-36.
Katsura, T. and M. Nagano (1976) J. Oceangraph. Soc. Japan, **32**, 139-150.
Kawano, Y. and Y. Ueda (1966) J. Pet. Min. Econ. Geol., **56**, 191-211.
Kitamura, N. (1962) Sci. Rept. Tohoku Univ., 2nd Ser. (Geol.), Spec. vol., **5**, 303-319.
Koga, K. (1982) Gruduation Thesis of Nihon University.
Masuda, K. (1970) Mem. Nat. Sci. Mus., **3**, 25-32.
Matsuhashi, S., K. Kiriu, Y. Nakashima, K. Fukumoto, T. Nemoto, and C.
Matsumoto, T. (1969) Mem. Nat. Sci. Mus., **2**, 5-18.
Matsuo, H. (1969) Mem. Nat. Sci. Mus., **3**, 19-24.
Minami, A. (1979) Jour. Japanese Assoc. Petrol. Technologists, **44**, 321-328.
MITI(Ministry of International Trade and Industry) (1972) Report on the regional geological survey, Tsushima-Kamigata district of the 1971's fiscal year.
MITI (1973) ibid. of the 1971's fiscal year.
MITI (1974) ibid. of the 1972's fiscal year.
MITI (1975) ibid. of the 1973's fiscal year.
Murauchi, S. (1972) Kagaku, **42**, 367-375.
Otofuji, Y. and T. Matsuda (1983) Earth Planet. Sci. Lett., **62**, 349-359.
Otofuji, Y., A. Hayashida, and M. Torii in: Formation of Active Ocean Margins, N. Nasu et al. eds., TERRAPUB, Tokyo (in press).
Otofuji, Y., T. Matsuda, and S. Nohda (1985) Nature, **317**, 603-604.
Shimada, N. (1977) Mem. Fac. Sci. Kyushu Univ., Ser. D, **23**, 417-480.
Takahashi, K. (1969) Bull. Fac. Lib. Arts, Nagasaki Univ., Nat. Sci., **10**, 67-82.
Takahashi, K. and T. Nishida (1974) Bull. Fac. Lib. Arts, Nagasaki Univ., Nat. Sci., **15**, 15-20.
Takahashi, K. and M. Hayashi (1985) Bull. Fac. Lib. Arts, Nagasaki Univ., Nat. Sci., **25**, 9-19.
Tomita, S., A. Yamashita, K. Ishibashi, T. Miki, R. Takahashi, T. Shuto, H. Urata, I. Hashimoto, E. Honza, and C. Igarashi (1975) Sci. Rep. Dep. Geol., Kyushu Univ., **12**, 77-90.
Zijderveld, J. D. A., (1967) In: Methods in Paleomagnetism, D. W. Collinson, K. M. Creer, and S. K. Runcorn eds. Elsevier, Amsterdam, 254-268.

(to be submitted to J. Geomagn. Geoelectr.)

A PALEOMAGNETIC RECONNAISSANCE OF PERMIAN TO CRETACEOUS SEDIMENTARY ROCKS IN SOUTHERN PART OF KOREAN PENINSULA

Yo-ichiro OTOFUJI*, Kwang Ho KIM**, Hiroo INOKUCHI*, Hayao MORINAGA***, Fumiyuki MURATA***, Hiroshi KATAO*† , and
Katsumi YASKAWA*

* Department of Earth Sciences, Faculty of Science, Kobe University, Kobe 657, Japan
** Department of Earth Science Education, College of Education, Chonbuk National University, Chonju, 520, Korea(Seoul)
Division of Environmental Science,
*** The Graduate School of Science and Technology, Kobe University, Kobe 657, Japan

Paleomagnetic results have been obtained from ten Korean sedimentary rock formations ranging in age from Permian to Cretaceous (Fig. 1). The magnetizations of almost all the rocks from Permian to Jurassic formations have been severely overprinted (Fig. 2). Estimation of paleomagnetic direction of the period between Permian and Jurassic is hindered by this. The Cretaceous rocks from the Gyeongsang Supergroup, however, have recorded the paleomagnetic direction at the period of formation of sedimentary rocks during Cretaceous. Some strata in the Hasandong Formation of lower part of the Gyeongsang Supergroup show the reversed magnetization which is presumably ascribed to reversedly magnetic polarity epoch of M-series in Mesozoic polarity scale. Paleomagnetic direction of the upper part of the Gyeongsang Supergroup (Middle to Late Cretaceous) is estimated to be Dec=28.4°, Inc=58.2° and α_{95} =6.4°. The pole position of Middle to Late Cretaceous obtained for the Korean Peninsula (202°E, 67°N) is in good agreement with other Cretaceous data for Asian continent, implying that the Korean Peninsula has not been subjected to rotational movement relative to the Asian continent since Cretaceous.

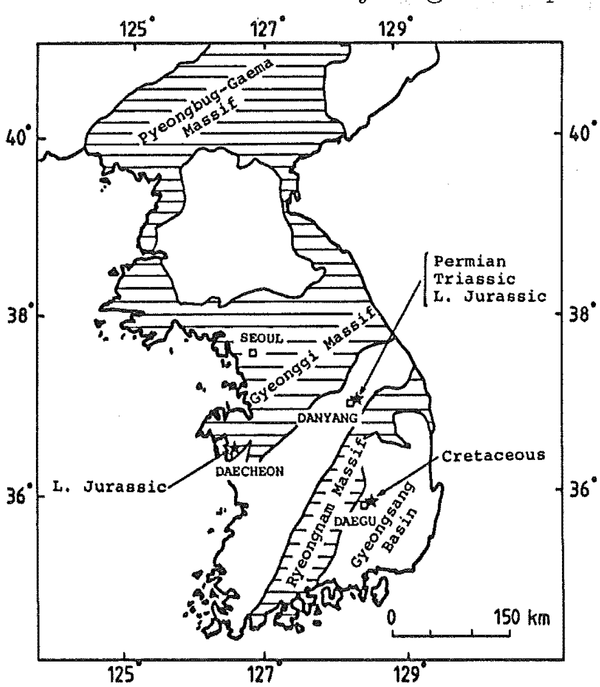

Fig. 1 Site map with major massifs in the Korean Peninsula shown schematically.

† Present address: Earthquake Research Institute, University of Tokyo, Tokyo

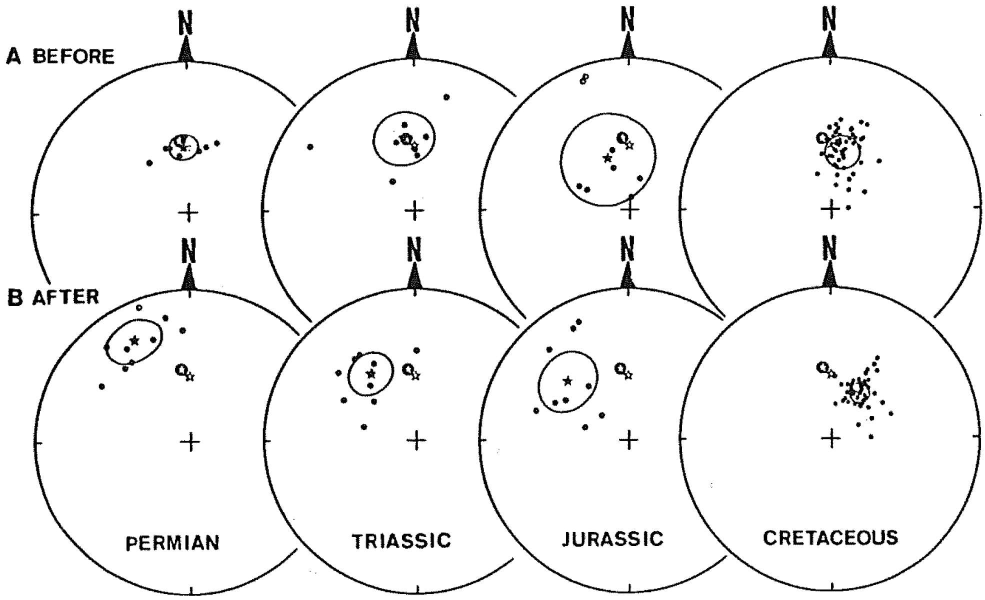

Fig. 2 Equal area plot of site mean magnetization directions after alternative field demagnetization (the closed star) and 95 % confidence limits of four period from the Permian to Cretaceous strata: (A) before bedding correction and (B) after bedding correction. The solid (open) symbols refer to the lower (upper) hemisphere. The open star and circled star represent the axial dipole and present field directions, respectively.

(In press in J. Geomag. Geoelectr.)

MAGNETIZATION OF PELAGIC CLAY IN PENRHYN BASIN, SOUTH PACIFIC: EVIDENCE OF MAJOR AEOLIAN ORIGIN

Toshitsugu YAMAZAKI and Akira NISHIMURA

Geological Survey of Japan, Yatabe, Tsukuba, Ibaraki, 305, Japan

Introduction

In large area of the Pacific except the region shallower than the CCD (Carbonate Compensation Depth) and except biogenic high productive province near the equator or high latitude, pelagic clay (In this paper this term is defined as deep-sea pelagic sediments which has no calcareous or siliceous fossil) has been deposited very slowly, less than few meters per million years. It is well known that calcareous or siliceous fossil bearing deep-sea clay has stable initial remanent magnetization and its secondary components can be easily cleaned by alternating field (AF) demagnetization technique. Paleomagnetic studies of these sediments have yielded many fruitful results, especially about the nature of the geomagnetic field and magnetic stratigraphy. On the contrary, several authors reported that the pelagic clay in the middle latitude of the North Pacific has large secondary magnetization which cannot be removed by AF demagnetization (Opdyke and Foster, 1970; Kent and Lowrie, 1974; Johnson et al., 1975; Prince et al., 1980), and no valuable paleomagnetic information could be obtained from them.

In this paper, we show that thermal demagnetization is effective to remove the secondary magnetization of the pelagic clay. Then we discuss about the paleolatitude of the Penrhyn Basin and about the origin of the pelagic clay on basis of the characteristics of magnetization.

Sampling and experimental results

Two piston cores of about 4 m in length, Core P411 (13°06.16'S, 159°18.01'W) and Core P412 (13°04.40'S, 159°17.31'W) were taken from the Penrhyn Basin in the South Pacific during research cruise GH833 of R/V Hakurei-maru. The depth of the basin is about 5200 m, well below the CCD there, and the age of the basement is estimated to be the late Cretaceous, about 90 Ma (Sclater et al., 1981). Lithology of the cores is pelagic clay since this area is off the equatorial biogenic high productive zone. These cores have a visually remarkable hiatus with manganese crust at the depth of 2.4 m and 0.4 m, respectively. Below the hiatus, consolidation has gone on for surface sediments. That is why the cores penetrated only less than 4 m. Calcareous or siliceous microfossil, which is usually used for age determination of deep-sea sediments, is not contained at all. We can get rough age assignments of pelagic clay by ichthyoliths (microscopic fish skeletal debris). Compared with Doyle and Riedel (1979), the age of the sediments below the hiatus is estimated to be the Oligocene (P411) and the late Cretaceous to the early Paleocene (P412), and above the hiatus it is not older than the middle Miocene (Table 1). The age of the formation of the hiatus, therefore, may be the early Miocene.

Specimens for paleomagnetic measurements were taken from the half-splitted cores in succession using cubic plastic case of about 10 cm^3 immediately after core-recovery. Care was taken not to be dehydrated before measurements. A SCT's cryogenic rock magnetometer was used for measurements of the remanence. Fig. 1 shows the NRM direction of Core P411 before the partial AF demagnetization by a three axis tumbler system

Table 1 Occurrences of ichthyoliths in three samples from Core P411 and Core P412.

SAMPLE		dry weight of analyzed sample	total number of triangle-shaped	Elliptical with line across	Circular with line across	Large triangle saw-toothed margin	Triangle with high inline apex	Small dendritic row radiating lines	Rectangular saw-toothed	Flexed narrow triangle 120-128	Flexed triangle 102-112	Curved triangle pointed margin	Triangle crenulate	Rectangular irregularly saw-toothed	Flexed triangle shallow inbase	Asymmetrical peak wide depression	Wide triangle straight inbase	Triangle short wing	Triangle pointed margin ends	Pointed and skirted	Prominence with wye-line	Poligonal cavity	Kite-shaped longitudinal line	Straight triangle keeled edges	Narrow triangle sharply pointed	Triangle smooth surface	Spiky palmate
P411	221 cm	23.9 g	294	X	X	X	X	X	X		X	X	X	X	X	X	X		X			X	D				
	281	26.0	138							X					X			X					X				D
P412	210	19.4	43																	X	X		X	X	X	X	X

X; present
D; derived

(a) and after that (b). Declination is relative because the cores were not oriented horizontally. Positive inclination means reversed polarity as the Penrhyn Basin is on the southern hemisphere. As for upper 1.5 m, the quality of the data has made some improvement by the AF demagnetization, but below it the scatter of the direction has increased. Overprint of the present geomagnetic field direction is not removed effectively. The result of the progressive AF demagnetization (Fig. 2) revealed that more than 90 % of the initial intensity was removed only a peak field of 5 mT, and that not only that the secondary component was eliminated insufficiently but also it seems that an artificial remanence which may be anhysteretic origin was attached. These features of the remanence of the pelagic clay in the Penrhyn Basin is similar to those in the middle latitude of the North Pacific (Opdyke and Foster, 1970; Prince et al., 1980).

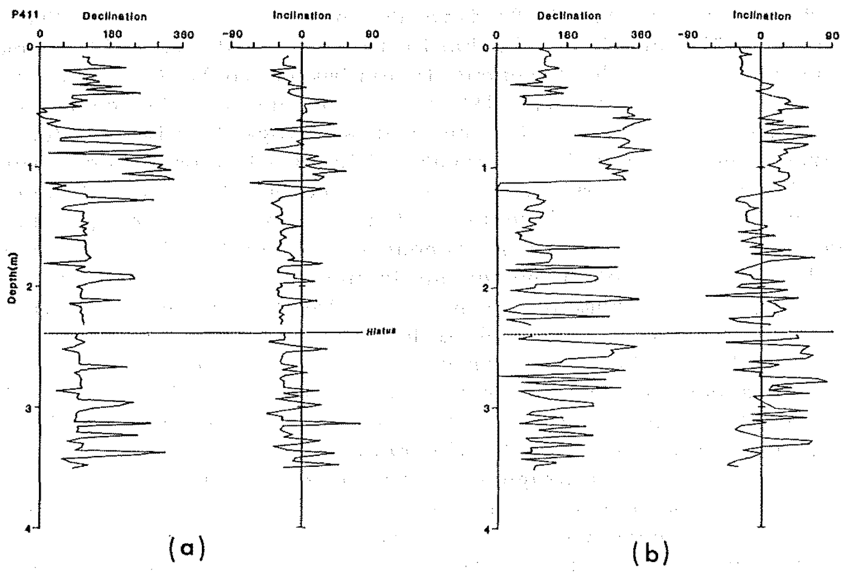

Fig. 1 Direction of the remanence of Core P411 (a) before and (b) after partial AF demagnetization of 10 mT. Declination is relative.

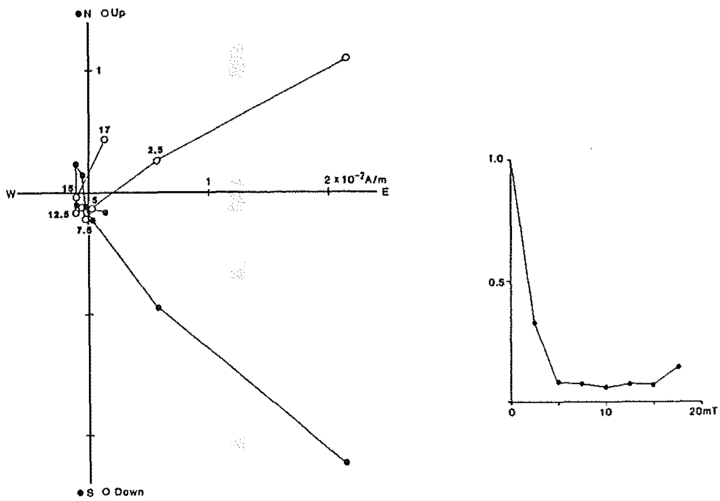

Fig. 2 Vector orthogonal projection of the remanence during progressive AF demagnetization of red clay (P411 282cm). Numbers along vertical component represents a peak field of AF demagnetization in mT.

Next, we attempted thermal demagnetization for the purpose of eliminating the overprint. The pelagic clay below the hiatus which seems to have been affected by the overprint more seriously was treated more elaborately. Residual field in the furnance of the thermal demagnetization apparatus in our laboratory is less than 100 nT during a cooling cycle. A part of experiments was conducted using the furnance of Kyoto University which has the residual field of less than 10 nT. Specimens were heated in air. When wet specimen dries, it shrinks approximately isotropically without serious deformation or being cracked. Fig. 3 illustrates the example of the progressive thermal demagnetization studies. Strong secondary component of normal polarity is effectively

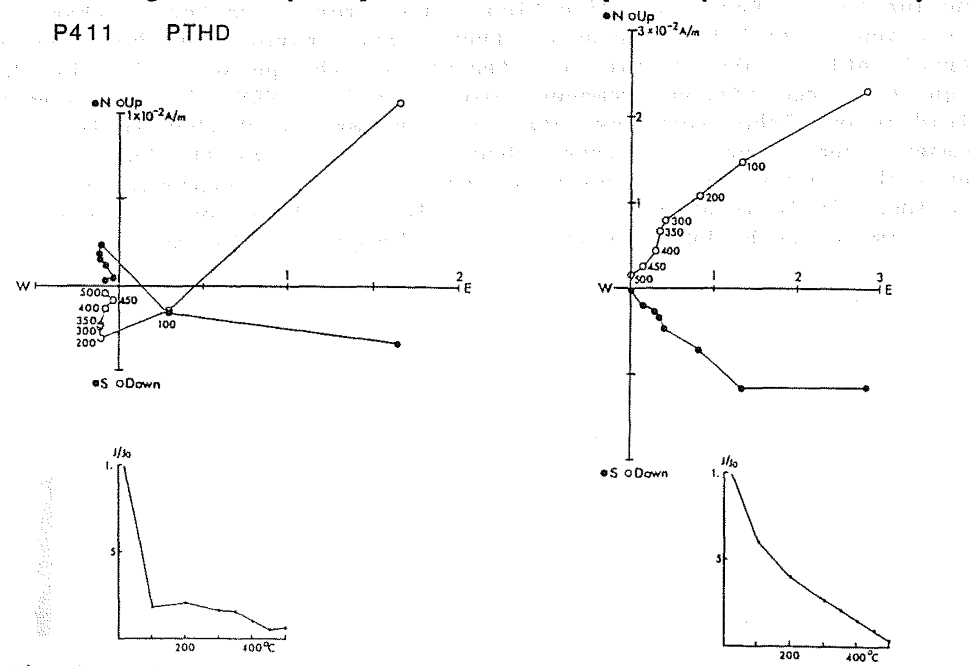

Fig. 3 Typical examples of progressive thermal demagnetization of pelagic clay (P411 317cm (left), 340cm (right)) shown on vector orthogonal projection. Numbers along vertical component represents temperatures (°C). Horizontal component is relative.

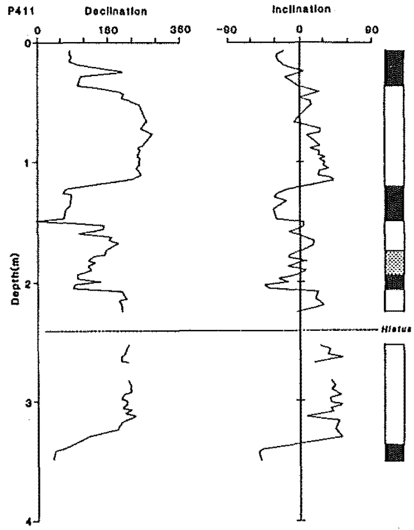

Fig. 4 Direction of the remanence of Core P411 after thermal demagnetization of 300 °C. The right column represents the polarity. Declination is relative.

removed up to 300 °C. Two specimens in this figure showed nearly the same normally magnetized direction before the demagnetization, but it separated into normal and reversed direction after the treatment above 300 °C. We adapted thermal demagnetization of 300 °C to the whole Core P411 (Fig. 4). As compared with Fig. 1, the effectiveness of the thermal demagnetization is clear. The Quality of the data has been much improved and now we can assign the polarity. Core P412 showed the same property (Fig. 5). Thermal treatment of 300°C on the whole core which showed present field direction could isolate stable normal and reversed direction of steeper inclination. Reversed directions are more scattered than normal directions, probably because there are minor residual secondary magnetization. One distinctive feature of the pelagic clay is that it acquires large viscous remanent magnetization (VRM) in the geomagnetic field in our laboratory instantaneously no matter whether it is partially demagnetized or not. It takes about 5 minutes that the VRM decays to a negligible level in the magnetic shield of the cryogenic magnetometer (residual field is about 50 nT). The origin of the secondary magnetization is estimated to be VRM from that before demagnetization specimens which

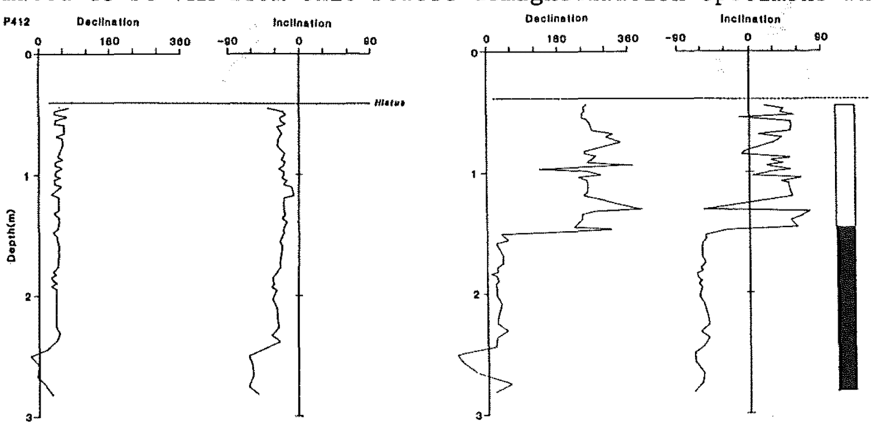

Fig. 5 Direction of the remanence of Core P412 (a) before and (b) after thermal demagnetization of 300 °C. Declination is relative.

have large secondary magnetization have nearly the same inclination as expected from an axial dipole hypothesis at the cored site independently to the age of the sediments, and from that large VRM easily adheres in the geomagnetic field in the laboratory.

Discussion

The Penrhyn basin has moved northwestward with the motion of the Pacific plate. At the ages of the pelagic clay below hiatus, the Oligocene (P411), the late Cretaceous to the early Paleocene (P412), the latitude of the cored sites was higher in the southern hemisphere than that of the present (13°S). Absolute motion of the Pacific plate since the late Cretaceous has not yet entirely been made clear though several models have been presented (Clague and Jarrard, 1973 together with Dalrymple et al., 1977; Lancelot and Larson, 1975; van Andel et al., 1975). Average inclination can be calculated from Fig. 4 and 5; about 25° for the pelagic clay above the hiatus of Core P411, about 40° for below the hiatus of Core P411 and about 55° for Core P412, which correspond to the paleolatitude of 13°, 23° and 36°, respectively. The models give nearly the same paleolatitudes of around 20°S for within the range of the Oligocene, which agrees with our results. For the age of the Core P412, the late Cretaceous to the early Paleocene, however, there are some differences among these models. Calculated paleolatitudes at 70 Ma are 38° (van Andel et al, 1975), 33° (Lancelot and Larson, 1975) and 28° (Clague and Jarrard, 1973 together with Dalrymple et al, 1977). The former two models are in accordance with ours but the latter is not. More paleomagnetic studies on the South Pacific are needed to improve the absolute motion model since those models were constructed on the basis of the data (hot spots, sedimentary facies, paleomagnetism) from mainly the North Pacific.

Next, we discuss about the origin of pelagic clay. Recently, the hypothesis that the source of the pelagic clay in the middle latitude of the North Pacific is for the most part atmospherically transported dust out of Asia is presented from atmospheric chemistry (Uematsu et al., 1985) and mineralogy (Blank et al., 1985). All the characteristics of the magnetization of the pelagic clay in the Penrhyn Basin mentioned in this paper have strikingly close resemblance to that of Chinese loess deposits of aeolian origin (Torii et al., 1983; Heller and Tungsheng, 1984). In brief, both sediments have the large secondary overprint of the present field which is thought to be VRM in origin which can be removed by thermal demagnetization up to 300 °C and cannot be eliminated sufficiently by AF demagnetization. It is considered that this affinity is not the one acquired by chance among the post-depositional alteration process in the different environment between on land and in deep-sea. We believe that it reflects the common feature of magnetic minerals in aeolian dust. The source of the pelagic clay in the South Pacific may be arid regions of continents in the southern hemisphere. It is difficult to consider that little difference in the deep-sea pelagic environment between near the equator and the middle latitude of the Pacific causes much variation in post-depositional alteration process which arises the large secondary overprint only in the pelagic clay in the middle latitude. It can be explained by the differences in origin of the sediments. Pelagic clay in the middle latitude is majorly aeolian origin which has large secondary magnetization. In the equatorial biogenic high productive zone the sediments have small ratio of aeolian inputs because the fluxes of aeolian dust are much smaller than those of the middle latitude (Uematsu et al.,

1985) but the sedimentation rate is higher (Opdyke and Foster, 1970). Then, the features of aeolian sediments are masked.

Conclusion

Pelagic clay with no calcareous or siliceous fossil has deposited since the late Cretaceous in the Penrhyn Basin in the South Pacific. Previous workers showed that the pelagic clay in the North Pacific has large secondary magnetization which cannot be removed sufficiently by AF demagnetization. The pelagic clay in the Penrhyn Basin has the same feature. It is revealed that initial stable direction can be isolated by thermal demagnetization up to 300 °C. Lancelot and Larson's (1975) and van Andel and other's (1975) models of absolute motion of the Pacific plate since the late Cretaceous agree with our paleolatitudes derived from the inclination of the remanence and age assignments from ichthyoliths. The characteristics of the magnetization of pelagic clay strikingly resemble to those of Chinese loess deposits of aeolian origin. This is an supporting evidence of the recently presented hypothesis that atmospherically transported dust is a major source of pelagic clay in the middle latitudes.

References

Blank, M., M. Leinen and J.M. Prospero (1985) Nature, 314, 84.

Clague, D.A. and R.D. Jarrard (1973) Geol. Soc. Amer. Bull., 84, 1135.

Dalrymple, G.B., D.A. Clague and M.A. Lanphere (1977) Earth Planet. Sci. Lett., 37, 107.

Doyle, P.S. and W.R. Riedel (1979) SIO/REF 79/16, 1.

Heller, F. and L. Tungsheng (1984) Geophys. J. R. astr. Soc., 77, 125.

Johnson, H.P., H. Kinoshita and R.T. Merrill (1975) Geol. Soc. Amer. Bull., 86, 412.

Kent, D.V. and W. Lowrie (1974) Jour. Geophys. Res., 79, 2987.

Lancelot, Y. and R.L. Larson (1975) Initial Rept. DSDP, 32, 925.

Opdyke, N.D. and J.H. Foster (1970) Geol. Soc. Amer. Memoir, 126, 83.

Prince, R.A., G.R. Heath and M. Kominz (1980) Geol. Soc. Amer. Bull. Part 2, 91, 1789.

Sclater, J.G., B. Parsons and C. Jaupart (1981) Jour. Geophys. Res., 86, 11535.

Torii, M., L.P. Yue, A. Hayashida, K. Maenaka, T. Yokoyama, Y.Y. Wang and S. Sasajima (1983) Some Problems on the Quaternary Chronology of Chinese Loess with Special Emphasis on Luochuan Loess Sequence of Shaanixi Province (Ed. Sasajima S. and Wang Y.Y) 15. (Japanese with English Abst.)

Uematsu, M. and R.A. Duce (1985) Jour. Atmos. Chem., 3, 123.

van Andel, T.H., G.R. Heath and T.C. Moore, Jr. (1975) Geol. Soc. Amer. Memoir, 143, 1.

PALEOMAGNETISM OF MIOCENE ROCKS IN THE WESTERN AREA OF BARAGOI, NORTHERN KENYA

Tadashi NAKAJIMA* and Masayuki TORII**

* Geological Laboratory, Faculty of Education, Fukui University, Fukui 910
** Department of Geology and mineralogy, Faculty of Sience, Kyoto University, Kyoto 606

1. Introduction

Field surveys focusing on discoveries of Miocene hominoids and geological and paleontological analyses of the paleoenvironments of the homonoids have been conducted in Kenya since 1980 (Ishida et al., 1982; Ishida, 1984). In 1984 the field survey of the third Japan-Kenya expedition was carried out in the Samburu Hills, the Nachola area, and the middle reaches of the Baragoi River, west of Baragoi, Kenya, where Miocene hominoid fossils were discovered during the second expedition in 1982 (Ishida et al., 1984). In the 1984 field season Miocene volcanic rocks were intensively collected for paleomagnetic measurements and K-Ar age determinations. This area is underlain by Miocene and Pliocene volcanic rocks composed of basalt, trachyte and alkali ryolite intercalated with sedimentary rocks,

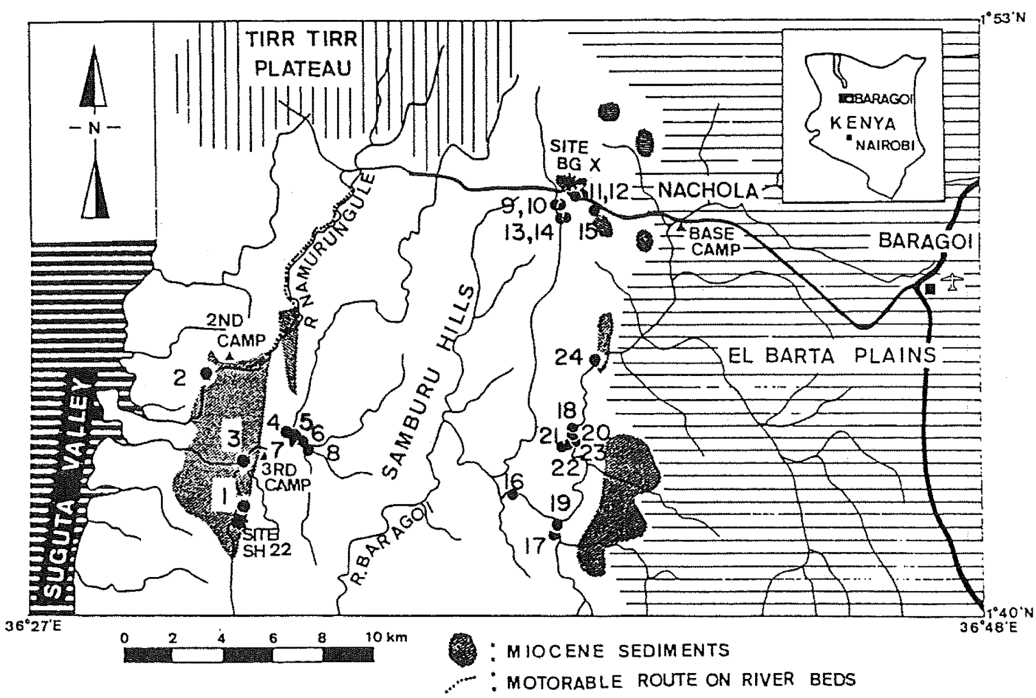

Fig. 1 Investigated area (modified from Ishida, 1982). Solid dots show sampling localities. Numbers correspond to Site Nos. in Table 1. Miocene hominoid fossils were discovered from sites SH 22 and BG X.

Table 1. Paleomagnetic results from the Nachola and Aka Aiteputh Formations.

Site	Rock Type	K-Ar age (Ma) (Itaya,1986) (*Matsuda et al., 1984)	Strike (°)	Dip (°)	ODF (Oe)	N	Dc (°E)	Ic (°down)	α_{95} (°)	k	Lat (°N)	Lon (°E)	dp (°)	dm (°)
AKA AITEPUTH FORMATION														
(Samburu Hills)														
1)	basalt	10.3, 10.3	N03E	30W	150	6	214.9	-16.2	5.0	181.6	-54.6	294.6	2.7	5.2
2)	basalt	12.0*	N20E	20W	570°C	3	187.0	0.2	14.2	76.7	-82.8	321.4	7.1	14.2
3)	basalt	12.8, 12.7	N30E	30W	150	7	180.8	- 1.6	3.7	263.9	-88.8	355.7	1.9	3.7
4)	basalt	13.3, 13.3	N05W	18W	350	3	196.4	-10.1	39.3	10.9	-73.3	294.6	20.1	39.8
5)	sodalite trachyte		N20E	20W										
6)	basalt	13.6, 13.6	N25E	20W	200	8	357.5	-17.9	9.1	37.8	78.8	229.3	4.9	9.4
7)	basalt		N20E	20W	520-570°C	6	356.3	9.6	8.7	24.0	85.2	346.6	4.4	8.8
8)	basalt	14.5, 14,2	N25E	20W	300	4	244.4	-44.1	21.6	18.9	-23.7	279.0	17.0	27.1
(Nachola Area)														
9)	basalt	10.3,10.5,11.8*	N90W	10S	100	9	13.2	4.6	7.3	50.7	76.8	124.3	3.7	7.3
10)	welded tuff		N90W	10S	100	10	12.9	4.3	4.3	126.9	77.1	125.0	2.2	4.3
11)	basalt	9.73,9.66,10.1*	N12W	13W	100	8	3.1	0.0	5.1	119.3	86.4	157.0	2.6	5.1
12)	sandstone		N-S	5W										
13)	tuff		N-S	5W	100	5	10.3	-17.8	9.6	64.2	75.0	173.6	5.2	10.0
14)	tuff		N-S	5W	400	4	3.9	-44.0	5.0	342.0	62.1	209.1	3.9	6.3
NACHOLA FORMATION														
(Nachola Area)														
15)	trachyte	13.4,13.4	N42E	12N	500	7	192.4	23.3	30.7	4.8	-71.4	355.6	17.4	32.7
(Middle Reaches of the Baragoi River)														
16)	trachyte	13.4, 13.4	N25E	15W	350	9	204.8	56.4	14.3	13.9	-45.0	8.3	14.9	20.6
17)	aphiric trachyte	13.5,14.1	N33E	12W	500	7	200.4	52.3	17.1	13.3	-50.4	9.3	16.1	23.5
18)	welded tuff	16.9,16.8	N-S	15W	200	10	354.0	-13.1	5.3	84.0	79.7	252.2	2.8	5.4
19)	tuff		N30E	20W	100	10	0.2	-13.0	16.2	9.9	81.7	215.3	8.4	16.5
20)	basalt		N10W	5W	300	8	315.4	-22.4	14.4	15.8	43.7	288.7	8.1	15.3
21)	basalt	16.3, 16.9	N10W	5W	100	7	335.1	-15.3	11.7	27.4	63.4	285.4	6.2	12.0
22)	basalt	17.3	N10W	5W	100	7	355.1	-36.2	4.3	193.6	67.6	228.8	2.9	5.0
23)	basalt		N10W	5W	500	5	188.8	-28.9	33.4	6.2	-73.8	248.5	20.2	36.8
24)	porphyritic basalt	16.9, 16.8	N30E	8W	100	10	356.1	-31.6	11.4	18.8	70.8	228.0	7.2	12.8

ODF: optimum demagnetization field (1 Oe= 0.1 mT), N: number of samples, Dc: declination after tilt correction, Ic: inclination after tilt correction, α_{95} and k: Fisher's statistic parameters, Lat and Lon: latitude and longitude of VGP, dp and dm: error angles of VGP. Data of sites 2 and 7 are referred to Matsuda et al. (1984).

unconformably overlying Precambrian metamorphic complex. The Miocene rocks are divided into the Nachola, the Aka Aiteputh, and the Namurungule Formations in ascending order, the stratigraphy of which was studied in detail by Makinouchi et al. (1984) and Sawada et al. (1986). In this paper we describe the preliminary paleomagnetic results obtained from the Nachola and the Aka Aiteputh Formations.

2. Samples

Paleomagnetic samples were collected by hand sampling, and independently oriented using a magnetic compass. Strike and dip of the strata were also measured in the field for a tilt correction of the remanent magnetic direction. Fig. 1 shows the sampling localities, where rock samples for K-Ar age determinations were also collected by Itaya (1986). These rock types, K-Ar ages and tiltings of the strata are listed in Table 1. The K-Ar ages of the Nachola and the Aka Aiteputh Formations range from 17 Ma to 13 Ma and from 14 Ma to 9 Ma, respectively. These formations gently dip west by angles of less than 30°.

3. Measurements

Remanent magnetization was measured with an astatic magnetometer at Fukui University and a Schonstedt SSM-1A spinner magnetometer at Toyama University. Three to four pilot samples from each site were first tested by progressive demagnetization method in alternating field (AF) in steps of 50 or 100 Oe up to a maximum field of 500 Oe. Results of the progressive AF demagnetization of typical samples are illustrated in Fig. 2. Most samples show considerable changes in magnetic direction

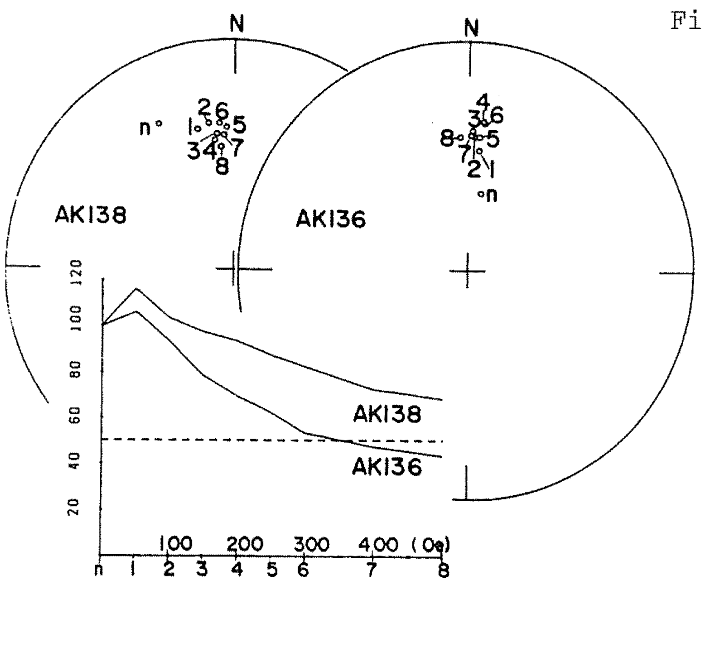

Fig. 2 AF demagnetization plots for typical samples (AK 136 and AK138) showing decay of normalized remanent intensity and changes in direction on equal area projection of upper hemisphere. n: 0 Oe, 1: 50 Oe, 2: 100 Oe, 3: 150 Oe, 4: 200 Oe, 5: 250 Oe, 6: 300 Oe, 7: 400 Oe, 8: 500 Oe.

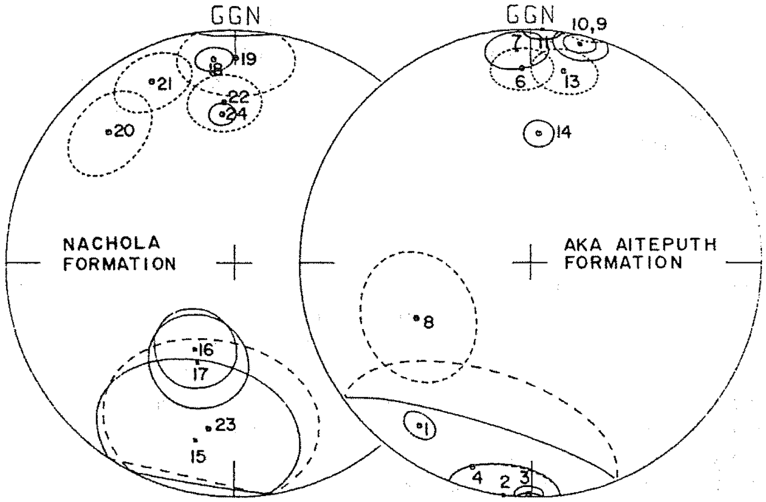

Fig. 3 Site mean directions with α_{95} values plotted on equal area projection. Solid symbols and lines are on lower hemisphere, and open symbols and dashed lines on upper hemisphere. Numbers correspond to Site Nos. in Table 1.

on beginning of the AF treatment, such as in peak fields of 50 or 100 Oe. The soft component of remanent magnetization which was cleaned by the AF up to 100 Oe can be interpreted as a secondary overprint of viscous remanent magnetization. No remarkable change, however, is observed in magnetic direction by the AF demagnetization in fields above 100 Oe. The stable directions with respect to the AF can be regarded to show those of the primary magnetization. The optimum demagnetization field (ODF) was selected from the results of the AF cleaning at 100 to 500 Oe on the basis of the smallest value of α_{95} (Fisher, 1953). The rest of samples for each site was demagnetized at the ODF. Site mean directions cleaned by the ODF and corrected for tiltings of strata are tabulated in Table 1. We could not obtain reliable paleomagnetic data from sites 5 and 12 because intensities of remanent magnetization of the samples were too week to be measured after the AF demagnetization. The table includes the data of sites 2 and 7 reported by Matsuda et al. (1984). Their samples, of which magnetic stabilities were confirmed to be stable by progressive thermal demagnetization method, were collected from the Aka Aiteputh Formation in the 1982 field season of the second Japan-Kenya expedition.

4. Magnetostratigraphy

The site mean directions together with their α_{95} values are plotted on the equal area projection diagram in Fig. 3. These directions are grouped into two separate clusters in antipodal directions, which are regarded as of normal and reversed polarity, respectively. The stratigraphic distribution of the normal and reversed polarity sites is illustrated in Fig. 4. The Nachola and the Aka Aiteputh Formations are magnetostratigraphically divided into two and three zones, respectively, which are called Magneto-zones and numbered from I to V in ascending

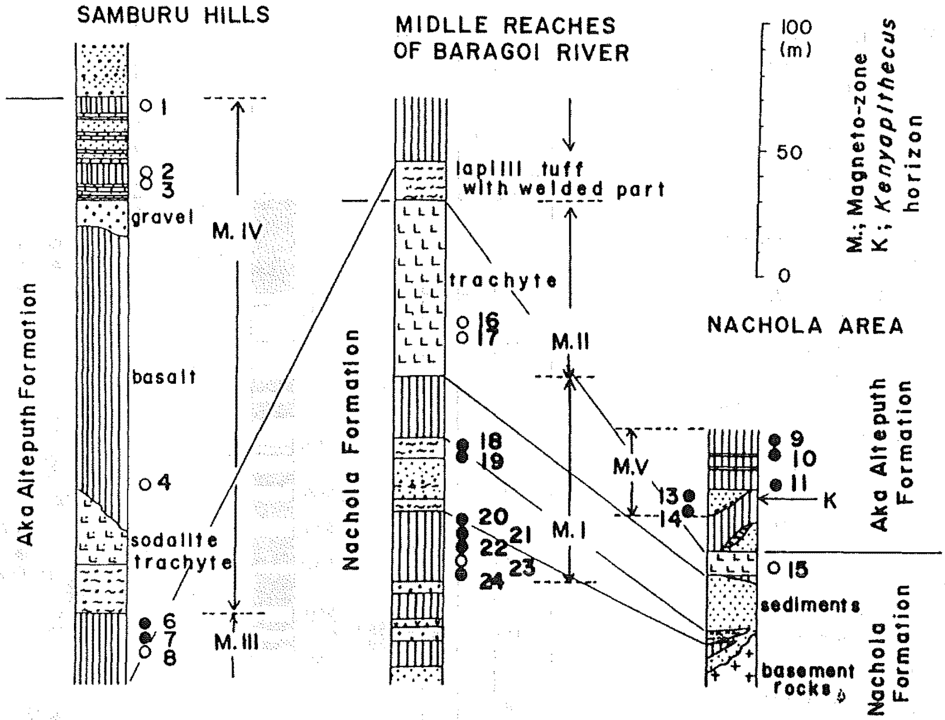

Fig. 4 Magnetostratigraphy for the Nachola and Aka Aiteputh Formations. Columnar sections are simplified from Sawada et al., 1986. Solid and open circle symbols show normal and reversed polarities, respectively. Numbers correspond to Site Nos. in Table 1.

order as shown in Fig. 4. Magneto-zones I, III and V are typified by a dominance of normal polarity sites, whereas Magneto-zones II and IV are composed of reversed polarity sites. Fig. 5 shows the tentative correlation of the magneto-zones with the geomagnetic reversal time scale (GRTS) (Harland et al., 1982) based on the K-Ar ages (Table 1) The normal Magneto-zones (I, III and V) are determined by well-concentrated paleomagnetic data. The reversed zones (II and IV), however, consist of a limited number of data compaired with the normal zones. Thus we consider that the correlation of the normal zones with the GTRS are more reliable than that of the reversed zones. Magneto-zone I is assigned to the polarity chron 5C ranging from 16.98 Ma to 16.20 Ma (Harland et al., 1982), Magneto-zone III to the chron 5AC ranging from 14.04 Ma to 13.65 Ma, and Magneto-zone V to the older part of the chron 5 in a period between 10.30 Ma and 9.78 Ma.

The horizon of the hominoid fossil: *Kenyapithecus* which was discovered in the 1982 Japan-Kenya expedition (Ishida et al., 1984) is assigned to Magneto-zone V in the period between 10.30 Ma and 9.78 Ma as can be observed in Fig. 4. The age estimated from the magnetostratigraphy almost coinsides with the chronological (Matsuda et al., 1984) and biostratigraphical (Pickford et al., 1984) results.

5. VGPs

Virtual geomagnetic poles (VGP) are also listed in Table 1, and plotted on the polar equal area net of the Northern Hemisphere in Fig. 6. Most of the VGPs deviate somewhat from the present geographic pole, and cluster in the Arctic Ocean between the longitudes of 110°E and 260°E. The deviations are almost all in the direction of the "far-sided and right-handed" effect first noted by Wilson (1970), whereby inclinations are systematically lower and declinations systimatically eastward of what would be expected for a simply geocentric axial dipole model of the geomagnetic field. The similar shift of the VGPs was observed in the paleomagnetic study of the Miocene rocks in the Kirimun district, central Kenya (Ishida et al., 1982).

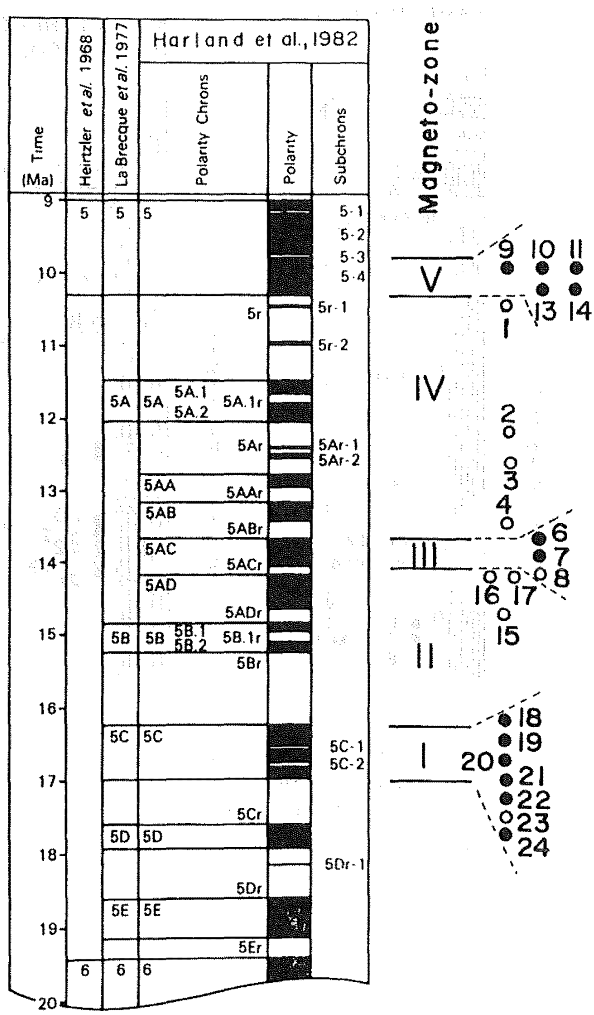

Fig. 5 Correlation of polarity sequence from the Nachola and Aka Aiteputh Formations with the geomagnetic reversal time scale (Harland et al., 1982). Solid and open symbols show normal and reversed polarities, respectively. Numbers correspond to Site Nos. in Table 1.

6. Conclusions

A total of 22 reliable paleomagnetic data are obtained from Miocene rocks in this area. The magnetic polarity sequence is divided into five Magneto-zones, which are tentatively correlated with the geomagnetic reversal time scale. The *Kenyapithecus* horizon is assigned to Magneto-zone V in the period between 10.30 Ma and 9.78 Ma. The VGPs obtained from this area show the deviations in the direction of the "far-sided and right-handed" effect from the geographic pole.

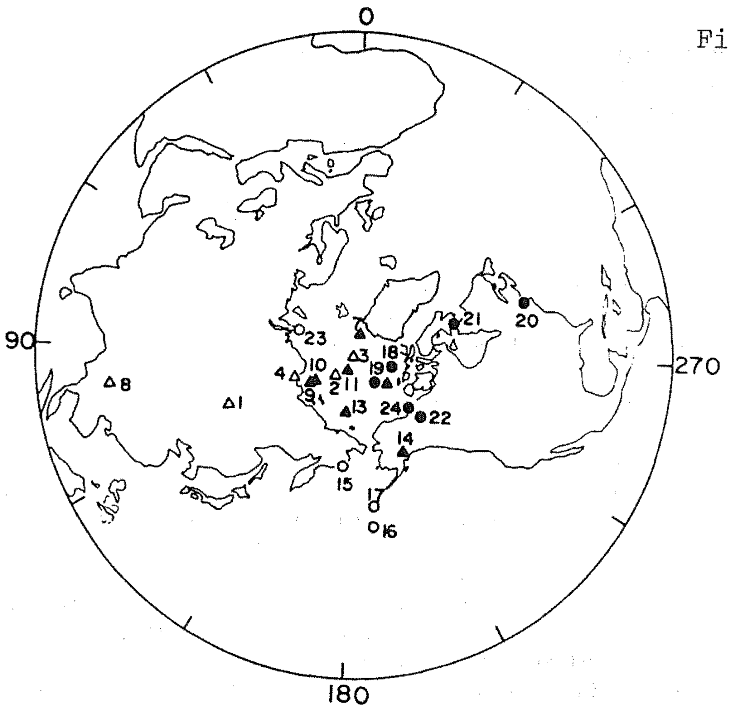

Fig. 6 VGPs plotted on polar equal area projection of Northern Hemisphere. Triangle and circle symbols are from the Nachola and Aka Aiteputh Formations, respectively. Numbers indicate Site Nos. in Table 1. Solid symbols correspond to north poles, and open symbols to south poles.

References

Fisher, R.A. (1953) Proc. Roy. Soc. London, A 217, 295.
Harland, W.B., A.V. Cox, P.G. Llewellyn, C.A.G. Pickton, A.G. Smith and R. Walters (1982) A geologic time scale, (Cambridge University Press, Cambridge), pp. 131.
Heirthler, J.R., G.O. Dickson, E.M. Herron, W.C.III Pitman and X. Le Pichon (1968) J. Geophys. Res., 73, 2119.
Ishida, H. (1984) African Study Monographs, Suppl. 2, 1.
Ishida, H., S. Ishida, M. Torii, T. Matsuda, K. Kawamura, K. Koizumi, H. Nakaya and M. Pickford (1982) Report of of field survey in Kirimun, Kenya, 1980. Study of the Tertiary Hominoids and their Paleoenvironments in East Africa 1, (Osaka University, Osaka), pp. 181.
Ishida, H., M. Pickford, H. Nakaya and Y. Nakano (1984) African Study Monographs, Suppl. 2, 73.
Itaya, T. (1986) African Study Monographs, (to be published).
LaBrecque, J.L., D.V. Kent and S.C. Cande (1977) Geology, 5, 330.
Makinouchi, T., T. Koyaguchi, T. Matsuda, H. Mitsushio and S. Ishida (1984) African Study Monographs, Suppl. 2, 15.
Matsuda, T., M. Torii, T. Koyaguchi, T. Makinouchi, H. Mitsushio and S. Ishida (1984) African Study Monographs, Suppl. 2, 57.
Pickford, M., H. Nakaya, H. Ishida and Y. Nakano (1984) African Study Monographs, Suppl. 2, 67 .
Sawada, Y., M. Tateishi and S. Ishida (1986) African Study Monographs, (to be published).
Wilson, R.L. (1970) Geophys. J. Roy. Astron. Soc., 19, 417.

(to be published in African Study Monographs)

OPAQUE MINERALOGY AND PALEOMAGNETISM IN THE NUMAJIRI HYDROTHERMAL ALTERATION ZONE, NORTHEASTERN JAPAN

Hirotomo UENO* and Munetomo NEDACHI**

* Institute of Mineralogy, Petrology and Economic Gology, Faculty of Science, Tohoku University, Sendai 980, Japan.
** Departmemt of Geology, College of Liberal Arts, Kagoshima University, Kagoshima 890, Japan.

Hydrothemal Alteration and Opaque Minerals

The Numajiri sulfur deposits (37°38'N, 140°15'E) and hydrothermal alteration zones around them are situated in the Adatara volcano which belongs the Nasu volcanic zone in northeastern Japan. Consisting rocks of the volcano are mainly andesite and partly basalt of both tholeiite and calc-alkali series. The age of the volcano is considered to be of Late Pleistocene to Holocene (Hirokawa, 1978). There are violent explosions at a crater, Numanotaira in 1898 and 1899. The Adatara volcanic activity is divided into three essential stages (Fujinawa, 1980). The latest stage productions are composed of many lava flows and domes, and a few of pyroclastic flows (Fig. 1). Replacement type sulfur deposits accompanying alteration zones around them occur sporadically in the latest stage lava flows and pyroclastics.

Two sampling routes containing continuous section from unaltered to altered are studied; one is a part of the Shojigaiwa lava flow at the underground of the Toward N tunnel of the -30 meter level of the mine , and the other is a part of the Shiraitonotaki lava flow at the surface along the Yukawa River. The Shojigaiwa lava flow was separated into two parts by the explosions mentioned above (Fig. 1). The Shojigaiwa and Shiraitonotaki lava flows consist of hyperthene-augite andesite belongs to the calc-alkali rock series (Fujinawa, 1980). Unaltered rocks have phenocrysts of plagioclase, hyperthene, augite, titanomagnetite, ilmenite and olivine. Olivine occurs only from the Shojigaiwa lava flow (underground route). The main constituents of groundmass are plagioclase, hyperthene, augite, titanomagnetite, ilmenite and glass. Titanomagnetite includes lamella of ilmenite as high temperature oxidation products. Grain sizes of titanomagnetite are 100 to 400 μm in phenocryst, and 1 to 5 μm in groundmass.

From the field occurrence, the hydrothermal alteration zones are divided into three ; Zones I, II and III. By opaque mineralogy Zone I is divided into two subzones; Zone I-a and I-b. In Zone I, rocks are black and hard andesite. Fe-Ti oxide minerals in Zone I-a are titanomagnetite, meanwhile those of Zone I-b are titanomaghemite and subordinately titanomagnetite and hematite. In Zone II, rocks are brownish altered andesite. In Zone III rocks are extremely altered, and those colors are pale brown or yellow. Small amounts of visible sulfur are included in these rocks within Zone III of the underground. In Zones II and III, titanomagnetite changes to titanohematite and hematite with pseudobrookite, and also

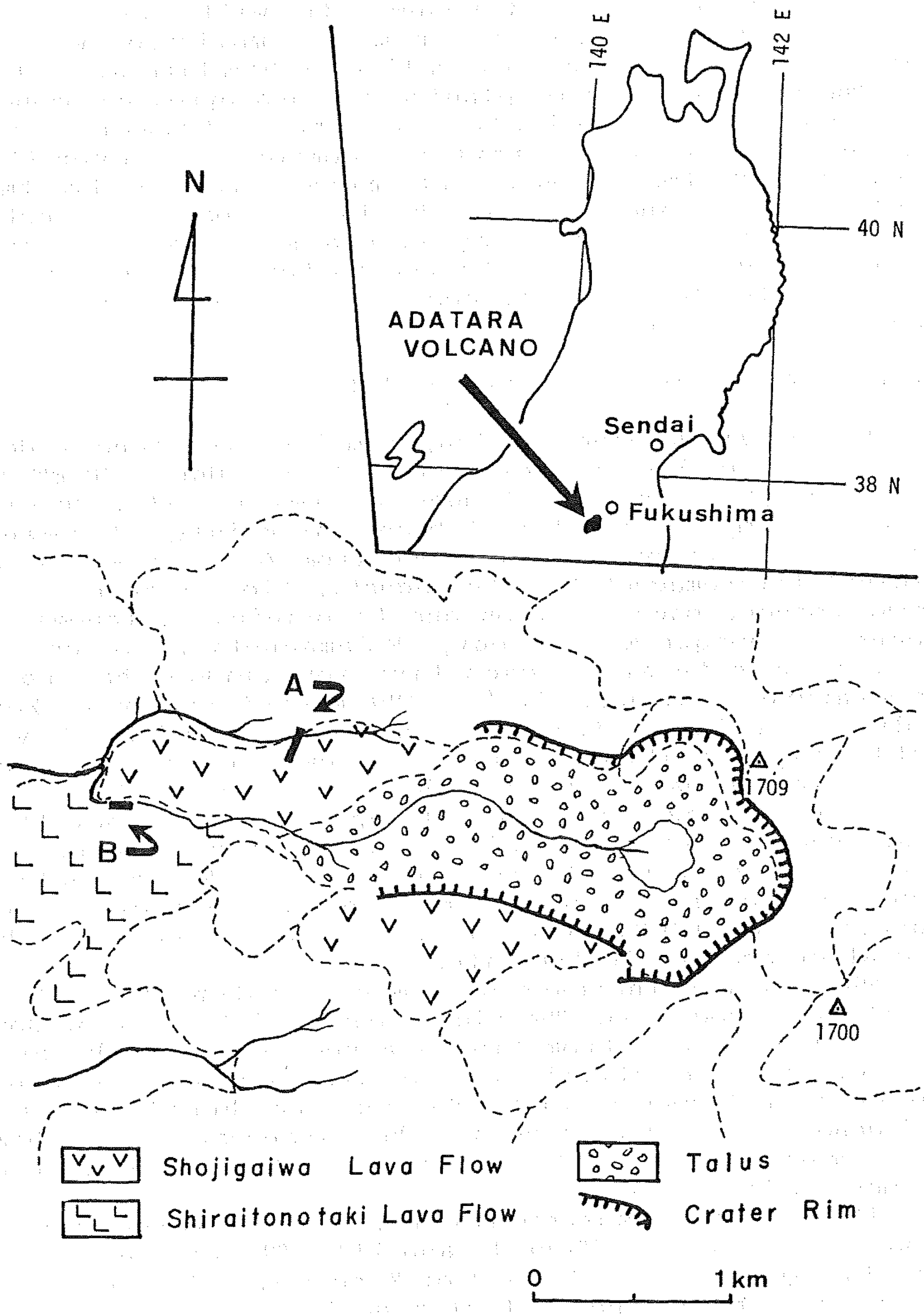

Fig.1. Location of the sampling routes (A and B) around the Numajiri sulfur deposits in the western half parts of the Adatara volcano.
Other lava flow units are indicated by dotted line.

ilmenite changes to titanohematite with rutile and to hematite with pseudobrookite in more complicated way. These hematite solid solutions are called as hematite after here.

The decomposition of plagioclase and pyroxene phenocrysts are used as an indicator of the alteration degree. Olivine phenocrysts are partly decomposed, if even the most fresh rock. Momtmorillonite determined after the treatment of ethylene-glycol and kaolinite having the basal reflection of 7.15 Å are detected as clay minerals in Zones II and III. Montmorillonite is not detected in Zones II and III of the surface route, but jarosite occurs within the zones. Alunite occurs in Zone III.

Magnetic Measurement and Interpretation

During AF demagnetization, samples from Zone I decrease relatively rapidly in their intensities. Until 20 mT(200 Oe) of AF step the direction changes are small, after 30 mT those are wild. Samples from Zone I-b contain mainly titanomaghemite show the similar pattern to those from Zone I-a which contain original titanomagnetite. The magnetization in Zone I-a is the thermoremanent magnetization due to original titanomagnetite, because of opaque mineralogy, AF demagnetization curves and reversible saturation magnetization curves having Curie temperature of around 570 °C. The magnetization of Zone I-b is discussed later. Samples from Zones II and III have very stable magnetization. Samples from both underground and surface routes have similar behavior in each alteration zone during AF demagnetization. By opaque mineralogy the main constituent magnetic minerals are fine grained hematite. Even in groundmass, hematite is 3 μm or less. The magnetization found in Zones II and III may be the chemical remanent magnetization (CRM) which is acquired during hydrothermal alteration and due to hematite.

The extreme increase of remanent intensity in Zones II and III is recognized. The high remanent intensity of Zones II and III may result from fine grained hematite, because the fine grain size attributes to high coercivity and high remanent intensity and CRM due to hematite is very hard(Ueno,1975). According to the disappearance of hematite in the most altered part of Zone 111, the remanent intensity becomes gradually low.

The magnetic susceptibility show a large difference between "Zone I" and "Zone II and III". The average of volume magnetic susceptibility(κ) of Zone I is 39×10^{-3} SI Units (3.1×10^{-3} emu), and that of Zone II and III is 1.6×10^{-3} SI Units. The Q ratios denoting the remanent intensity,M, divided the volume magnetic susceptibility,κ, and the geomagnetic field,H, are 0.70 in Zone I, and 23 in Zone II and III.

The mean direction of each zone is listed in Table 1. The whole magnetization is normal. There is no difference between Zone I-a and Zone I-b at the surface and also underground routes. At the surface the direction of Zone I is similar to that of Zones II and III, but at the underground there is a significant difference between " Zone I" and "Zone II and III". Moreover the direction of Zone I-b is similar to

Table 1. Summary of the paleomagnetic measurements.

	Initial Remanence						After AF demag. (20 mT)					
Zone	N	M	D°,I°	R	k	α°	N	M	D°,I°	R	k	α°
Underground												
I-a	22	1.0	352,+63	20.51	14	9	22	0.27	355,+55	21.47	39	4
I-b	13	0.85	346,+55	12.56	12	8	13	0.25	357,+54	12.61	31	8
I-a & b	35		349,+60	32.92	17	6	35		356,+54	34.08	37	4
II & III	17	1.5	338,+52	16.75	65	4	17	1.1	339,+51	16.77	70	4
Surface												
I-a	12	1.8	000,+54	11.93	150	4	12	0.78	358,+55	11.89	102	4
I-b	6	1.7	359,+54	5.96	135	6	6	0.76	359,+56	5.95	111	6
I-a & b	18		000,+54	17.88	153	3	18		358,+56	17.84	111	3
II & III	14	7.6	007,+53	13.72	46	6	14	5.2	002,+56	13.86	95	4

N is the number of samples. M is the mean intensity in A/m. D° is the direction, clockwise from the true north. I° is the inclination, positive downwards. R is the vector resultant. k is Fishers best estimate of precision. α° is the half angle of the cone of confidence at P=0.95[15].

that of Zone 1-a at the underground. Those are confirmed by a ststistical test on mean directions by Watson and Irving (1957). As shown in Table 2, the results for "Zone I-b" and "Zone II and III" do not indicate no significant difference ($F_0 > F$), while for Zone I-b and Zone I-a indicate no significant difference($F_0 < F$).

Table 2. Statistical test on mean directions of the underground.

Zones (Underground)	N	R	F_0	ϕ_1	ϕ_2	$F(\phi_1, \phi_2)0.05$
I-b & II + III	30	29.24	6.46	2	56	3.16
I-b & I-a	35	34.08	0.11	2	66	3.12
I-a & II + III	39	38.09	5.98	2	74	3.14

$F = (N-2)\ (R_1+R_2-R)/(N-R_1-R_2)$.
N is total number of samples. R_1, R_2 and R are the vector resultants (for R_1 and R_2 in Table 1). $F(\phi_1, \phi_2)0.05$ is F-ratio at 5 percent level from F-table.

The hydrothermal alteration from Zone I-b to Zone III through Zone II in both underground and surface routes is continuous in its degree. Then, it appears that the alteration was occurred successively within the limited period. Even if the small alteration spots found at surface might occur immediately late after the cooling of the lava, the large scale alteration zones accompanying sulfur deposits such as the underground route needs the sufficient time gap between the cooling and the alteration. That is to say it is need to be covered by another hard lava flow as a cap rock for sulfur deposits. This means that there are possibilities of the different direction of geomagnetic field by events of tilting or secular variation. Although there is no positive evidence of these events, Zones II and III have the different magnetization direction from Zone I-a at the underground route. In this case Zones I-b, II and III should acquire the same magnetization direction of the CRM. Actually the direction of Zone I-b is different from that of Zones II and III, and similar to Zone I-a. This fact supports that the direction of magnetization in Zone I-b is controlled by the direction of the original TRM during the alteration process from titanomagnetite to titanomaghemite as reported by Marshall and Cox (1972), and Johnson and Atwater (1977). But, the remanent directions of Zone II and III due to hematite are controlled by the geomagnetic field during alteration. The magnetic polarity change due to hematite in the hydrothermal alteration zone of a dacite lava flow around the Kosaka Kuroko deposits has been reported (Ueno, 1982).

Conclusions

The conclusions are summarized as follows.

(1) The two routes including fresh andesite and hydrothermally altered andesite were studied. Zone I-a of fresh site carries a TRM due to primary titanomagnetite.

(2) Zone II (altered site) and Zone III (highly altered site) carry a very stable CRM due to hematite. The large intensity in Zones II and III is probably resulted from the fine gain size of hematite. As hematite changes to marcasite in Zone 111, the remanent intensity becomes weak.

(3) Although each zone of the surface route has similar magnetization direction, the direction of Zone I-b at the underground route is different from that of Zones II and III, but similar to Zone I-a. The magnetization direction in Zone I-b which is mainly due to titanomaghemite is probably controlled by the primary TRM rather than by the geomagnetic field during the alteration.

(4) The values of magnetic susceptibility are 39 x 10^{-3} SI Units in Zone I where titanomagnetite and titanomaghemite occur, and 1.6x10^{-3} SI Units in Zones II and III where hematite occurs.

References

Fisher, R. A. (1953) Proc. R. Soc. London, Ser. A, 271, 295-305.

Fujinawa, A. (1980) J. Japan. Assoc. Miner. Petr. Econ. Geol., 75, 385-395, (in Japanese).

Hirokawa, O.[Chief ed.] (1978) Geological map of Japan, 1:1,000,000, Geological Survey of Japan, Kawasaki.

Johnson, H. P. and Atwater, T. (1977) Geol. Soc. Amer. Bull. 88, 637-647.

Marshall, M. and Cox, A. (1972) J. Geophys. Res., 77, 6459-6469.

Ueno, H. (1975) Econ. Geol., 70, 547-553.

Ueno,H.(1982) Sci. Rept. Tohoku Univ., Ser.3, 15, 273-280.

Watson G. S. and Irving, E. (1957) Mont. Note R. Astron. Geophys., Supp. 7, 289-300.

(Submitted to Earth Planet. Sci. Lett.)

CHANGES IN TRM AND ARM IN A BASALT DUE TO LABORATORY HEATING

Masaru KONO

Department of Applied Physics, Tokyo Institute of Technology
Ookayama 2-12-1, Meguro-ku, Tokyo 152, Japan

1. Introduction

In a recent paper, it was shown that substantial changes occur in the magnetic hysteresis properties of a natural basalt when the sample was heated in air at a moderate temperature of 640°C for a duration of 3 to 300 minutes (Kono, 1985). The sample was taken from a hypersthene basalt lava flow on Oshima Island, about 100 km south of Tokyo, which erupted in 1951. The main ferromagnetic mineral in this sample is a titanomagnetite with a composition of approximately x = 0.4, i.e., $Fe_{2.6}Ti_{0.4}O_4$ (Akimoto, 1955). In addition, this sample contained a second magnetic phase of approximately magnetite composition.

The original sample contains low Curie temperature (Tc, about 300°C) and high Tc (about 540°C) fractions as main and secondary magnetic components, respectively. With the heating, the high Tc component steadily increased at the expense of low Tc fraction, indicating the progression of high-temperature oxidation (Strangway et al., 1968; Buddington and Lindsley, 1964). It can be inferred that the original sample contained titanomagnetite which has already underwent partial high-temperature oxidation (Ozima and Larson, 1970).

In the experiments reported by Kono (1985), saturation magnetization and the capacity to acquire thermoremanent magnetization (TRM) did not change much for different heating times, but other parameters showed substantial changes. The most affected parameter was the coercive force (Hc). These results suggest that heating induced high-temperature oxidation, and that the low-Tc component (original, stoichiometric titanomagnetite) was replaced by the high-Tc component (Ti-poor titanomagnetite, or more appropriately magnetite-ilmenite intergrowths as judged from the increase of coercivity).

As a next step of the investigation, characteristics of the remanences were examined in the same basalt before and after heating.

2. Samples and Experimental Procedures

Samples were prepared as disks 25 mm diameter and 4 to 9 mm thick. TRM was induced by cooling the samples in a constant magnetic field of 0.5 Oe after they were kept at 640°C for periods ranging from 3 to 300 minutes. Anhysteretic remanent magnetization (ARM) was produced by a constant field of 5.2 Oe and a maximum alternating field (AF) of 1000 Oe. AF and thermal demagnetizations were carried out in a nonmagnetic space with residual field less than 200 gammas.

Three sets of samples were used. The first set was heated to 640°C, cooled in 0.5 Oe field, and the resulting TRM was subjected to stepwise thermal demagnetization. The second set was heated to 640°C and cooled in a nonmagnetic field and an ARM was given and was also subjected to thermal demagnetization. In the third set, the NRM was stepwisely AF demagnetized and then ARM's were given and were AF demagnetized. After that, these samples were heated to 640°C, cooled in 0.5 Oe field to impart the TRM, and AF demagnetization was again carried out on the TRM and then ARM's were produced and AF demagnetized. In other words, this set underwent treatments similar to the Shaw's (1974) method of paleointensity determination.

3. Results

Fig. 1 shows the results of thermal demagnetization of the TRM and ARM in the first and second set of the samples. Heatings cause a shift in the blocking temperature (T_B) spectrum towards higher temperatures in both the TRM and ARM, but such change is much more pronounced in the TRM. In the TRM demagnetization, the growth of the high blocking temperature component with the heating is apparent. Similar change also occurs in the ARM, but is less pronounced. This suggests that the ARM, although thought very similar to the TRM, contain more low temperature blocking component than the TRM.

In the blocking temperature spectra, median demagnetizing temperatures (indicated by arrows) increase with the heating time in both the TRM and ARM. The TRM spectra show that they contain two components, one centered near 300°C and the other at about 540°C. Undoubtedly, they correspond to the low and high Curie

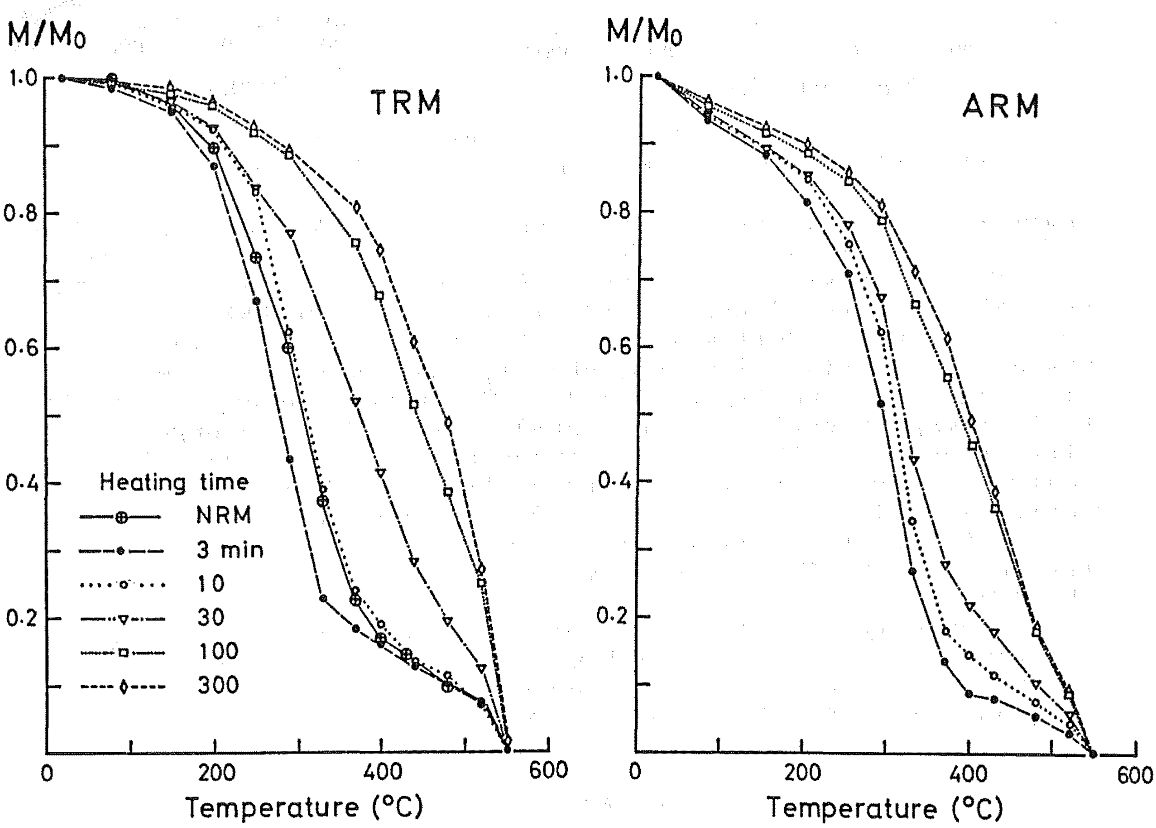

Fig. 1 Thermal demagnetization of the TRM and ARM of the samples after heating.

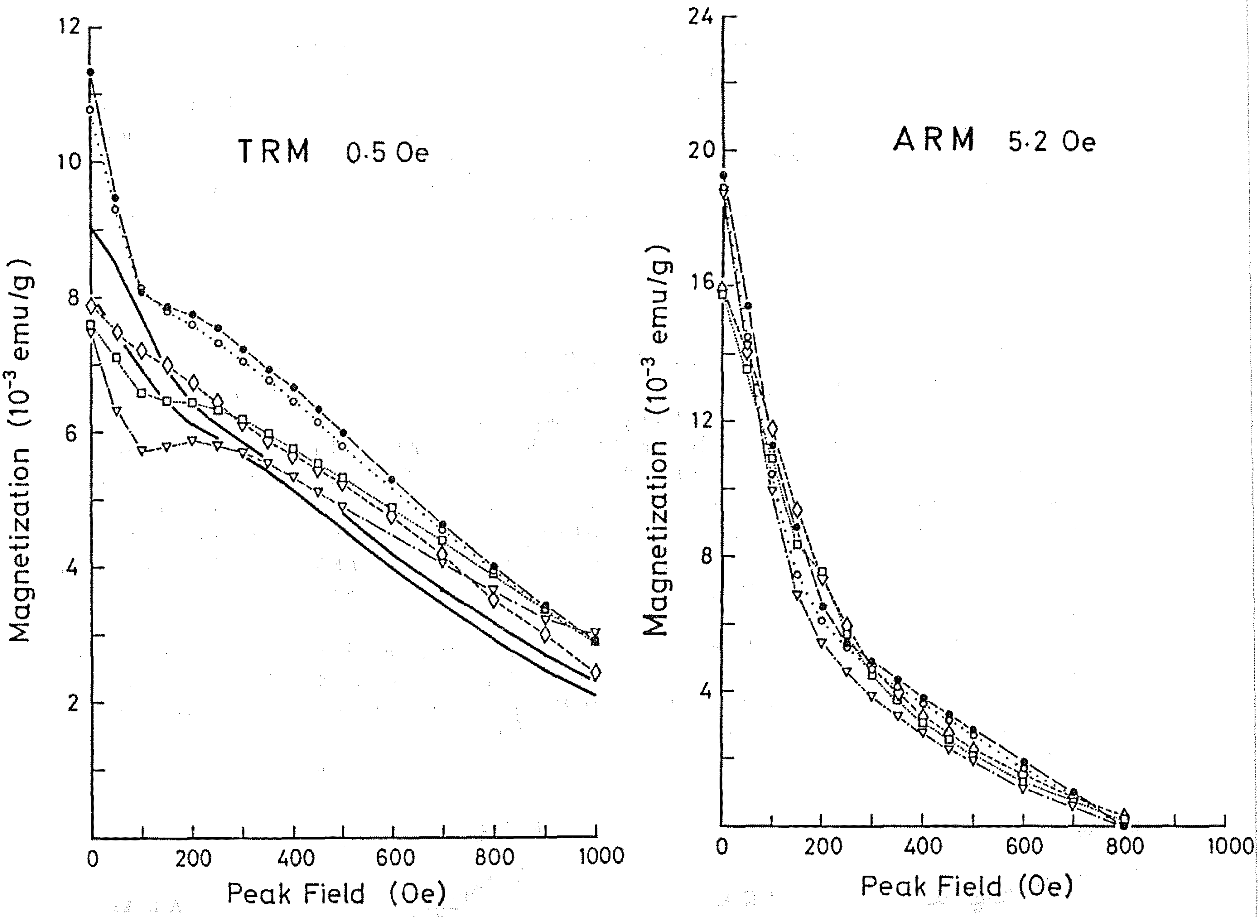

Fig. 2 Alternating field demagnetization of the TRM and ARM of the samples after heating.

temperature fractions. In the case of the ARM, the distinction is not so clear as in the TRM, but some effects really exists.

Fig. 2 shows the results of AF demagnetization of the TRM and ARM. All the demagnetization curves of the NRM's in the original samples fall within the two thick lines indicated in the TRM demagnetization diagram, showing that sample-to-sample differences are negligibly small. The rate of decay of the TRM by AF demagnetization becomes smaller with the prolonged heating time, because of the relative increase of high coercivity components due to heating induced changes. Though the AF demagnetization is limited at 1000 Oe, large difference can be seen between the demagnetization curves of the two remanences. Apparently, the TRM contains more high coercivity component than the ARM.

Apprently, the TRM is composed of two components, separated at about 150 oersteds. The low coercivity portion decreases and the high coercivity portion increases with the increase in heating time. The ARM is also composed of the low and high coercivity components, but their distinction is not so clear as in the case of the TRM, and there is no dominance of high coercivity component in the ARM.

4. Discussion and Conclusions

The main conclusion drawn from these experiments is that high-temperature oxidation proceeds in the time intervals comparable with the laboratory experiments even at a moderately high temperature of 640°C and that the original titanomagnetite is subdivided to magnetite/ilmenite intergrowths, which behave as SD-like particles. Due to this oxidation, the low coercivity, low blocking temperature portion of the TRM is lost and replaced by the stable, high coercivity, high blocking temperature remanence.

This is clearly demonstrated by Fig. 3, where the abscissa is the TRM in the first set of the samples remaining after themal demagnetization to temperatures indicated by the numerals in the figure. The ordinate is the NRM component for a reference sample. The samples for the abscissa and ordinate are different, but such comparisons are permissible as the magnetic properties of the samples are so similar (Fig. 2).

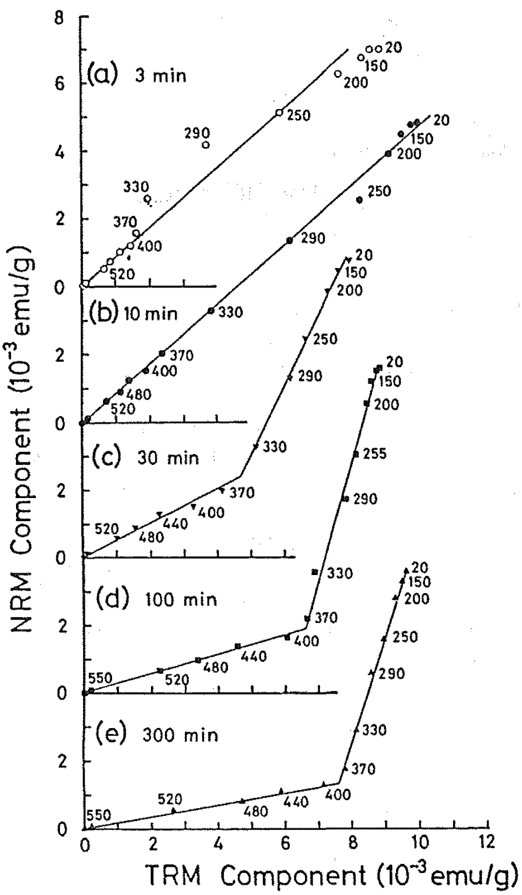

Fig. 3 NRM-TRM diagrams produced from the data of thermal demagnetization (Fig. 1). Note the two linear segments corresponding to low and high blocking temperatures.

Two linear segments are apparent in Fig. 3 (c-e), which suggests that only the proportion of the low and high T_B components changes by the heating. The amount of the low T_B TRM decreases and that of the high T_B TRM increases as the heating time becomes longer, but the blocking spectrum of each of the two separate components remain essentially the same during the present series of experiments.

In natural as well as in laboratory environment, high-temperature oxidation is by no means limited to the unmixing of Ti-rich titanomagnetite into magnetite/ilmenite intergrowths. Generation of hematite and/or pseudobrookite minerals are commonly observed (Buddington and Lindsley, 1964; O'Reilly and Banerjee, 1966; Larson et al., 1969; Ozima and Larson, 1970). In the present experiments, however, the change was not so extensive that the remanences kept the same properties as indicated by the linearlity in the NRM-TRM diagram (Fig. 3). In such cases, the remanences can be understood as a combination of different mixing ratios of two components. This conclusion is in good agreement with the results of the former experiments (Kono, 1985).
A less important conclusion of the present study is the limitation of the ARM as an analog of the TRM in natural rocks. Fig. 4 shows the present experimental results plotted in

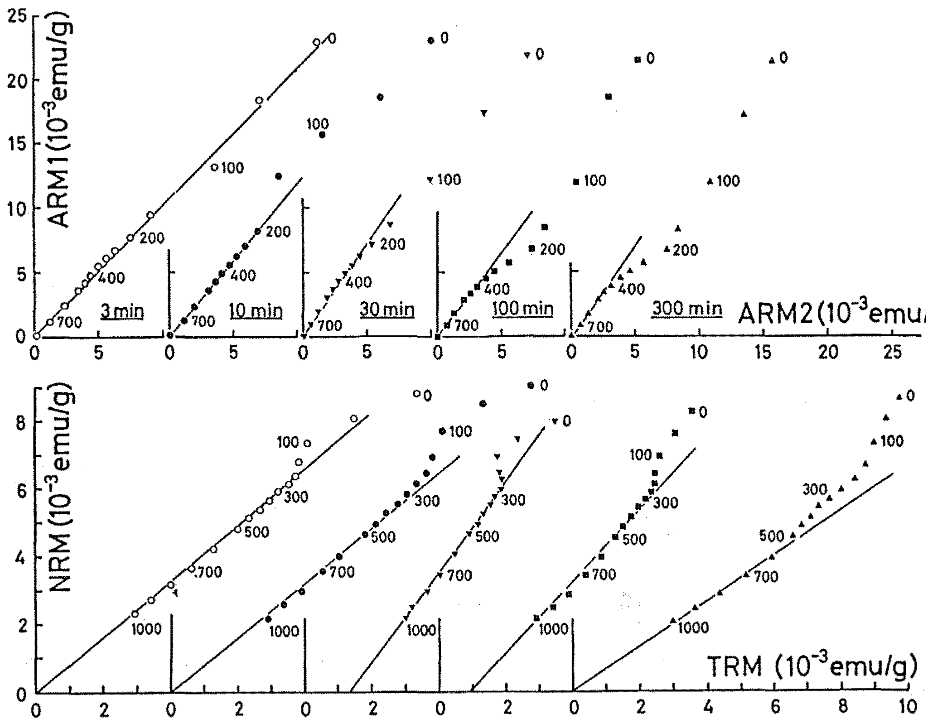

Fig. 4 NRM-TRM and ARM-ARM diagrams constructed from the AF demagnetization data for various heating times. Numerals indicate demagnetizing field in Oe.

a form similar to the Shaw's (1974) method of paleointensity determination. Although the gradient in the ARM1-ARM2 diagram is close to one, there is significant changes due to heating. This is because of the difference in apparent susceptibilities of the TRM and ARM with low and high coercivities. Different versions of Shaw's method were proposed to 'correct' the paleointensity estimates when ARM1-ARM2 relation no longer follows the 45^{o} straight line. However, present results warn us to be very careful to use such 'corrections' since the TRM behaves distinctly different from the ARM in heating induced changes.

References

Akimoto, S. (1955) Japan. J. Geophys., 1, 1.
Buddington, A.F. and D.H. Lindsley (1964) J. Petrol., 5, 310.
Gromme, C.S., T.L. Wright, and D.L. Peck (1969) J. Geophys. Res., 74, 5277.
Kono, M. (1985) J. Geomag. Geoelectr., 37, 589.
Larson, E.E., M. Ozima, M. Ozima, T. Nagata, and D.W. Strangway (1969) Geophys. J. Roy. Astron. Soc., 17, 263.
Ozima, M. and E.E. Larson (1970) J. Geophys. Res., 75, 1003.
O'Reilly, W. and S.K. Banerjee (1966) Nature, 211, 26.
Shaw, J. (1974) Geophys. J. Roy. Astron. Soc., 39, 133.
Strangway, D.W., E.E. Larson, and M. Goldstein (1968) J. Geophys. Res., 73, 3787.

(Submited to Physics of Earth and Planetary Interiors)

ON THE THERMOMAGNETIC STUDY OF THE KO-YAMA METAMORPHIC ROCKS, NORTHEASTERN YAMAGUCHI PREFECTURE, WEST JAPAN

Haruo DOMEN

Institute of Physical Sciences, Faculty of Education
Yamaguchi University, Yamaguchi 753, Japan

In the previous report (Domen, 1982), the experimental data were shown on the natural remanent magnetization of the Susa Tertiary rocks at the Ko-Yama Peninsula, northeastern Yamaguchi Prefecture, southwest Japan. There is the so-called "magnetic stone (jishaku-ishi)" which shows the extraordinarily strong remanent magnetization at the summit of Mt. Ko-Yama (533 m). And of this "magnetic stone", the rock magnetic study had also been carried out (Domen, 1958). In recent, Ito (Ito and Notsu, 1982) also reported on the remanent magnetization of the Ko-Yama intrusive complex.

In this report, the data of the thermomagnetic analysis on the metamorphosed rock specimens previously examined (Domen, 1982) as mentioned above, are shown.

The test specimen was taken from each sample, as in pieces of the order of thousand milligrams in weight. The bulk specimens thus prepared were examined thermomagnetically in the open air by means of an automatic thermomagnetic balance.

The typical examples of the thermomagnetic curve (Js-T curve) are shown in figures (Fig. 1).

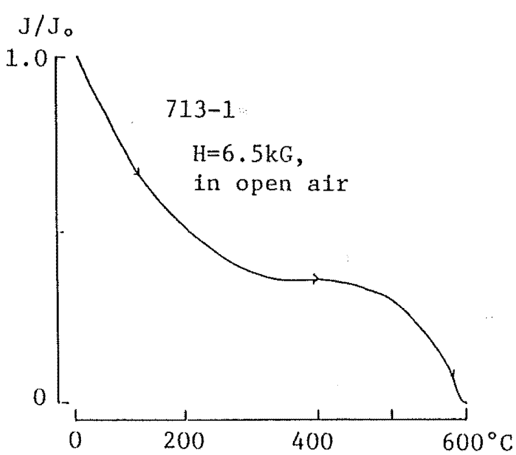

Fig. 1-1. Normalized Js-T curve for the unaltered(?) rock.

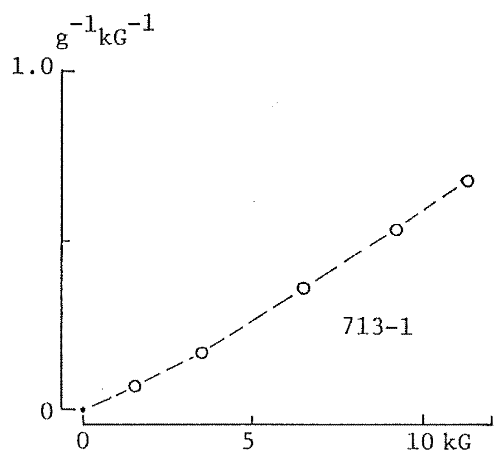

Fig. 2-1. Bulk magnetic susceptibility of the specimen as in Fig. 1-1.

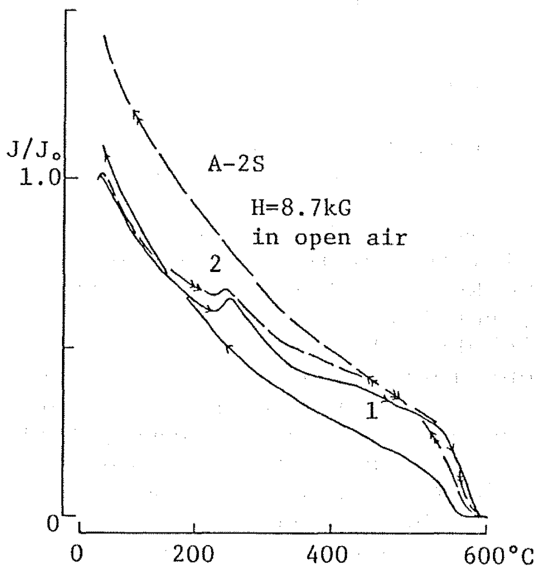

Fig. 1-2. Js-T curves for the slightly altered rock.

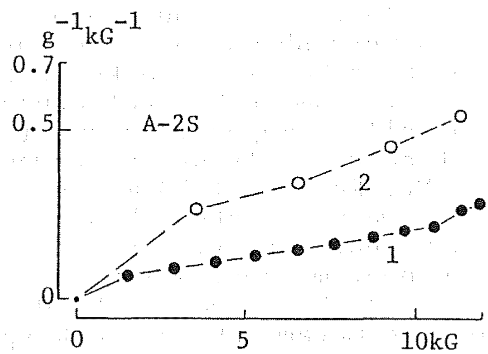

Fig. 2-2. Magnetic susceptibility standing for Fig. 1-2 specimens.

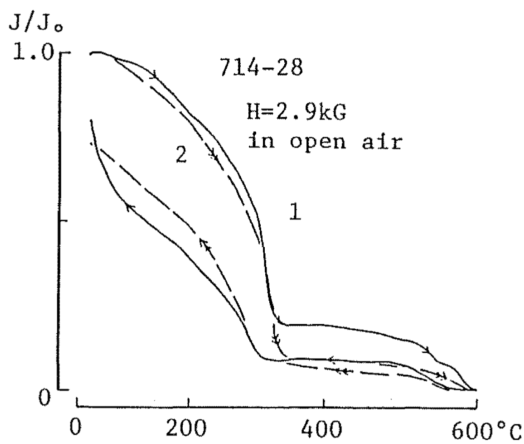

Fig. 1-3. Js-T curves for the slightly altered rock.

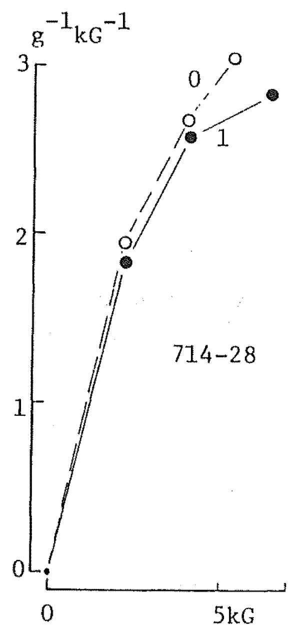

Fig. 2-3. Magnetic susceptibility for the samples in Fig.1-3.

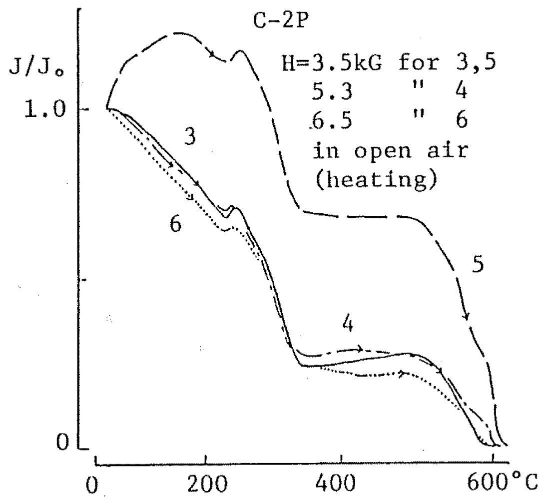

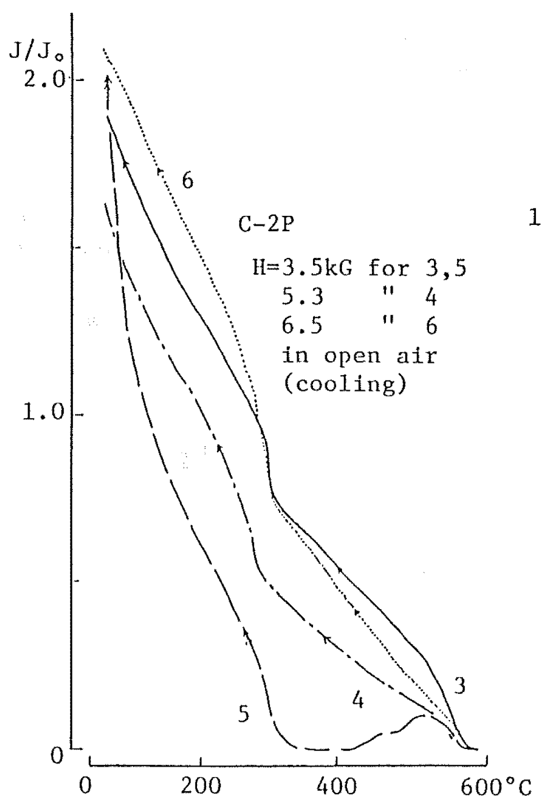

Fig. 1-4. Js-T curves for the slightly altered rock. Top; heating process, Bottom; cooling one.

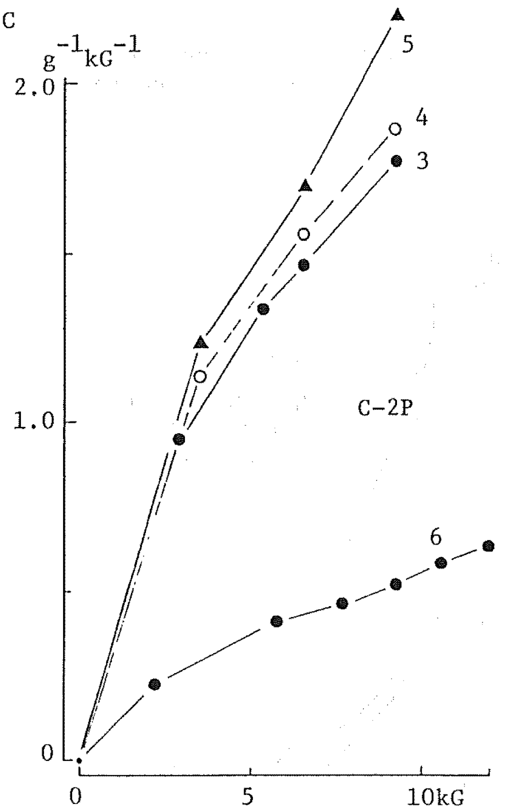

Fig. 2-4. Magnetic susceptibility for the samples in Fig. 1-4.

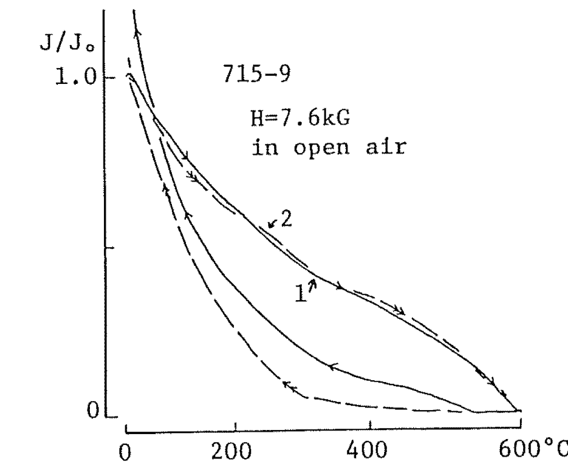

Fig. 1-5. Js-T curves for the highly altered rock.

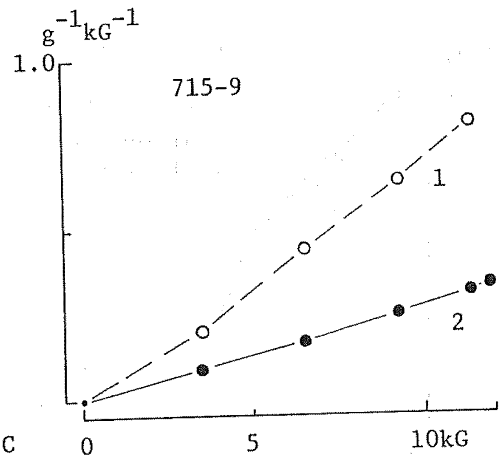

Fig. 2-5. Magnetic susceptibility for the samples in Fig. 1-5.

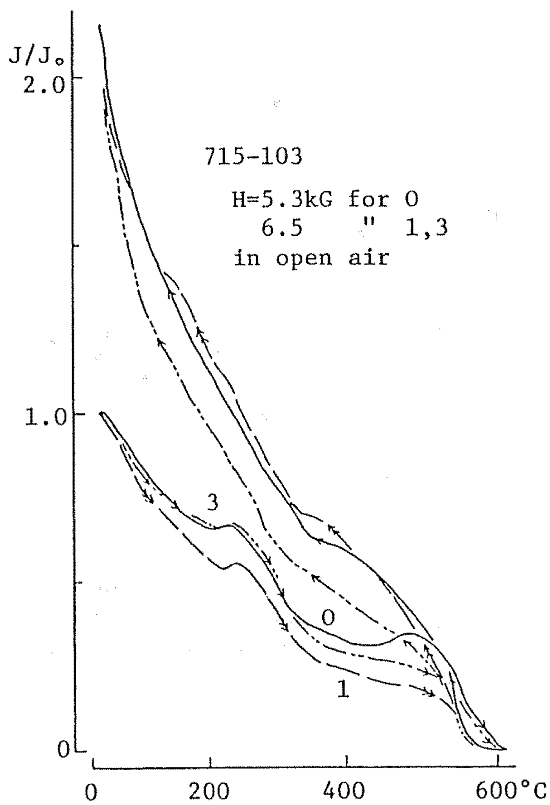

Fig. 1-6. Js-T curves for the highly altered rock.

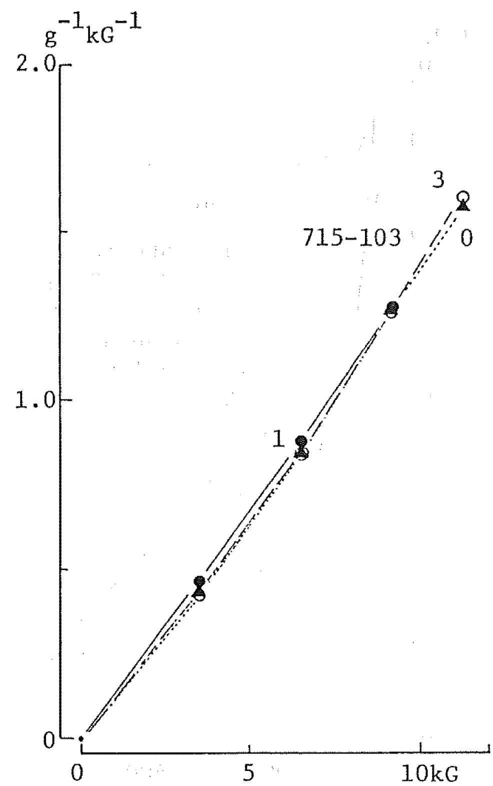

Fig. 2-6. Magnetic susceptibility for the samples in Fig.1-6.

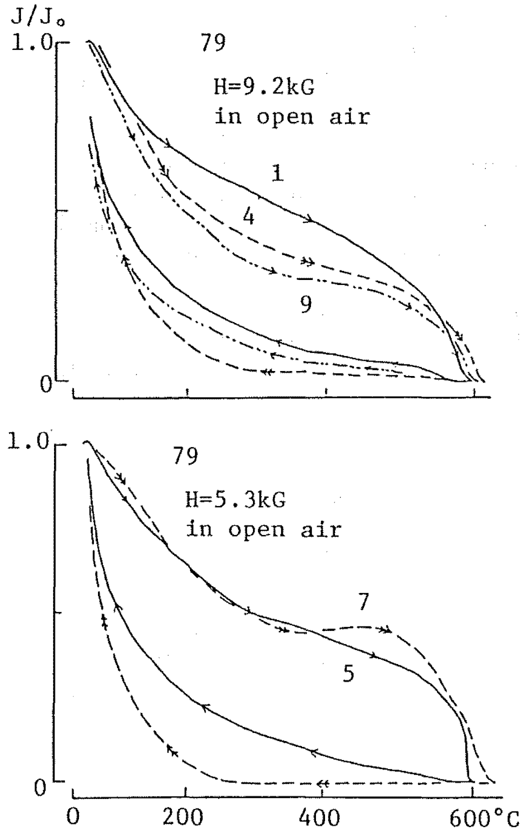

Fig. 1-7. Js-T curves for the unaltered rock newly sampled from the site closed with the Site No. 713-1.

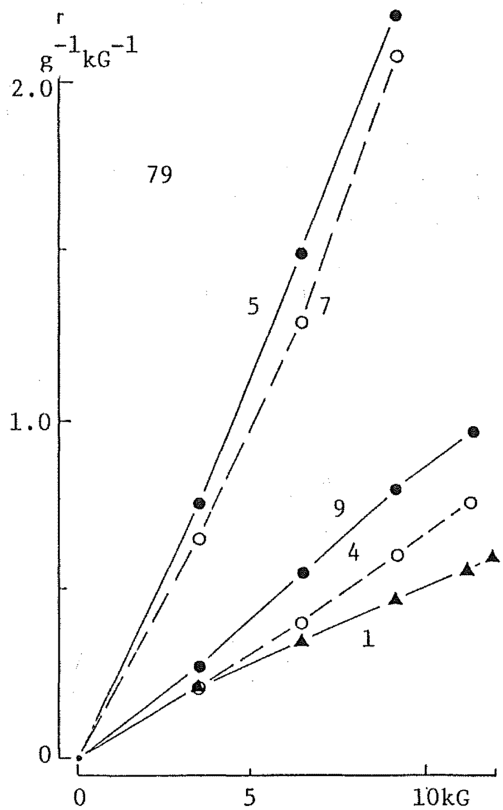

Fig. 2-7. Magnetic susceptibility for the sample in Fig.1-7.

The Js-T curves thus obtained show rather characteristic of those modes during the thermal treatments; heating and cooling cycles as have been shown in the figures.
So far as the present study is concerned, it seems that the rock forming ferromagnetic minerals are not only magnetites but also several ferromagnetics having the lower Curie points. And each Js-T curve shows rather irreversible process on the thermal treatments. However, it is also difficult to recognize of any correlation between the mode of the Js-T curve and the degree of the alteration of each sample.

On the other hand, the magnetic susceptibility of the bulk specimen was decided. The obtained results are also shown in Fig. 2.

Generally speaking, the Ko-Yama metamorphosed rocks show the characteristic Js-T curves which are somewhat similar to those of the specimens highly altered of the quartzporphyry rock samples come from the Ii-no-Ura district, Shimane Prefecture; the nearest neighbour to the Ko-Yama area (Domen, 1983). There is also seen the "magnetic stone" in this Ii-no-Ura district.

On the contrary, both the Ko-Yama and Ii-no-Ura "magnetic stones" were also examined previously as mentioned above, of those ferromagnetic constituents. The modes of these Js-T curves obtained are rather simple (single phased) and the main Curie points are consistent to that of magnetite.

For the comparison, the typical examples of the Js-T curves are shown in Fig. 3, which are for the highly altered Ii-no-Ura rock and for both Ko-Yama and Ii-no-Ura "magnetic stones" respectively.

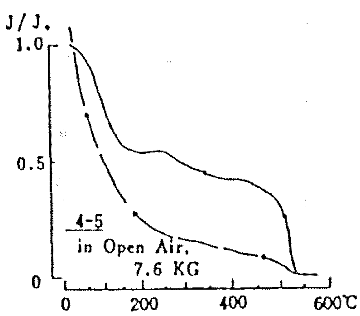

(a) Ii-no-Ura highly altered

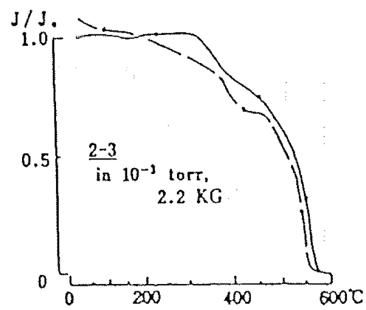

(b) Ii-no-Ura 'Magnetic Stone'

Fig. 3. Typical examples for Js-T curves; for rhe highly altered quartzporphiry rock from Ii-no-Ura district, Shimane Pref. (a), for the 'Magnetic Stones' form the Ii-no-Ura (b), and from the Ko-Yama (c) respectively. (a) and (b); after Domen, 1983. (c); after Domen, 1958.

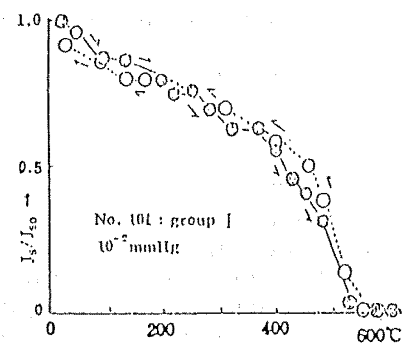

(c) Ko-Yama 'Magnetic Stone'.

Referecnes

Domen, H., 1958. Bull. Fac. Educ., Yamaguchi Univ., 7 (Pt. 2), 35.

Domen, H., 1982. Rock Mag. Paleogeophys., 9, 96.

Domen, H., 1983. Bull. Fac. Educ., Yamaguchi Univ., 33 (Pt. 2), 1.

Ito, H. and K. Notsu, 1982. Rock Mag. Paleogeophys., 9, 24.

MAGNETIC PROPERTIES OF LAMELLAR TETRATAENITE IN TOLUCA IRON METEORITE

Minoru FUNAKI and Takesi NAGATA

National Institute of Polar Research
9-10 kaga 1-chome, Itabashi-ku, Tokyo 173

1. Introduction

Atomically ordered FeNi, which is detected as a tetragonal super lattice, was first discovered by Albertsen et al. (1978a) in isolated lamellae from the Cape York and Toluca iron meteorites by Mössbauer spectroscopy and X-ray diffraction studies. Recently the magnetic properties of tetrataenite in chondrites have been clarified by Wasilewski (1982, 1985) and Nagata and Funaki (1982). The thermomagnetic curves (I_S-T curves) of tetrataenite-rich chondrites are characterized by a very flat heating curve up to 400-450°C and then an abrupt decrease to the Curie point which ranges 550-580°C, depending on composition. Chondrites containing tetrataenite grains have a highly stable NRM component against alternating field (AF) demagnetization up to 180 mT. Magnetic coercivity of the tetrataenite phase is much larger than that of ordinary (disordered) taenite.

The Toluca iron meteorites is a polycrystalline coarse octahedrite with Widmanstatten pattern of bandwidth 1.4±0.2 mm (Buchwald, 1975). The tetrataenite lamellae were prepared from the bulk sample of Toluca by using 2.5 N diluted HCl etching over a period of 20 days. By consecutive microscopical observations, we observe that the tetrataenite sandwiched the plessite and cloudy taenite, and these are etched away completly. By this method a couple of tetrataenite lamellae are obtained from one high nickel lamella.

2. Characteristics of natural remanent magnetization

Natural remanent magnetization (NRM) of ten tetrataenite lamellae was measured using the superconducting rock magnetometer. The NRM intensities of maximum and minimum values are 37.42 and 2.58 $\times 10^{-2}$ Am^2/Kg, respectively. The intensities of 50% occurrence are between 1 and 5 $\times 10^{-2}$ Am^2/Kg. Since the bulk sample was 2.24 g in weight, and has 8.727 $\times 10^{-4}$ Am^2/Kg of NRM intensity, the intensity of lamellae is about 100 times stronger than that of bulk Toluca.

A cubic sample of bulk Toluca (a) and three lamella samples (b), (c) and (d) were demagnetized by AF field up to 120 mT as shown in Fig. 1. Original intensity of bulk sample (a) is demagnetized by 65% steeply from 0 to 5 mT and then gradually from 5 to 30 mT. The changes of direction of NRM is very unstable on the whole. Compared with the bulk sample, the NRM stability of the lamellae is fairly high, not only in intensity as shown in Fig. 2, but also in direction. The original NRM is demagnetized gradually, having a median demagnetization field (MDF) of more than 50 mT.

NRM of the lamella samples was thermally demagnetized in steps of 50°C from 50 to 650°C. Thermal demagnetization curves of NRM intensities for three lamellae show very similar characteristics each others. They show an almost flat demagnetization curve up to 500°C and then an abrupt breakdown at 600°C. Significant residual remanence is not observed at 600 and 650°C. The changes of directions are only few degrees up to 550°C, and then a larger shift at 600 and 650°C.

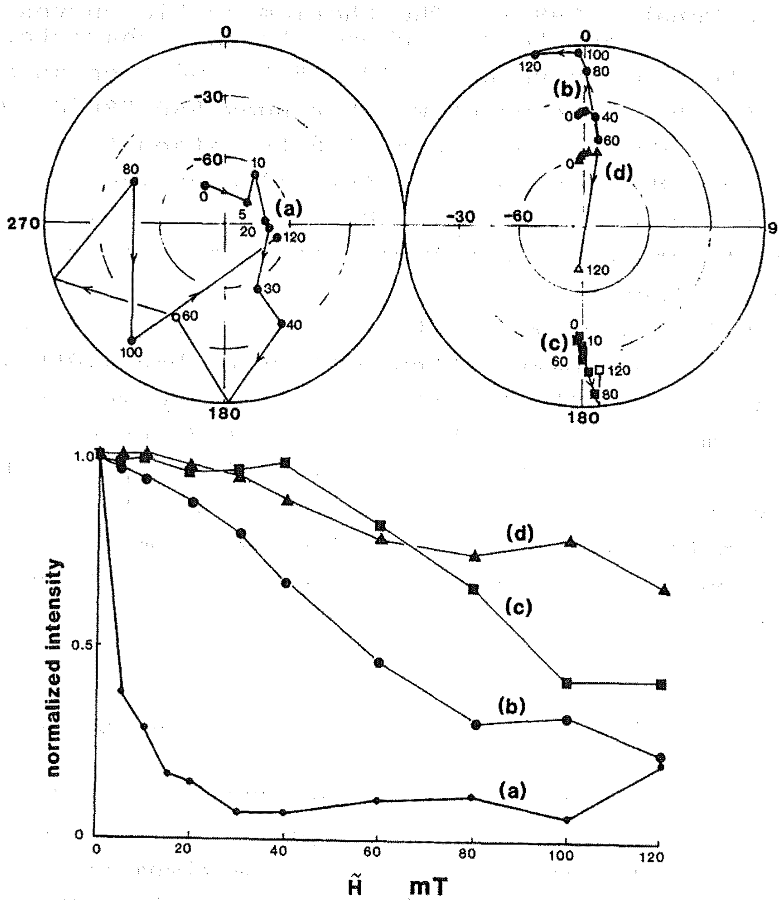

Fig. 1 AF demagnetization curves of NRM of Toluca bulk(a) and tetrataenite lamellae (b),(c) and (d).

3. Thermomagnetic curves (I_S-T curves)

Representative I_S-T curves of a lamella sample, Fig. 2, were obtained from -269(4K) to 650°C(933K), using 1000 mT of external field. Significant characteristic behavior in the heating curves is a very flat decreasing curve from -269 to 550°C and then it abruptly breaks down from 550 to 575°C. In the cooling curve, the magnetization increases gradually from 620 to -269°C. The abrupt break for temperatures in the heating curves and the Curie points in the cooling curve for eight lamella samples are in the range of 550 to 585°C and 545 to 595°C, respectively. In the 2nd run heat treatment, the I_S-T curve is reversible and resembles the cooling curve of the 1st run treatment. The intensity of representative samples at room temperature increases 18% after the 1st run heating. This may be explained by the degree of saturation at 1,000 mT in room temperature; before heating the sample is not saturated at 1,000 mT for the high coercive force of tetrataenite but after heating it is saturated for the small coercive force of disordered taenite under the same conditions.

Figure 2 also shows the 1st run I_S-T curves of a man-made alloy of 50% Fe and 50% Ni. Its 515°C Curie point is reasonably consistent with the expected 517°C for the same composition. The cooling curves for lamellae resemble the man-made alloy curves with regard to magnetization and aspect of the curve as shown in this figure. However, the Curie point at 575°C is higher than that of the alloy. Since the Curie point after heat treatment of eight lamella samples ranges from 545 to 595°C, the nickel contents are evaluated as 52 to 60% atomic percent. We measured the chemical compositions of pre-heating lamellae by EPMA, obtaining Fe=51.45 and Ni=49.05 wt% (Fe 52.44, Ni 47.56 at%) as well as minor amounts of Co=0.19 and Cr=0.02 wt%.

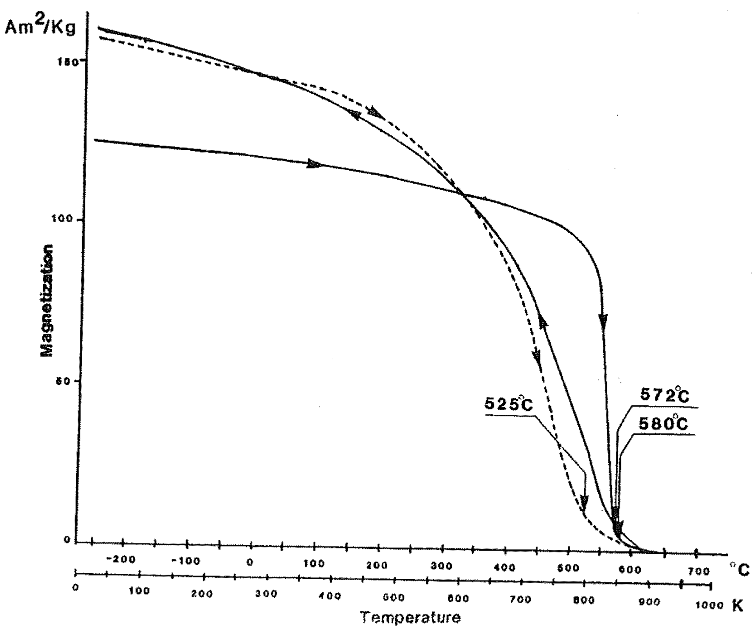

Table 2
Thermomagnetic curves of Toluca and man-made alloy of 50%Fe 50%Ni.

4. Magnetic hysteresis properties

Basic magnetic properties derived from magnetic hysteresis loops, saturation magnetization (I_S), saturation isothermal magnetization (I_R), coercive force (H_C) and remanent coercive force (H_{RC}), were measured at room temperature for the samples before and after heating up to 650°C as summarized in Table 1. The I_S values are estimated by the law of approach to saturation magnetization. The evaluated I_S values are shown in Table 1 together with other hysteresis data and the ratio of post-heating values to pre-heating ones which is denoted by * on each parameter. Values of H_C=44.5-69.5 mT and H_{RC}=70.4-87.7 mT decrease to H_C=1.2-2.2 mT and 2.3-3.0 mT by heating at 600°C. These coercivity values in the pre-heating samples are extremely high compared with chondrites, and the post-heating values are almost the same as those for low nickel chondrites (E, H chondrite). The value of I_S^* is very close to 1.0, suggesting no great chemical composition changes in magnetic materials by heat treatment. Other rates I_R^*, H_C^*, and H_{RC}^* are very small for all samples. The plausible reason for coercivity changes of such magnitude in FeNi alloys must be the transition from an ordered state to a disordered state by heat treatment up to 650°C. The small value of H_C=2.45 mT in the bulk sample illustrates the dominance of the coercive force by kamacite, because the dominant iron phase of Toluca is kamacite as estimated by I_S-T curves. The large value of H_{RC}=129.6 mT may be related to high coercivity materials such as lamellar tetrataenite and tetrataenite in plessite included in this meteorite.

Table 1. Magnetic properties of Toluca iron meteorite.

Sample	heating	I_S Am^2/Kg	I_R Am^2/Kg	H_C mT	H_{RC} mT	I_S^*	I_R^*	H_C^*	H_{RC}^*
block	before	208.4	1.0	2.45	129.6	1	0.02	0.16	0.05
	after	208.4	0.015	0.4	6				
lamella 1	before	143.5±8.6	28.0±1.68	45	72.9	0.09	0.18	0.03	0.04
	after	141.8±8.5	5.0±0.30	1.2	3				
lamella 2	before	152.5±19.8	70.8±9.2	69.5	87.7	1.07	0.68	0.05	0.03
	after	163.5±21.3	19.0±2.3	2.2	3				
lamella 3	before	133.5±21.4	27.0±4.3	4.45	70.4	0.98	0.57	0.04	0.03
	after	130.4±20.9	15.5±2.5	1.8	2.3				

I_S- Saturation magnetization. I_R- Saturation remanent magnetization. H_C- Coercive force, H_{RC}- Remanent coercive force.
I_S^*, I_R^*, H_C^* and H_{RC}^*- Rates of after heating values to before ones.

5. Discussion

Tetrataenite grains have extremely high H_C and H_{RC} values, but the values decrease by heating to 550-580°C (Nagata and Funaki, 1982). In Ym-74160, for example, the respective values change from 22.5 and 40.6 mT to 0.8 and 24 mT by heating above 550°C. As summarized in Table 1, lamellae of Toluca have very high magnetic coercivities, H_C=44.5-69.5 mT, pre-heating and small coercivities, H_C=1.2-2.2 mT, post-heating to 650 °C. This is consistent with the results from tetrataenite grains. The values of H_C^*=0.03-0.05 and H_{RC}^*=0.03-0.04 suggest that the decreasing ratio of the coercive force to the remanent coercive force is very similar within each lamella.

The characteristic flat 1st run heating curve of lamellae shows the typical I_S-T curve of a single component of magnetically homogeneous material. The abrupt breakdown of magnetization between 550 and 570°C is consistent with the transformation of an ordered phase (tetrataenite) to a disordered one (taenite) reported by Wasilewski (1982, 1985) and Nagata and Funaki (1982) using Bjurbole (L_4), Ym-74160 (LL_7), ALH-77260 (L_3) and St. Séverin (LL_6) chondrites and Estherville mesosiderite. For the Toluca lamellae, the breakdown of magnetization between 550 and 570 °C appears to be influenced by a phase transition from order to disorder states.

The Mössbauer spectrum of Toluca lamellae (Albertsen et al., 1978b) indicated a paramagnetic γ-phase and an ordered phase. If the paramagnetic component is included in the lamella samples, it should be detected by some magnetization in the I_S-T curves from -269 to 800°C. However, we find no magnetization above 650 °C and no steeply increasing magnetization below -240 °C in the I_S-T curves. If lamellar tetrataenites include a paramagnetic component, the saturation magnetization, I_S, should be smaller than that of standard 50 wt% FeNi alloy; the I_S values of three lamellae in the range of 133.5±21.4 - 152.5±19.8 Am^2/Kg, as shown in Table 1, are similar to the values 150.5 Am^2/Kg of 50 wt% FeNi (Hoselitz, 1952). These magnetic observations suggest that the lamellar tetrataenite does not include any large amount of paramagnetic component as observed in the Mössbauer spectrum analyses.

The NRM directions of lamellar tetrataenite are fairly stable up to 550°C but become unstable at 600°C against thermal demagnetization. The thermal demagnetization curves of these samples essentially resemble those of Ym-74160 (Nagata and Funaki, 1982); the temperature at which unstable NRM is developed is 530°C; it has a very flat curve up to about 500°C and then an abrupt breakdown at 600°C. These breakdown temperatures are in the same range as the phase transition temperature of 550-575°C obtained from the I_S-T curves. From these viewpoints and the observed decreasing coercive force at that temperature, it seems likely that the breakdown of NRM is caused by phase transition from order to disorder rather than conventional NRM thermal blocking.

References

Albertsen, J.F., Jensen, G.B. and Knudsen, J.M. (1978a): Nature, 273, 453-454.

Albertsen, J.F., Aydin, M. and Knudsen, J.M.(1978b): Phys. Scripta, 17, 467-472.

Buchwald, V.F. (1975): University of California Press. p1209.

Hoselitz, K. (1952): Clarendon Press, Oxford, p299.

Nagata, T.and Funaki, M. (1982): Mem. Natl. Inst. Polar Res., Spec. Issue 25, 222-250.

Wasilewski, P.J. (1982): Lunar and Planet. Sci. XIII. Houston, Lunar Planet. Inst., 843-844.

Wasilewski, P.S. (1985): EOS 66, No18, 296.

POSSIBLE OCCURRENCE OF EXCESS ^{129}Xe ASSOCIATED WITH RELATIVELY LOW $^{40}Ar/^{36}Ar$ RATIOS IN OLIVINE MEGACRYST NODULES IN SOUTH AFRICAN KIMBERLITES

Ichiro KANEOKA*, Nobuo TAKAOKA**
and Ken-Ichiro AOKI***

* Geophysical Institute, Faculty of Science, University of Tokyo, Bunkyo-ku, Tokyo 113
** Department of Earth Sciences, Faculty of Science, Yamagata University, Yamagata 990
*** Institute of Mineralogy, Petrology and Economic Geology, Faculty of Science, Tohoku University, Sendai 980

Excess ^{129}Xe compared with the atmospheric Xe has been identified in CO_2 well gases (Boulos and Manuel, 1971; Hennecke and Manuel, 1975a; Phenney et al., 1978), ultramafic nodules (Hennecke and Manuel 1975b; Kaneoka and Takaoka, 1978; Kyser and Rison, 1982) and oceanic basalt glasses (Kirsten et al., 1981; Staudacher and Allègre, 1982), which is generally attributed to the decay product of a now extinct nuclide ^{129}I ($T_{1/2}$ = 17 Ma). Based on such information, early degassing of the terrestrial atmosphere has been discussed (Staudacher and Allègre, 1983; Thomsen, 1980). Furthermore, it is argued that the occurrence of excess ^{129}Xe is accompanied with high $^{40}Ar/^{36}Ar$ ratios (Allègre et al., 1983; Manuel and Sabu, 1983; Staudacher and Allègre, 1982). If it is, it also gives us a constraint for considering the early history of the earth unless excess ^{129}Xe remained only in limited portions within the earth. In the present study, we have revealed that excess ^{129}Xe in olivine megacryst nodules in South African kimberlites is associated with relatively low $^{40}Ar/^{36}Ar$ ratios as low as 279.3 ± 1.5 even as an observed value. The apparent $^{40}Ar/^{36}Ar$ ratios seem to increase with the increase of their K contents in olivine megacryst samples, from which their formation age is estimated to be about 900 Ma ago. Thus, excess ^{129}Xe might also occur in a region whose $^{40}Ar/^{36}Ar$ ratios are relatively low. This suggests that the occurrence of excess ^{129}Xe might be complicated and gives a possibility that it might be distributed in rather limited portions in the earth's interior.

In the discussion of the degassing history of the earth on the basis of excess ^{129}Xe, it is implicitly assumed that the occurrence of excess ^{129}Xe should have ubiquitously occurred in a region of the concern from which main portions of the terrestrial atmospheric gases were derived. In this context, it is important to testify a hypothesis that excess ^{129}Xe is accompanied with high $^{40}Ar/^{36}Ar$ ratios (Allègre et al., 1983; Manuel and Sabu, 1983), which may imply that such excess ^{129}Xe is significant in a depleted mantle. CO_2 well gases show high $^{40}Ar/^{36}Ar$ ratios as high as 16,000 (Phinney et al., 1978). In this case, however, the $^{3}He/^{4}He$ ratio is not so high (3.1 R_A; $R_A = 1.4 \times 10^{-6}$ for the air) and the Xe isotopes clearly show the contribution of fissiogenic components from ^{238}U. Hence, it is probable that CO_2 well gases were largely contaminated with crustal components, resulting in a higher $^{40}Ar/^{36}Ar$ ratio than the original one. For oceanic basaltic glasses, the common occurrence of excess ^{129}Xe has been reported by Allègre et al. (1983), but Ozima and Zashu (1983) found no observable excess ^{129}Xe within their analytical uncertainties. Kirsten et al. (1981) reported both cases. In the case of ultramafic nodules from Hawaii, the occurrence of excess

^{129}Xe has been confirmed by three groups (Hennecke and Manuel, 1975b; Kaneoka and Takaoka, 1978; Kyser and Rison, 1982) and the samples also show high $^{40}Ar/^{36}Ar$ ratios together with MORB-type $^{3}He/^{4}He$ ratios. Although olivine megacryst nodules in South African kimberlites also suggest the occurrence of excess ^{129}Xe, they seem to show rather low $^{40}Ar/^{36}Ar$ ratios (Kaneoka et al., 1978). Hence it is important to re-examine the last case and they were studied again.

Two olivine megacrysts (MO-32, MO-36) which are about 3 cm in size were used for analyses. They were carried out on the surface as nodules in kimberlites, erupted at Monastery mine, Orange Free State, South Africa about 90 Ma ago. Based on their chemical compositions (Fo_{80}) together with their associated minerals, their derived depth is estimated to be 150 - 200 Km. They are slightly altered to serpentine along cracks. Hence, purified samples (MO-32, P; MO-36, P) were prepared in this study, where the grain size of the powdered samples was adjusted to be more than 100 meshes to prevent from degassing during each process. Previously analysed sample MO-32 had not been purified and designated as MO-32, N. All noble gas isotopes were analysed on a Nier-type mass spectrometer with a resolving power of about 600 to separate ^{3}He from $HD + H_3$ at Yamagata University. To separate secondary atmospheric components, two stage (700° C and 1800°C, 30 minutes) stepwise heating was applied. Other analytical procedures were the same as those reported before (Kaneoka and Takaoka, 1978).

The selected isotopic ratios for higher temperature fractions are summarized in Table 1. All isotopic ratios other than those in Table 1 were almost of atmospheric composition. Present results suggest the occurrence of excess ^{129}Xe for these samples, but their $^{40}Ar/^{36}Ar$ ratios are relatively low especially for MO-36, P. However, their $^{3}He/^{4}He$ ratios are similar one another in spite of the difference in the observed $^{40}Ar/^{36}Ar$ ratios. The occurrence of excess ^{129}Xe in these samples is more clearly shown in Fig. 1, where the apparent excess ^{129}Xe cannot be ascribed to mass fractionation or any other analytical problems. MO-32, N and MO-32, P were analysed under very different conditions including the analytical periods, which were separated more than one year. In the case of MO-36, P, the excess ^{129}Xe seems less reliable, because it overlaps with the atmospheric value marginally within the uncertainty of 2σ. For this sample,

Table 1. Noble gas isotopic ratios of olivine megacrysts in kimberlites from Monastery, S. Africa

Sample No.	$^{3}He/^{4}He$ ($\times 10^{-6}$)	R/R_A	$^{20}Ne/^{22}Ne$	$^{40}Ar/^{36}Ar$	$^{129}Xe/^{132}Xe$	$^{136}Xe/^{132}Xe$
Mo-32, N	6.55 ± 0.27	4.75 ± 0.20	9.79 ± 0.26	1183 ± 11	1.014 ± 0.005	0.334 ± 0.005
Mo-32, P	7.94 ± 1.01	5.75 ± 0.73	9.77 ± 0.22	676.8 ± 4.0	1.009 ± 0.008	0.332 ± 0.004
Mo-36, P	8.36 ± 0.62	6.06 ± 0.45	9.88 ± 0.20	279.3 ± 1.5	0.997 ± 0.007	0.330 ± 0.005
Atmosphere	1.38	1	9.81	295.5	0.983	0.329

N.B. ∘ $R/R_A \equiv (^{3}He/^{4}He)_{sample}/(^{3}He/^{4}He)_{atmosphere}$.
∘ All tabulated data are those of 1700°C or 1800°C fractions with an uncertainty of one standard deviation.

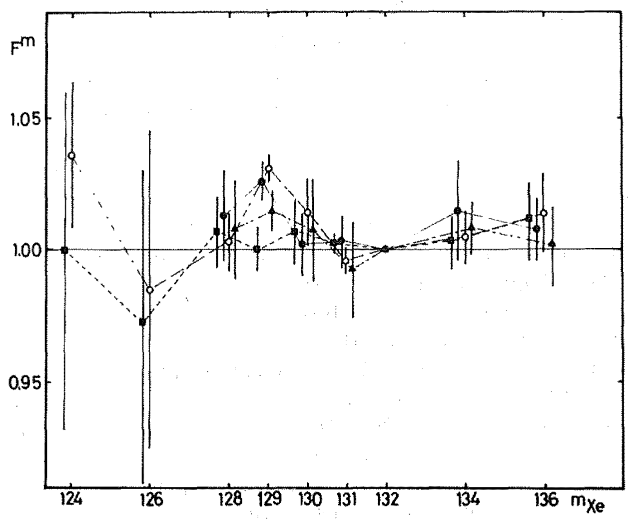

Fig. 1. Normalized Xe isotopic compositions of olivine megacryst nodules (MO-32, N; MO-32, P; MO-36, P) and an augite-ilmenite intergrowth nodule (MO-61) in kimberlites, Monastery mine, Orange Free State, South Africa. The error bar indicates one standard deviation. F^m is defined as follows.

$$F^m = ({}^{m}Xe/{}^{132}Xe)_{sample}/({}^{m}Xe/{}^{132}Xe)_{atmosphere}$$

o MO-32, N (1700°C); ● MO-32, P (1800°C);
▲ MO-36, P (1800°C); ■ MO-61 (Total fusion).

however, we observed also excess ^{129}Xe with a value of $F^m = 1.022 \pm 0.007$ in the 1700°C fraction in our previous study (Kaneoka et al., 1978). Hence, it is likely that excess ^{129}Xe was also included in this sample. For comparison, Xe isotopes for MO-61 (Augite-ilmenite intergrowth, kimberlite nodules from Monastery mine, derived depth : 100 - 150 Km) are shown in Fig. 1. This was also analysed previously (Kaneoka et al., 1978). This sample shows no excess ^{129}Xe. Among previously analysed nodules in South African kimberlites, only olivine megacrysts show such excess ^{129}Xe. Since they are regarded to have been derived from the deepest part among those nodules, the occurrence of excess ^{129}Xe may probably reflect the difference in the original sources for these nodules. Although present results suggest the occurrence of excess ^{129}Xe with the order of around 2% compared with the atmospheric value, its definite value is difficult to be estimated due to the uncertainty in the analytical data. Coupled with this fact, it is worth noting that the occurrence of excess ^{134}Xe and ^{136}Xe is possible, but cannot be confirmed due to the uncertainty in the analysed data. In order to establish this point, more refined techniques are required.

Concerning the $^{40}Ar/^{36}Ar$ ratio, it is interesting to note that the samples with higher $^{40}Ar/^{36}Ar$ ratios have higher K contents (46 ± 5 ppm for MO-32, N; 37 ± 5 ppm for MO-32, P; 5 ± 1 ppm for MO-36, P; determined by S. Zashu with the isotope dilution method). If we correct for the radiogenic ^{40}Ar based on these K contents and the age of 90 Ma, the $^{40}Ar/^{36}Ar$ ratios become 1139 for MO-32, N, 639.8 for MO-32, P and 274.0 for MO-36, P, respectively, with the condition that all radiogenic components were only degassed at higher temperatures. It is very significant that the sample

MO-36, P shows a very low $^{40}Ar/^{36}Ar$ ratio as low as 279.3 ± 1.5 even in the higher temperature fraction. The $^{40}Ar/^{36}Ar$ ratio of this sample for the 700°C fraction shows a slightly highter value of 283.6 ± 1.7. Since this low $^{40}Ar/^{36}Ar$ ratio is associated with the occurrence of excess ^{129}Xe together with the higher $^{3}He/^{4}He$ ratio than the atmospheric value (R_A = 1.4×10^{-6}), it is quite unlikely that this low ratio was caused due to the mass fractionated secondary atmospheric contamination. After purifying the sample MO-32, both the K content and the $^{40}Ar/^{36}Ar$ ratio decrease, resulting from the removement of impurities. From the mass balance, it is pointed out that the impurities contain lower $K/^{36}Ar$ ratio than the purified olivine megacryst, suggesting that the impurities are sources for incompatible elements including noble gases.

Ne isotopes are almost atmospheric within the analytical uncertainty. On the other hand, $^{3}He/^{4}He$ ratios are similar among these samples, though MO-32, N shows a slightly lower $^{3}He/^{4}He$ ratio. This apparent lowering would probably reflect the relative decrease of primordial component ^{3}He due to the occurrence of impurities in this sample. The samples MO-32, P and MO-36, P show similar $^{3}He/^{4}He$ ratios which are definitely lower than the present MORB value (0.8 - 1.0 R_A), but still higher than the present atmospheric value. If these components are associated with heavier noble gases such as Ar and Xe, the observed $^{3}He/^{4}He$ ratios might be different between the samples MO-32, P and MO-36, P and/or the definite value would be much higher than the MORB value due to the remaining of relatively large amount of primordial component ^{3}He. The similarity in the observed $^{3}He/^{4}He$ ratio suggests that He might have been equilibrated with the surrounding rocks when they were kept at the depth, because it is possible that He would be relatively easily equilibrated between two phases as long as the surrounding temperature is relatively high of more than 1000°C or more (Kaneoka et al., 1983). However $^{40}Ar/^{36}Ar$ ratios suggest that it did not occur at least for heavier noble gases than Ar.

Thus, present results indicate that the occurrence of excess ^{129}Xe is not always associated with the sample of high $^{40}Ar/^{36}Ar$ ratios. This raises a question in which portion such excess ^{129}Xe is remained in the earth's interior. Assuming that the samples MO-32, P and MO-36, P have been derived from the same source but associated with different amount of K content, we can infer both the formation age and its $^{40}Ar/^{36}Ar$ ratio. The calculated values show a formation age of about 890 Ma with an initial $^{40}Ar/^{36}Ar$ ratio of about 215. If we assume that all observed ^{40}Ar is radiogenic, we can get an upper limit for the formation age. Such a maximum age is estimated to be in the order of 2500 - 2800 Ma. Since this portion in the earth's interior contains excess ^{129}Xe, it would demonstrate the existence of a fertile part at the depth of about 150 - 200 Km or the deeper part, which shows a relatively low $^{40}Ar/^{36}Ar$ ratio. If it is, it gives an important information on the evolution of the mantle together with the degassing state of the earth. As discussed before, we cannot preclude a possibility that the occurrence of excess ^{129}Xe may be rather limited in the earth's interior. In this case, the occurrence of excess ^{129}Xe implies the incomplete mixing of mantle material since a few hundred millions later than the formation of the earth. To clarify this point, it is eargently required to settle the problem whether the excess ^{129}Xe occurs rather ubiquitously in some regions in the earth's interior on global scale or only remained in limited portions which are distributed heterogeneously.

References

Allègre, C.J., T. Staudacher, P. Sarda and M. Kurz (1983) Nature, 303, 762.

Boulos, M.S. and O.K. Manuel (1971) Science, 174, 1334.

Hennecke, E.W. and O.K. Manuel (1975a) Earth Planet. Sci. Lett., 27, 346.

Hennecke, E.W. and O.K. Manuel (1975b) Nature, 257, 778.

Kaneoka, I. and N. Takaoka (1978) Earth Planet. Sci. Lett., 39, 382.

Kaneoka, I., N. Takaoka and K. Aoki (1978), In Terrestrial Rare Gases (eds. E.C. Alexander and M. Ozima), 71 (Cent. Acad. Pub. Tokyo).

Kaneoka, I., N. Takaoka and D.A. Clague (1983) Earth Planet. Sci. Lett., 66, 427.

Kirsten, T., H. Richter and D. Störzer (1981) Abstr. Meteorol. Soc. Meet. Bern, 147.

Kyser, T.K. and W. Rison (1982) J. Geophys. Res., 87, 5611.

Manuel, O.K. and D.D. Sabu (1983) Geochem. J., 15, 245.

Ozima, M. and S. Zashu (1983) Earth Planet. Sci. Lett., 62, 24.

Phinney, D., J. Tennyson and U. Frick (1978) J. Geophys. Res., 83, 2313.

Staudacher, T. and C.J. Allègre (1982) Earth Planet. Sci. Lett., 60, 389.

Thomsen, L. (1980) J. Geophys. Res., 85, 4374.

NOISE AND STABILITY OF Ag-AgCl ELECTRODE

Akio HORIGUCHI[1], Hidefumi TANAKA[2], Masaru KONO[2], and Yozo HAMANO[3]

1)Mitsubisi Chemical Industries Limitted., Yokkaichi 510.
2)Dept. of Applied Physics, Tokyo Institute of Technology, Ookayama, Meguroku, Tokyo 152.
3)Geophysical Institute, University of Tokyo, Yayoi 2-11-16, Bunkyoku, Tokyo 113.

Introduction

Measurement of electric field at deep sea floors has large significance for magnetic method such as magneto-telluric measurements and controlled source electromagnetic sounding. However, measurements under the deep sea is much more difficult on land because of attenuated electric field within conductive sea water, and the largest noise arises from electrode itself. The best electrode to be used in the sea water is Ag-AgCl electrode (Filloux, 1973). The improved version of this type of electrode by Hamano et al. (1984) has much larger Ag-AgCl contact surface owing to the preparation method which include heat treatment of the mixture of AgCl and Ag_2O. This type of electrode, which was developed by Keston (1935), is called a sintered electrode because heating in air sinters the mixture to forme the coexistence of AgCl and Ag of large surface area. This study aims to obtain the best condition for preparaing the sintered Ag-AgCl electrode by comparing the performances of electrodes made under different parameters such as the mixture ratio of AgCl ang Ag_2O and sintering temperature.

Electrode

Figure 1 shows the cross section of electrode which was fabricated as follows. A 20 mm by 25 mm Ag mesh was wound around an Ag stem of 40 mm long and 1 mm diameter. The mixture of AgCl and Ag_2O powders of total weight of 1.5 g was ground in an agate motor and made pasty by adding a little water. This pasty mixture was plastered around on the Ag mesh, and then the electrode was heated in air to sinter it. The sintered electrode connected to lead wire with solder was set in a vinyl chloride tube with a porous alumina end cap which was stuffed with silica powder. Lastly, the electrode was filled with 2 N KCl solution after vented under vacuum.

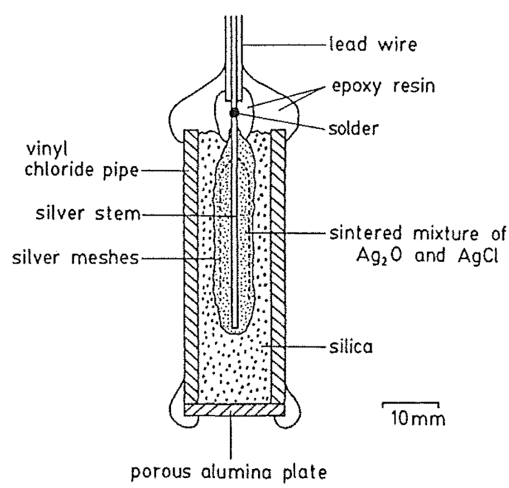

Fig.1 Cross section of sintered Ag-AgCl electrode.

Table 1. Comparison of performances of Ag-AgCl and Pt electrode

type	AgCl content (weight %)	temp. (°C)	time (min)	qt.	reciprocity (μV)	additivity (μV)	drift (μV/day)	temp. dependency (μV/deg)
sintered	11.1	450	15	10	−0.5±1.5	0.73±0.48	10.9±3.9	4.1±2.3
	20.0	450	15	9	−1.2±1.0	0.56±0.32	7.7±2.8	2.5±1.1
	33.3	450	15	10	−1.9±1.3	0.81±0.42	8.8±4.0	1.5±0.7
	50.0	450	15	10	−1.1±1.4	0.66±0.44	14.6±7.2	4.1±2.6
	66.7	450	15	10	−1.6±1.7	0.93±2.30	11.3±12.5	4.7±3.4
	33.3	450	7	6	−2.0±1.2	0.40±0.14	10.4±5.3	4.0±2.3
	33.3	450	1	10	−1.1±1.5	0.76±0.45	19.6±8.0	4.7±1.2
	33.3	350	15	10	−3±12	3±7	607±373	152±83
nonsintered	*	*	*	4	−11±52	12±4	454±38	209±74
platinum	*	*	*	3	180±150 (mV)	36±73 (mV)	27±1 (mV)	21±2 (mV)

Eight kinds of electrode were prepared under different conditions of fabrication. The parameters changed for comparison of electrode performances are the composition of the $AgCl-Ag_2O$ mixture, sintering temperature, and sintering time. Details of fabrication parameters are tabulated in Table 1. Ten electrodes were prepared for each kind with two exceptions, and the total number amounts to 75. Non-sintered type of Ag-AgCl electrode and simple platinum stem electrode were also examined.

Basic features of voltage differences among electrodes

To test the basic performances of electrode, we examined the next relation among voltage differences.

$v_{ij} = -v_{ji}$ (reciprocity)

$v_{ij} = v_{ik} + v_{kj}$ (additivity)

where v_{ij} represents the voltage difference between i-th and j-th electrodes. All electrodes of each type, usually ten in number, were placed within a container of 2N KCl solution which was held at constant temperature. We measured the following quantity which should be zero in principle for all combinations of electrodes.

$x = v_{ij} + v_{ji}$

$y = (v_{ki} - v_{ji}) - v_{kj}$

Figure 2 shows an example of histograms of observed x and y for a type of sintered Ag-AgCl electrode. Table 1

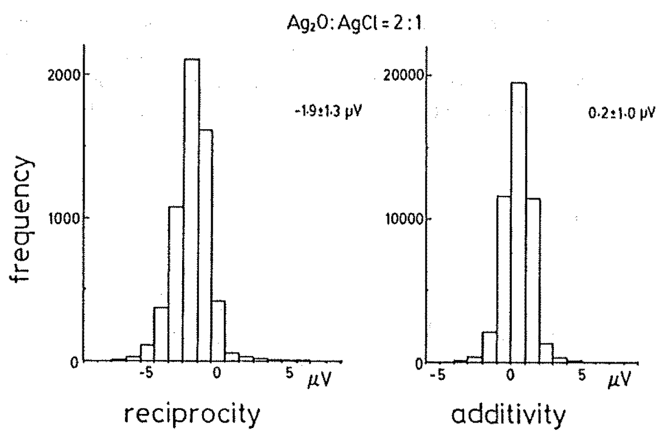

Fig.2 Basic relations among v_{ij}.

was around 10 - 20 μV peak to peak. Figure 6 shows the ratio of amplitude between the observation and source which was normalized by the value at the period of one minute. Phase delay of observed oscilation from the source is also shown in the figure although we could not measure for 1 second period. The reason of the negative correlation of amplitude and phase delay to period is unknown but may be related to the effect of polarization because the experiment was made in a small tub. In any case, clear observation of very small electric field of 15 μV peak to peak as shown by the inset of Figure 6 demonstrates the large performance of the sintered Ag-AgCl electrode for the application to the use under deep esa.

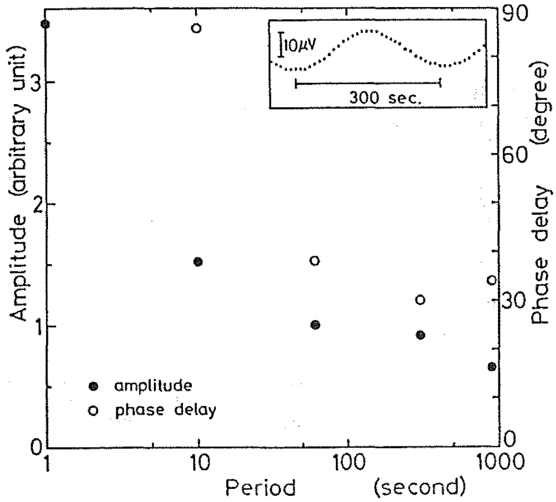

Fig.6 Dependency on periodic electric field of sintered Ag-AgCl electrode.

Structural difference between good and bad electrode

Structure of sintered Ag-AgCl electrodes were observed by a reflecting microscope. After completion of experiments, representative electrodes were selected from the best kind (20 % AgCl, 450°C, 15 min.), bad kind (67 % AgCl, 450°C, 15 min.), and the worst one (33.3 % AgCl, 350°C, 15 min.). Crystal cutter was used to cut the electrode. The cross section of the electrodes was flat enough for identification of Ag and AgCl grains as shown in Figure 7 although the polish process was omitted. The structure of the best electrode is characterized by the Ag grains of 20 - 30 μm diameter which we believe is connected to each other and interstitial AgCl grains of 5 - 10 μm diameter, while

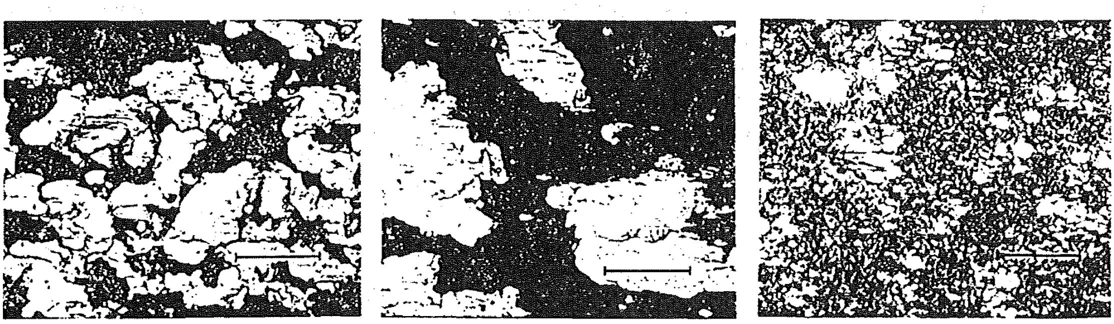

(a) The best kind (b) Bad kind (c) The worst kind

Fig.7 Structural difference among sintered Ag-AgCl electrodes. A scale bar indicates 20 um, for all photogrophs.

in the bad one large AgCl grains are not connected to each other and reduces the contact surface of Ag and AgCl. The Ag grains within the worst electrode are very small and scattered which means they are not electrically connected. We can conclude that the performance of Ag-AgCl electrode can be interpreted in terms of its structure especially contact surface of Ag and AgCl.

References

Corwin, R. F. and U. Conti (1973) Rev. Sci. Instrum., 44, 708.
Filloux, J. H. (1973) Phys. Earth Planet. Inter., 7, 323.
Hamano, Y., t. Yukutake, J. Segawa (1984) Proc. Conductivity Anomaly Working Group, 251.
Keston, A. S. (1935) J. Ame. Chem. Soc., 57, 1671.
Petiau, G. and A. Dupis (1980) Geophys. Prospect., 28, 792.

(To be submitted to J. Geomag. Geoelectr.)

AUTHOR INDEX

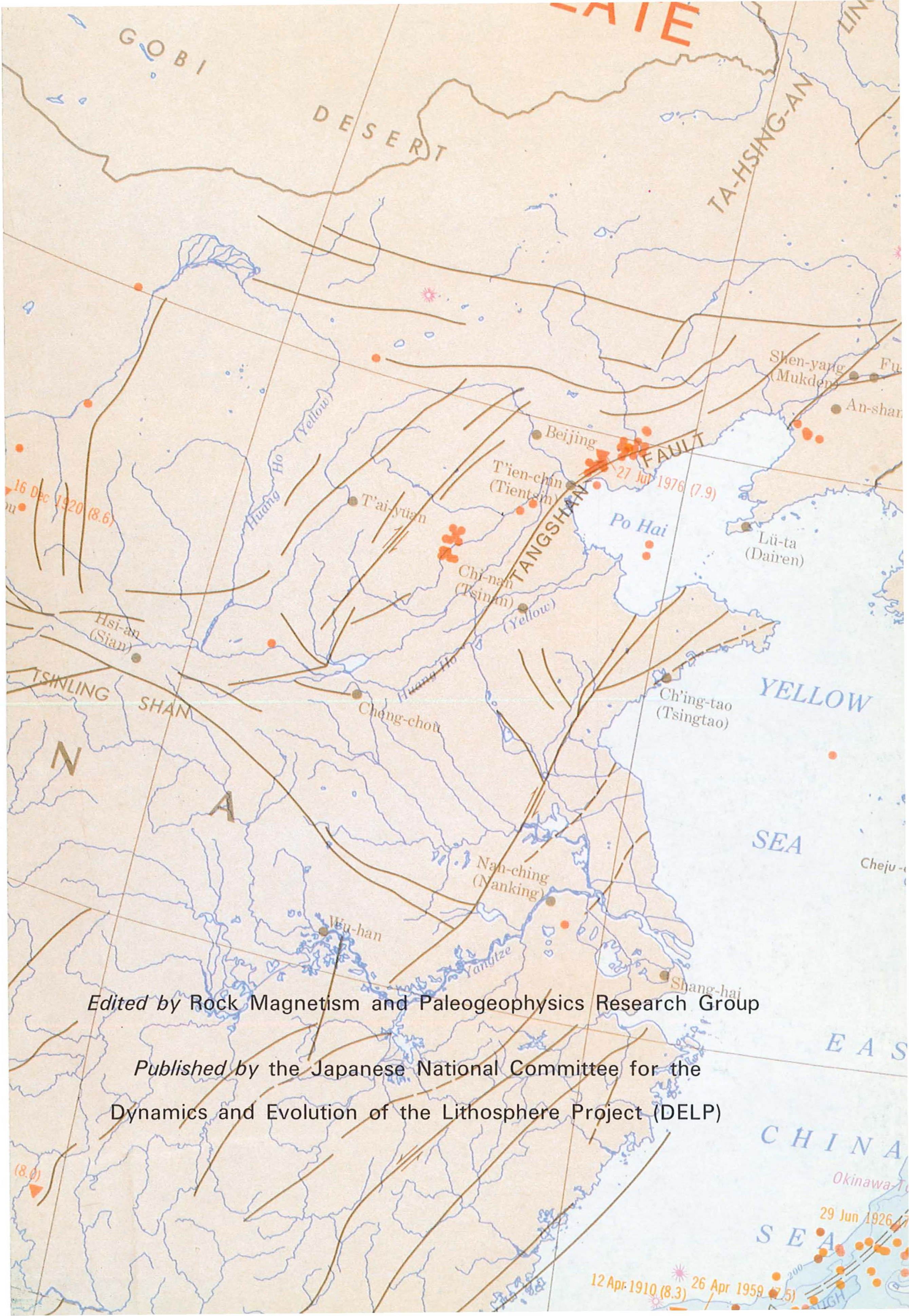

Edited by Rock Magnetism and Paleogeophysics Research Group

Published by the Japanese National Committee for the Dynamics and Evolution of the Lithosphere Project (DELP)